

**PALEOBIOLOGY, PALEOECOLOGY, AND MORPHOLOGY OF
VERTEBRATES: NEW APPROACHES TO OLD QUESTIONS**

A Dissertation
Submitted to the Faculty of
The Richard Gilder Graduate School
at the
American Museum of Natural History
in partial fulfillment of the requirements for the
degree of
Doctor of Philosophy

By

Shaena A. Montanari, B.S.

Richard Gilder Graduate School
at the
American Museum of Natural History
New York, NY
September 26, 2012

©
Copyright 2012
by
Shaena A. Montanari, B.S.
All Rights Reserved

**PALEOBIOLOGY, PALEOECOLOGY, AND MORPHOLOGY OF
VERTEBRATES: NEW APPROACHES TO OLD QUESTIONS**

Shaena Montanari, B.S.

Chair: Mark A. Norell, Ph.D.

ABSTRACT

Physical, chemical, and osteo-histological signatures in fossils can be extremely informative about organismal life history and ecological characteristics, yet these signatures have not yet been exploited to their fullest potential. Tools such as microscopy and mass spectrometry have the potential to address issues and questions in vertebrate paleontology that have, until now, remained elusive. First, this dissertation begins with traditional methods of anatomy and systematics with the addition of improved sampling and visualization of a historic specimen, *Macrerpeton huxleyi*. The edopoid temnospondyl *Macrerpeton huxleyi* is redescribed on the basis of new peels of the holotype. Phylogenetic analysis recovers *Macrerpeton* as the sister taxon of *Cochleosaurus* within the edopoid clade Macrerpetidae (formerly Cochleosauridae).

Histological signatures in fossil bone can be used to reconstruct information about extinct organisms, such as genome size. Nonetheless, intra-skeletal osteocyte lacunae size variation, which could cause error in genome size estimation, has remained unexplored. While there is variance in the sizes of these bone structures over the skeleton of modern tetrapods, this variation is not necessarily causing any issues with genome size estimate; instead, the actual methods of estimation create a wide range of potential values that these methods are not able to answer certain genetic questions at a fine scale.

Examining the carbon and oxygen isotopes in tooth enamel represents a quantitative method for discerning the paleoenvironments and paleoecology of fossil fauna. The Chinchilla Local Fauna from southeastern Queensland is a diverse assemblage of terrestrial Pliocene vertebrates from the Chinchilla Sand Formation. Isotopic analysis results from Chinchilla show that there were distinct dietary niches within the large marsupial vertebrate community. This study suggests that southeastern Queensland hosted a mosaic of tropical forests, wetlands and grasslands during the Pliocene. A review of the uses of biogenic materials in eggshells for stable isotope analysis is also provided. Stable isotope analysis is also used to determine paleoenvironments and paleoecology of dinosaurs during the Late Cretaceous in Mongolia. This study, which is the first to utilize stable isotope geochemistry on Mesozoic fossil tooth enamel from central Asia, documents that the environment was arid, but more importantly that dinosaur remains, such as eggshells, can be used for this type of study. These objectives are united by a need to use quantitative measurements to more accurately reconstruct vertebrate traits throughout earth history.

ACKNOWLEDGMENTS

If I have seen further it is by standing on the shoulders of giants –Sir Isaac Newton, 1676

The above quotation famously penned by Newton, but prevalent in some incarnation since the 12th century, may be clichéd, but it truly describes my feelings. The work I did in these four years could only have been accomplished because of the excellent education I have received from some sincerely gifted teachers.

When I saw the advertisement for the RGGGS Comparative Biology Ph.D. program back in the fall of 2007 never in my wildest dreams did I imagine I would ever have this unique opportunity. Some called us guinea pigs, some called us pioneers, but I just call my classmates some of the brightest young minds in science. Antonia, Bryan, Zach, and Sebastian- where would I be without you guys? We got through this together and I am so unbelievably proud of you all. Especially Sebastian, my ex-roommate and forever best friend in the world. I feel so lucky that through it all I have always had the finest classmates to rely on: Ed, Phil, Pedro, Yi, Steve, Isabelle, Alejandro, Dawn, Ansel, and John. Snorri, my margarita buddy, I never could have made it through without our lengthy, yet important conversations about food and television.

In my four years at RGGGS, I often leaned on our academic staff and without their patience, kindness, and hard-work, this program never would have turned out to be such an (accredited) success. Anna Manuel, Maria Rios, and Taylor Johnson made up the best team anyone could ask for. But lest I forget the original administrative pioneer, Adam Kashuba, who was a great adviser and is now a great friend. My dissertation committee has been there for me to lean on and approach with literally any question. I am so fortunate I had John Flynn, Mark Norell, and Meng Jin guiding such an important part of

my scientific career. John, your unwavering support in every single one of my endeavors has helped me attain so much success at this point in my career, and I thank you so much for it. Mark, you were always there when I needed you and you have given me some of the greatest opportunities up to this point in my life.

I owe the AMNH paleontology crew- you all helped me so much during my dissertation and I cannot even thank you enough for all that you did: Carl Mehling, Justy Alicia, Ana Balcarcel, Amy Davidson, Jack Conrad, and Mick Ellison. The AMNH Mongolia crew gave me two amazing summers in the field most grad students only get to dream of. Thanks to Jonah Choiniere, Amy Balanoff, Gabe Bever, Mike Novacek , and of course the illustrious Gobi mechanic, Tamir. I remember the first day Jonah arrived in New York- he was supposed to help me pack for the trip to Mongolia we would be taking the next day. I thought he was the nicest guy ever for coming up early and helping me out, and while I later learned that he was fairly annoyed that he had to help me pack on such short notice, over these two years he has truly become one of my closest friends (though now I probably like his wife Kelsey a bit more than him).

While not on my official academic committee per say, I am proud to say Susan Perkins was an incredible friend and inspiration throughout this process, even though she made me suffer through pilates with her (but we always made sure we ate enough spring rolls afterwards). I wish I could write more about every single person I have grown to respect so dearly. I thank Penny Higgins, Mark Siddall, Michelle Spaulding, Andres Giallambardo, Sterling Nesbitt, Gilbert Price, Robin Beck, Paul Sweet and Kristina Killgrove for being amazing scientists, collaborators, mentors, and friends.

I have saved the most important people for last. I am blessed my parents, Amy and Andy Montanari, have dedicated their lives to me since the day I was born. I owe all of my success to them and the generosity they have bestowed on me for my entire life; always supporting every endeavor I chased, no matter how far out it was. They trust every decision I make 110%, even when I doubt myself. The only regret I have in finishing this Ph.D. is that my grandmother, Helen Johnsen (aka Nana) is not here to see me achieve this dream because I know she would be the proudest of anyone. And finally, to my future husband Julien, who I had the pleasure of meeting because of this very work, I love you. You are my best friend and my most important collaborator. Despite the fact we were often oceans apart, I dedicate this dissertation to you because it wouldn't have happened without your help and support.

Reconstructing the picture; that's what fascinates me. We may not get all the details correctly, but the main facts are just as clear as though they had been written in stone and left for us to read.

–Roy Chapman Andrews, *This Business of Exploring*

TABLE OF CONTENTS

COPYRIGHT PAGE.....	ii
ABSTRACT.....	iii
ACKNOWLEDGMENTS.....	v
EPIGRAPH.....	viii
FIGURES AND TABLES.....	xi
CHAPTER I. INTRODUCTION.....	1
CHAPTER II. ANATOMY AND RELATIONSHIPS OF <i>MACRERPETON HUXLEYI</i> (TEMNOSPONDYLI: MACRERPETIDAE) FROM THE LATE CARBONIFEROUS OF LINTON, OHIO.....	13
CHAPTER III. VARIATION OF OSTEOCYTE LACUNAE SIZE WITHIN THE TETRAPOD SKELETON: IMPLICATIONS FOR PALAEOGENOMICS.....	34
CHAPTER IV. PLIOCENE PALEOENVIRONMENTS OF SOUTHEASTERN QUEENSLAND, AUSTRALIA INFERRED FROM STABLE ISOTOPES OF MARSUPIAL TOOTH ENAMEL.....	48
CHAPTER V. CRACKING THE EGG: THE USE OF MODERN AND FOSSIL EGGS FOR ENVIRONMENTAL AND ECOLOGICAL INTERPRETATION.....	77
CHAPTER VI. DINOSAUR EGGSHELL AND TOOTH ENAMEL GEOCHEMISTRY AS AN INDICATOR OF CENTRAL ASIAN CRETACEOUS PALEOENVIRONMENTS.....	103
CHAPTER VII. CONCLUSIONS.....	141
APPENDICES.....	144
APPENDIX A. SUPPLEMENTARY MATERIAL FOR CHAPTER II.....	144
APPENDIX B. SUPPLEMENTARY MATERIAL FOR CHAPTER III.....	150

APPENDIX C. SUPPLEMENTARY MATERIAL FOR
CHAPTER IV.....165

APPENDIX D. SUPPLEMENTARY MATERIAL FOR
CHAPTER VI.....171

FIGURES AND TABLES

Figures

2.1	Outline of sutures on the dorsal view of the skull roof of <i>Macrerpeton</i> (AMNH 6834)	20
2.2	Outline of cranial elements preserved in ventral view on the counterpart of <i>Macrerpeton</i> (AMNH 6834)	23
2.3	The strict consensus tree of 4 MPTs, length of 97 steps, retrieved from the phylogenetic analysis.....	28
3.1	An illustration of the automated contrast-based thresholding measurement method.....	37
3.2	A visual representation of estimated genome size measurements for all bones in each of the four taxa sampled.....	41
4.1	Map of Chinchilla Sand locality.....	57
4.2	Bivariate plot of carbon and oxygen for fossil and modern teeth..	65
5.1	Dinosaur eggs as they are found in the field (Grellet-Tinner et al. 2006).....	79
5.2	Schematic of egg and eggshell based on avian model.....	83
5.3	Bivariate plot of carbon versus oxygen from eggshell carbonate for seven species of seabird (Schaffner and Swart 1991)	86
5.4	CL and TLM photos of megaloolithid eggshell from Auca Mahuevo, Argentina (Grellet-Tinner et al. 2010).....	91
5.5	TLM and SEM images of dinosaur eggshell from <i>Deinonychus antirrhopus</i> (Grellet-Tinner et al. 2006).....	93
6.1	Map of Mongolia.....	110
6.2	Generalized stratigraphic columns.....	113
6.3	Photomicrographs of dinosaur eggshell.....	120
6.4	Bivariate plot of oxygen and carbon.....	123

Tables

3.1	ANOVA for Lacuna Area and Volume.....	39
4.1	Stable isotope general statistics.....	59
4.2	Summary of ANOVA results.....	60
4.3	Summary of results from Tukey's HSD test from the $\delta^{13}\text{C}$ and $\delta^{18}\text{O}$ fossil and modern ANOVAs.....	61
4.4	Summary of results from Tukey's HSD test from the $\delta^{13}\text{C}$ and $\delta^{18}\text{O}$ ANOVAs of modern <i>Macropus</i> and fossil <i>Macropus</i> from Chinchilla.....	62
4.5	$\delta^{13}\text{C}$ diet and %C3 diet of fossil and modern marsupials.....	66
4.6	Summary of general statistics for modern <i>Macropus</i> spp. values in different biogeographic and climatic regions from Murphy et al. (2007).....	69
6.1	Stable isotope results and statistics.....	124
6.2	Pairwise comparisons of all materials and localities.....	125
6.3	Results from t-tests.....	126

CHAPTER I

INTRODUCTION

Long past are the days when paleontology merely meant examining fossils with a magnifying glass and a pencil in hand. Recent technological and computational advances mean we are able to answer questions about extinct species with a level of precision and detail never before thought possible. The last decades have brought us refined estimates of feather color in dinosaurs and detailed dietary reconstructions of ancient beasts (Li et al. 2012, Koch 2007). Physical, chemical, and osteo-histological signatures in fossils can be extremely informative about organismal life history and ecological characteristics, yet these signatures have not yet been exploited to their fullest potential. Several of these discoveries have been made specifically using techniques in chemistry and microscopy. In this thesis I explore the use of these tools to tackle issues and questions in vertebrate paleontology whose answers have, until now, remained elusive. I begin my dissertation (Chapter 2) focusing on traditional methods of anatomy and systematics which, combined with new advances in sampling and visualization of historic museum collections allows hitherto unresolved evolutionary relationships of temnospondyls to be determined. Chapter 3 then introduces new methods and analyses in bone histology and microscopy used to obtain information about previously living cells from their remains in hard tissue, and hence paleogenomic inferences. Finally, I end with two studies and a review that use stable isotope geochemistry to assess and quantify underexplored areas of paleoecology and paleobiology across two separate continents and geological periods, highlighting the versatility of these analyses. The uses of these advanced methods have vastly improved

the science of paleontology, bringing a higher level of precision and accuracy to paleobiological and paleoecological interpretations which enrich and improve our understanding of the ancient world.

Systematics of ancient amphibians

Temnospondyl amphibians are a clade of early amphibians within Tetrapoda. This clade has a long fossil history spanning from the Carboniferous into the Cretaceous, yet their exact relationship to modern Lissamphibia remains unknown (Ruta et al. 2007). The basal most group in the temnospondyl clade is thought to be Edopoidea, characterized by enlarged upper marginal teeth near the maxilla/premaxilla suture and an exposed septomaxilla on the surface of the skull. Edopoid fossils are known from coal measures of the Czech Republic (Sequeira 2003) and the United States (Moodie 1916), and the red beds of Texas (Romer and Witter 1942). In the United States, the Carboniferous aged Linton coal measure is rich with vertebrate fossils, including edopoid temnospondyls. This Linton coal fauna was originally described 140 years ago by E.D. Cope (Cope 1874). A vast array of potentially related specimens have been described in recent years, however their precise phylogenetic relationships with species described in the late 19th century and early 20th century have remained elusive, due to different standards of description and previous lack of precise methods of analysis and comparison. Therefore, it is necessary to redescribe historic specimens in order to determine their relationships with more recently described taxa.

The taxon *Macrerpeton huxleyi* was first described in 1874 by E.D. Cope as a species of microsauro, but subsequently placed in the genus *Macrerpeton* by Moodie (1916). Various researchers had noted edopoid or cochleosaurid similarities of

Macrerpeton (e.g. Milner and Sequeira 1998), but until the study presented in this thesis it had never been included in a phylogenetic analysis. The systematic position of this specimen had been shrouded in confusion and had not been accurately incorporated into a taxonomic or phylogenetic framework. In chapter 2, I redescribe the original type specimen of *M. huxleyi* based on new molds and casts. Additionally, I refer two additional specimens to *M. huxleyi* based on my new, detailed examination. I present a revised phylogeny of edopoid temnospondyls based on information derived from this specimen, and discuss the paleoecology and paleoenvironment this species and its allies may have inhabited.

Methods in bone histology and paleogenomics

It was discovered early on in the pursuit of the discovery of heritable information in cells that genome size in mass varies over several orders of magnitude and has no connection to organismal complexity (Gregory 2001, 2005). C-value, or the haploid DNA, has been measured in organisms since the 1940s to determine patterns in amounts of genetic material. Vendrely and Vendrely (1948) noticed that all individuals within a species had the same amount of nuclear DNA, but this value varied greatly between different species. The combination of DNA consistency within a species and extreme variation among species was termed the C-value paradox by Thomas (1971) (Gregory 2005). It was later discovered that large portions of genomes contain non-coding DNA, so this paradox is not really a paradox at all; although it is still important to understand why genome sizes vary among species and groups so widely. Among vertebrates, cartilaginous fishes, lungfish, and amphibians have extremely large C-values compared

with mammals, birds, reptiles, and teleost fishes (Gregory 2005). The exact reason for this variation is not completely known and is a major source of inquiry in the field.

However, what is known is that there is a connection between the size of a cell and genome size in vertebrate species (Gregory 2001). This correlation was first observed with red blood cells, but it has been shown that the reservoir of bone cells in bone, known as osteocyte lacunae also conform to this same pattern (Organ et al. 2007). This is extremely valuable to the study of paleogenomics; in fossils, genetic material is not preserved beyond the scale of thousands of years, but the osteocyte lacunae shape can be preserved in fossils tens or hundreds of millions of years old. Hence this method can be used to study genome size evolution on a geological time scale.

Birds, on average, have a smaller genome size than mammals or other reptiles (Gregory 2005). The reasons behind this have been hotly debated, but it has been proposed that smaller genomes have evolved in organisms that are capable of powered flight (Hughes and Hughes 1995). A number of papers examining this possibility and its pattern in dinosaurs have been published in recent years (Organ et al. 2007, Organ, Brusatte and Stein 2009, Organ and Shedlock 2009) but the methods of measurement and estimation used in these studies ignored numerous fundamental issues about bone histology. In chapter 3 of my dissertation, I examine methods previously used for genome size estimation in fossil organisms and test them with measurements in extant organisms. Previous studies have been inconsistent in their choice of bones for bone cell measurements, and measurements from different types of bone such as long, irregular, and flat bones have been included in the same studies (Organ et al. 2007, Organ, Brusatte and Stein 2009). Here I provide the first rigorous examination of osteocyte lacunae size

variation in living vertebrates. I find that there is variation within the osteocyte lacunae. The vast amount of variation present in measurements made in the genome estimation process therefore renders the method imprecise. This chapter is extremely useful for those considering these types of analyses in the future, and demonstrates to future investigators studying paleontological questions that the assumptions behind such methods must be tested. In particular, my study has direct implications for researchers predicting genome size, and hence making paleobiological inferences, on the basis of lacunae size.

Stable isotope geochemistry: unstudied regions and fossil taxa

The use of stable isotope geochemistry for dietary and environmental reconstruction in vertebrate fossils effectively began with the pioneering work in the late 1970s and early 1980s. Since then study, countless taxa, systems, and time frames have been studied using similar methods; many of these studies are reviewed in publications such as Koch (1998), Koch (2007), and Sponheimer et al. (2009).

Stable isotope geochemistry is effective for environmental and ecological reconstruction because of a few basic principles of earth chemistry. Some elements have multiple stable forms with a different number of neutrons in the nucleus, which is known as an isotope. For example, a normal carbon atom has 6 protons and 6 neutrons in its nucleus, for an atomic weight of 12, but there is also a less common form of carbon that exists with an atomic weight of 13, meaning there are 6 protons and 7 neutrons in its nucleus. Heavier stable isotopes tend to be rarer on earth. The differing physical properties of isotopes of the same element led to a predictable and often times systematic variation in the ratio of heavy to light isotopes in organic materials. Stable isotope ratios

are measured using an isotope ratio mass spectrometer (IRMS). A variety of sample preparation methods, sample inlet methods, and other peripherals have been designed to increase the efficiency and accuracy of isotope measurements. In the past, samples were prepared and combusted offline, which means it would occur in a separate laboratory away from the actual mass spectrometer. Today, peripherals exist that are able to combust and digest samples for analyses and are combined with the IRMS, making the entire process occur online.

A kinetic isotope fractionation occurs when a reaction is unidirectional and mass dependent. This often occurs in biological systems due to enzymes that discriminate between isotopes of different masses during a reaction so substrate and product end up isotopically distinct (Dawson et al. 2002). Equilibrium isotope fractionations occur during isotopic exchange reaction that convert one phase to another, which leads to an isotopic redistribution that is identical in a closed system, but not in an open system (Dawson et al. 2002). Evaporation, condensation, and diffusion are the primary physical mechanisms that cause fractionation between a substrate and a product (Ben-David and Flaherty 2012). This means that all of these fractionation reactions are temperature dependent because temperature changes the velocity and strength of chemical bonds of molecules (Sulzman 2007). There are a number of reactions in an ecosystem that involve a predictable fractionation of isotopes from the atmosphere (substrate) to a biological product. Perhaps the most useful for paleoecologists is the pattern of carbon isotopic fractionation in plants. Due to a kinetic isotope fractionation, C3 photosynthesis plants preferentially fix ^{12}C bearing CO_2 during photosynthesis, resulting in $\delta^{13}\text{C}$ values that are strongly discriminated from the $\delta^{13}\text{C}$ of the atmosphere (currently $\sim -7\text{‰}$), ranging

between -25 and -35‰. In contrast, C4 photosynthesis plants have $\delta^{13}\text{C}$ values worldwide of between -15 and -9‰. C3 and C4 plants tend to grow under different climate regimes, and this clear delineation in $\delta^{13}\text{C}$ provides a way to track changes in ecosystems and understand dynamics of environments in deep time.

Similar predictable fractionations occur with water in the environment and water in the body of an organism, which allows oxygen isotope ratios, $\delta^{18}\text{O}$, to be useful for reconstructing the type of water the organism was drinking in their environment, for example, if it was highly evaporated or not. Oxygen isotope ratios recorded in tooth enamel are related to the drinking water of the organism, which is obtained from the environment. The $\delta^{18}\text{O}$ of environmental water is determined by the $\delta^{18}\text{O}$ of precipitation, which in turn is determined by temperature, evaporation, and the source of the precipitation air mass (Dansgaard 1964). Lighter isotopes of oxygen evaporate while heavier ones condense, meaning the greater the distance between the ocean and the air mass, rain will be lighter because heavy isotopes rainout preferentially earlier in travel of the air mass. Enrichment of $\delta^{18}\text{O}$ is greatest under arid, hot conditions. These systematic variations in the enrichment and fractionation of oxygen isotopes allow us to glean environmental information from the $\delta^{18}\text{O}$ contained in fossil tooth enamel.

Stable isotopes of Pliocene fossils in southeastern Queensland

In Australia, there are very few Pliocene (5.3-2.6 Ma) localities, so it is important to be able to obtain a reliable paleoenvironmental record from the handful of existing ones. Most of the previous stable isotope geochemistry work has been done on Pleistocene sites in southern Australia. Gröcke (1997) was one of the first to utilize bone collagen to look at the environments of a variety of megafauna. Prideaux et al. (2007) and

(2009) used stable isotopes of fossil tooth enamel to examine environmental change of mid Pleistocene localities in southern Australia. It was shown by these authors that an extinct species of kangaroo, *Procoptodon*, consumed primarily C4 browse and drank water in an environment that did not obtain a large amount of rainfall (Prideaux et al. 2009). Forbes et al. (2010) also used fossils from a late Pleistocene locality in southern Australia to compare the diets of kangaroos and wallabies from the Pleistocene to the modern day. It is clear that there has been environmental change over the last 100,000 years in that region, as macropods (kangaroos) from the Pleistocene had stable isotopic signatures of a mixed habitat with a C4 vegetation component, while the macropods that currently live in this environment have a signature in their tooth enamel of a completely C3 dominated ecosystem (Forbes et al. 2010). These studies have created a viable record in southern Australia to track paleoenvironmental and paleoecological change over the Pleistocene to the present; in chapter 4 of my dissertation I begin to create a similar record for Queensland beginning in the Pliocene. It is vital to determine such records in order to examine potential causes for extinction based on environmental change, and also to create a baseline of earlier environmental reconstruction to understand how the arrival of humans could have altered the landscapes these fauna were living in.

Stable isotopes and paleoenvironments using Mongolian dinosaur remains

It is only in recent years that there has been a surge in the number of studies that use stable isotope geochemistry of dinosaur tooth enamel for paleoenvironmental reconstruction (Fricke et al. 2008, Fricke, Rogers and Gates 2009). Previously, non-avian dinosaur tooth enamel was not widely used for stable isotope geochemistry. However studies by Fricke et al. (2008) and Amiot et al. (2004) have sufficiently shown that this

can be a useful proxy for environmental reconstruction. Dinosaur remains from central Asia have never been studied isotopically even though they could provide an important proxy for terrestrial paleoenvironments and ecology. The only stable isotope studies of dinosaur remains in central Asia have focused on dinosaur eggshells from China. In chapter 5, I review stable isotope methods that have specifically been used on modern and fossil eggs and explore their potential for additional inquiry. In chapter 6 of my dissertation, I focus on stable isotopic studies of two important localities in the Gobi Desert of Mongolia.

All of these methods highlight how much we can learn from the fossil record by applying chemical and microscopic methods in innovative and exciting ways. The aforementioned objectives of this dissertation are united by a need to use quantitative measurements to more accurately reconstruct vertebrate life-history traits, and more effectively integrate techniques to obtain a more complete understanding of life-history trait evolution. It is vital for paleontologists to continue exploring old questions using advances in other fields of science in order to create new interdisciplinary methods to address these problems. It is only in this way that new groundbreaking discoveries will be made.

References

- Amiot, Romain, Christophe Lécuyer, Eric Buffetaut, Frédéric Fluteau, Serge Legendre, and François Martineau. 2004. Latitudinal temperature gradient during the cretaceous upper campanian–middle maastrichtian: $\Delta 18\text{O}$ record of continental vertebrates. *Earth and Planetary Science Letters* 226 (1-2): 255-272
- Ben-David, Merav and Elizabeth A Flaherty. 2012. Stable isotopes in mammalian research: A beginner's guide. *Journal of Mammalogy* 93 (2): 312-328.
- Cope, Edward Drinker. 1874. Supplement to the extinct batrachia and reptilia of north america I. Catalogue of the air-breathing vertebrata from the coal-measures of linton, ohio. *Transactions of the American Philosophical Society* 15 (2): 261-278.
- Coplen, Ty B. 1994. Reporting of stable hydrogen, carbon, and oxygen isotopic abundances. *Pure and Applied Chemistry* 66:273-273.
- Dansgaard, Willi. 1964. Stable isotopes in precipitation. *Tellus* 16 (4): 436-468.
- Dawson, Todd E, Stefania Mambelli, Agneta H Plamboeck, Pamela H Templer, and Kevin P Tu. 2002. Stable Isotopes In Plant Ecology. *Annual Review of Ecology and Systematics* 33 (1): 507-559.
- Forbes, Matt S, Matt J Kohn, Erick A Bestland, and RT Wells. 2010. Late pleistocene environmental change interpreted from $\delta 13\text{c}$ and $\delta 18\text{o}$ of tooth enamel from the black creek swamp megafauna site, kangaroo island, south australia. *Palaeogeography, Palaeoclimatology, Palaeoecology* 291 (3-4): 319-327.
- Fricke, Henry C, Raymond R Rogers, and Terry A Gates. 2009. Hadrosaurid migration: Inferences based on stable isotope comparisons among late cretaceous dinosaur localities. *Paleobiology* 35 (2): 270.
- Fricke, Henry C, Raymond R Rogers, Robert Backlund, Christopher N Dwyer, and Susan Echt. 2008. Preservation of primary stable isotope signals in dinosaur remains, and environmental gradients of the late cretaceous of montana and alberta. *Palaeogeography, Palaeoclimatology, Palaeoecology* 266 (1-2): 13-27.
- Gregory, T. Ryan. 2001. The bigger the c-value, the larger the cell: Genome size and red blood cell size in vertebrates. *Blood Cells, Molecules, and Diseases* 27 (5): 830-843.
- . 2005. The c-value enigma in plants and animals: A review of parallels and an appeal for partnership. *Annals of Botany* 95 (1): 133-146.

- Gröcke, Darren R. 1997. Distribution of C3 and C4 plants in the late pleistocene of south australia recorded by isotope biogeochemistry of collagen in megafauna. *Australian Journal of Botany* 45 (3): 607-617
- Hughes, Austin L and Marianne K Hughes. 1995. Small genomes for better flyers. *Nature* 377 (6548): 391.
- Koch, Paul L, Daniel C Fisher, and David Dettman. 1989. Oxygen isotope variation in the tusks of extinct proboscideans: A measure of season of death and seasonality. *Geology* 17 (6): 515-519.
- Koch, Paul L. 1998. Isotopic reconstruction of past continental environments. *Annual Review of Earth and Planetary Sciences* 26 (1): 573-613
- . 2007. Isotopic study of the biology of modern and fossil vertebrates. In *Stable Isotopes in Ecology and Environmental Science*. 2nd ed. Boston: Blackwell Publishing.
- Li, Quanguo, Ke-Qin Gao, Qingjin Meng, Julia A Clarke, Matthew D Shawkey, Liliana DAlba, Rui Pei, Mick Ellison, Mark A Norell, and Jakob Vinther. 2012. Reconstruction of microraptor and the evolution of iridescent plumage. *Science* 335 (6073): 1215-1219.
- Milner, Andrew R and Sandra E K Sequeira. 1998. A cochleosaurid temnospondyl amphibian from the middle pennsylvanian of linton, ohio, USA. *Zoological Journal of the Linnean Society* 122 (1-2): 261-290.
- Moodie, Roy L. 1916. *The Coal Measures Amphibia of North America*. Carnegie Institution of Washington.
- Organ, Chris L, Andrew M Shedlock, Andrew Meade, Mark Pagel, and Scott V Edwards. 2007. Origin of avian genome size and structure in non-avian dinosaurs. *Nature* 446 (7132): 180-4.
- Organ, Chris L, Stephen L Brusatte, and Koen Stein. 2009. Sauropod dinosaurs evolved moderately sized genomes unrelated to body size. *Proceedings of the Royal Society B: Biological Sciences* 276 (1677): 4303-4308.
- Organ, Chris L and Andrew M Shedlock. 2009. Palaeogenomics of pterosaurs and the evolution of small genome size in flying vertebrates. *Biol Lett* 5 (1): 47-50.
- Prideaux, Gavin J, John A Long, Linda K Ayliffe, John C Hellstrom, Brad Pillans, Walter E Boles, Mark N Hutchinson, et al. 2007. An arid-adapted middle pleistocene vertebrate fauna from south-central australia. *Nature* 445 (7126): 422-5.

- Prideaux, Gavin J, Linda K Ayliffe, Larisa R G DeSantis, Blaine W Schubert, Peter F Murray, Michael K Gagan, and Thure E Cerling. 2009. Extinction implications of a chenopod browse diet for a giant pleistocene kangaroo. *Proceedings of the National Academy of Sciences* 106 (28): 11646-11650.
- Romer, Alfred S and Robert V Witter. 1942. Edops, a primitive rhachitinous amphibian from the texas red beds. *The Journal of Geology* 925-960.
- Ruta, Marcelo, D Pisani, Graeme T Lloyd, and Michael J Benton. 2007. A supertree of temnospondyli: Cladogenetic patterns in the most species-rich group of early tetrapods. *Proceedings of the Royal Society B: Biological Sciences* 274 (1629): 3087-3095.
- Sequeira, Sandra E K. 2003. The skull of cochleosaurus bohemicus frič, a temnospondyl from the czech republic (upper carboniferous) and cochleosaurid interrelationships. *Transactions of the Royal Society of Edinburgh: Earth Sciences* 94 (01): 21-43.
- Sulzman, Elizabeth W. 2007. Stable isotope chemistry and measurement: A primer. *Stable Isotopes in Ecology and Environmental Science* 1-21.
- Thomas, C A. 1971. The genetic organization of chromosomes. *Annual Review of Genetics* 5 (1): 237-256.
- Vendrely, R and C Vendrely. 1948. L'acide desoxyribonucleique du noyau cellulaire, depositaire des caracteres hereditaires; arguments d'ordre analytique. *CR Acad. Sci* 226:1061-1063.

CHAPTER II

ANATOMY AND RELATIONSHIPS OF *MACRERPETON HUXLEYI* (TEMNOSPONDYLI: MACRERPETIDAE) FROM THE LATE CARBONIFEROUS OF LINTON, OHIO

(Adapted from Montanari, S., Kammerer, C.F. In review. Anatomy and relationships of *Macrerpeton huxleyi* (Temnospondyli: Macrerpetidae) from the Late Carboniferous of Linton, Ohio. Journal of Vertebrate Paleontology.)

Abstract

The edopoid temnospondyl *Macrerpeton huxleyi* is redescribed on the basis of new peels of the holotype. Phylogenetic analysis recovers *Macrerpeton* as the sister taxon of *Cochleosaurus* within the edopoid clade Macrerpetidae (formerly Cochleosauridae). Although distinctive preserved morphology is limited, *Macrerpeton* can be identified as an edopoid based on the exclusion of lacrimal from the orbital margin and enlarged marginal teeth toward the premaxillary-maxillary suture. *Macrerpeton* possesses a carnivorous dentition, and is autapomorphic in its unusually large, sharp marginal teeth, lack of an intertemporal bone, and fine dermal ornament. There are also lateral line sulci on the skull roof of this individual, which can indicate an aquatic lifestyle. A phylogenetic analysis places *Macrerpeton* in a polytomy with the two species of *Cochleosaurus*, which leads to the renaming of the node-based family Cochleosauridae to Macrerpetidae, as it takes precedence as the name of the clade containing *Macrerpeton*. Although *Macrerpeton* was described in brief over 130 years ago, we present the first analysis of this specimen in a phylogenetic framework.

Introduction

Temnospondyl amphibians have a long fossil record spanning from the Carboniferous into the Cretaceous and are integral to the understanding of the origins of the modern Lissamphibia (Ruta et al., 2007). Edopoids are primarily known from coal measures of the Czech Republic (Sequeira, 2004) and the United States (Moodie, 1916), and the red beds of Texas (Romer and Witter, 1942). One North American coal measure locality is located in Linton, Ohio, USA. The Pennsylvanian aged fauna of the Linton coal measures has been known since the mid-19th century and has helped paint a vivid, diverse picture of an ancient Paleozoic terrestrial ecosystem. Famed paleontologist Edward D. Cope was almost entirely responsible for the original taxonomy and description of these fossils nearly 140 years ago (Cope, 1874). Since this time, a myriad of new temnospondyl discoveries have led to the need for a re-examination of the Linton temnospondyl assemblage.

The Linton tetrapod assemblage has been subject to extensive revision in recent years, but *Macrerpeton huxleyi* has received little attention. This taxon was first named (Cope, 1874) as a species of the microsaur *Tuditonus*, but subsequently placed in a separate genus (Moodie, 1909). Moodie (1916) named a second species of *Macrerpeton*, *M. deani*, but this species has subsequently been recognized as a junior synonym of the colosteid *Colosteus scutellatus* (Hook and Baird, 1986). Although various researchers have noted edopoid or cochleosaurid affinities for *Macrerpeton* (e.g., Milner and Sequeira, 1998), it has never been included in a phylogenetic analysis.

In particular, a seemingly basal temnospondyl, *Macrerpeton huxleyi* Cope 1874 has never been thoroughly described or placed within a phylogenetic framework.

Throughout the years, the taxa in Linton Fauna have been subject to a number of supposed taxonomic revisions that have only compounded confusion in this diverse and plentiful assemblage (Moodie, 1909; Moodie, 1916; Romer, 1930), with *M. huxleyi* falling victim to misclassifications in each publication. The Linton Fauna was subject to several extensive revisions in the early 20th century, although these revisions were strongly criticized in subsequent studies (Romer, 1968; Hook, 1983). Moodie (1916) referred several additional specimens to *M. huxleyi* and named a second species, *M. deani*, based on a partial jaw (AMNH FARB 2934). Romer (1930) considered *M. huxleyi* as a loxommatid (=baphetid). Steen (1931) named numerous new specimens, including *Mytaras macrognathus*.

Romer (1966, 1968) considered *Mytaras* a junior synonym of *Macrerpeton*. Hook (1983) removed *M. deani* from *Macrerpeton*, recognizing the holotype of this species as an individual of the common Linton colosteid *Colosteus scutellatus*. Hook and Baird (1986) reviewed the Linton vertebrate fauna and reaffirmed the synonymy of *Leptophractus dentatus* and *Mytaras macrognathus* with *Macrerpeton huxleyi*. Milner and Sequeira (1998) described a new taxon of Linton cochleosaurid, *Adamanterpeton ohioensis*, based on material formerly referred to *M. huxleyi* (Moodie, 1916).

Until now, *Macrerpeton* has been shrouded in taxonomic and phylogenetic confusion. With recent discoveries and redescriptions of hypothesized relatives of *Macrerpeton*, such as *Nigerpeton* (Steyer et al., 2006) and *Adamanterpeton* (Milner and Sequeira, 1998), *Macrerpeton* can be examined in a phylogenetic framework in order to help elucidate the early evolutionary history of edopoids. It is important to understand the lifestyle modes of early temnospondyls to trace the evolution of life histories (e.g.,

aquatic versus terrestrial) in amphibians. In this paper, a detailed description of *Macrerpeton* is provided, along with a phylogeny illustrating the ecological and morphological diversity of this ancient clade.

Institutional abbreviations

AMNH FARB, American Museum of Natural History, Fossil Amphibians, Reptiles, and Birds Collection, New York, USA; **FMNH**, Field Museum, Chicago, Illinois, USA; **MB**, Museum für Naturkunde, Berlin, Germany; **MCZ**, Museum of Comparative Zoology, Harvard University, Cambridge, Massachusetts, USA; **MNN**, Musée National de Niger, Niamey, Niger; **NHMUK**, Natural History Museum, London, UK; **USNM**, National Museum of Natural History, Washington, DC, USA.

Anatomical abbreviations

art, articular; **cp**, cultriform process; **dent**, denticles; **ex**, exoccipitals; **f**, frontal; **j**, jugal; **l**, lacrimal; **m**, maxilla; **n**, nasal; **p**, parietal; **pf**, postfrontal; **po**, postorbital; **pp**, postparietal; **prf**, prefrontal; **psp**, parasphenoid; **pt**, pterygoid; **sq**, squamosal; **st**, supratemporal; **t**, tabular.

Materials and methods

Redescription of *Macrerpeton huxleyi* is based on new, high quality silicone peels of the holotype skull impressions (AMNH FARB 6834), with additional information based on AMNH FARB 23395 (latex peel of BMNH R2657, the holotype of *Mytaras macrognathus*) and AMNH FARB 6946 (holotype of *Leptophractus dentatus*). Comparisons with other taxa are based on personal examination of the holotypes of *Adamanterpeton ohioensis* (AMNH FARB 2933), *Chenoprosopus lewisi* (USNM 437646), *Chenoprosopus milleri* (FMNH UC 670), and *Nigerpeton ricqlesi* (MNN

MOR69), casts and latex peels of other edopoid specimens (AMNH FARB 7614, a cast of MCZ 1378, a referred specimen of *Edops craigi*; AMNH FARB 23376, a peel of MB Am 80, a referred specimen of *Cochleosaurus bohemicus*), and reference to Langston (1953), Rieppel (1980), Hook et al. (1993), Godfrey and Holmes (1995), Sequeira (1996, 2004), Milner and Sequeira (1998), Sidor et al. (2005), and Steyer et al. (2006).

Systematic paleontology

TEMNOSPONDYLI Zittel, 1887-1890

EDOPOIDEA Romer, 1945

MACRERPETIDAE Moodie, 1909

Cochleosauridae Broili in Zittel and Broili 1923:193.

Chenoprosopidae Romer 1947:313.

Diagnosis

Edopoid based on the presence of the edopoid synapomorphy: prefrontal excludes the lacrimal from the orbital margin. Distinguished from other edopoids by the following unambiguous synapomorphies: maximum length of naris being much less than half the orbit length, and presence of subdued ornament adjacent to midline suture.

MACRERPETON HUXLEYI (Cope, 1874)

(Figs. 2.1-2.2)

Tuditanus huxleyi Cope 1874:274.

Macrerpeton huxleyi Moodie 1909:72.

Leptophractus dentatus Moodie, 1916:169.

Mytaras macrognathus Steen 1931:868.

Holotype

AMNH FARB 6834, impression of partial adult skull, part and counterpart.

Partial palate and lateral surface of jaws visible in ventral view, partial skull roof visible in dorsal view.

Type locality and horizon

Ohio Diamond Coal Mine, Linton, Jefferson County, Ohio. Fossiliferous layer is a cannel coal underlying the Upper Freeport coal of the Allegheny Group, Middle Pennsylvanian (Upper Carboniferous).

Diagnosis

Macrerpetid distinguished by the following autapomorphies: anterior maxillary teeth large and posterior small; finely pitted dermal ornament; small, widely set orbits; lateral line sulci on skull roof of adult; and intertemporal bone absent.

Referred material

AMNH FARB 6946 (holotype of *Leptophractus dentatus*), impression of partial skull (left premaxilla, maxilla, and partial skull roof); NHMUK R2657 (holotype of *Mytaras macrognathus*), impression of partial skull (palatal view), lower jaws, shoulder girdle, and forelimb.

Description

AMNH FARB 6834 consists of a partial skull roof, with much of the preorbital portion absent. The left posterior portion of the skull is missing, with only the right post parietal lappet preserved. The right orbit is distorted while the left has kept its shape. The intertemporal and a pineal foramen are seemingly absent. The counterslab to the skull roof contains a visible partial palate. Two interpterygoid vacutities are filled with small

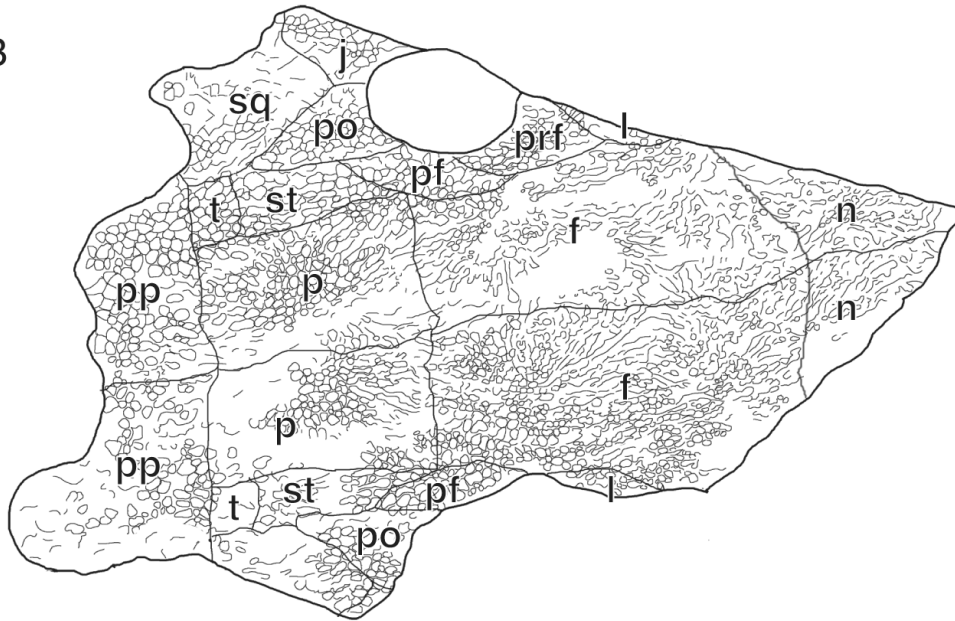
Figure 2.1. Outline of sutures on the dorsal view of the skull roof of *Macrerpeton* (AMNH 6834). A, Photograph of cast of specimen B, Outline of cast of with sutures. Abbreviations: **f, frontal; **j**, jugal; **l**, lacrimal; **n**, nasal; **p**, parietal; **pf**, postfrontal; **po**, postorbital; **pp**, postparietal; **prf**, rontal; **sq**, squamosal; **st**, supratemporal; **t**, tabular. Scale bar equals 2 cm.**

A



2 cm

B



ossicles. The parasphenoid and cultriform processes are present, along with the basisphenoid, basioccipital, and exoccipital bones. Additionally, there are visible fragments of both the right and left mandibles.

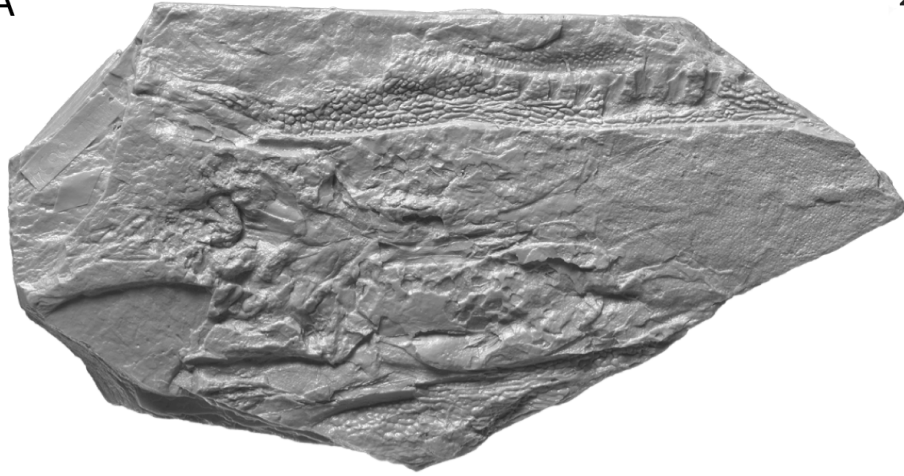
Skull roof

The preserved portion of the skull roof of AMNH FARB 6834 does not preserve the majority of the preorbital portion of the skull, the midline length cannot be measured. Longitudinally oriented ridges are present on the preserved portion of the snout, and between them is a zone of reduced ornamentation, a synapomorphy of *Macrerpetidae* (= *Cochleosauridae* sensu Milner and Sequeira, 1998, see Discussion). Shallow lateral line sulci are present parallel to the longitudinal ridges. Lateral line sulci are absent in most edopoids, with the exception of *Nigerpeton* (Sidor et al., 2005; Steyer et al., 2006). The dermal ornament is comprised of small honeycomb-like pits and ridges, with grooves radiating from centers of ossification in the zone of reduced ornamentation on the frontals and nasals. Compared to other edopoids, such as the rugosely pitted *Adamanterpeton* (Milner and Sequeira, 1998) and *Cochleosaurus bohemicus* (Sequeira, 2004), *Macrerpeton* has smoother dermal ornament with shallower pits and less pronounced ridges.

Although the sutures on the skull roof of AMNH 6834 are difficult to discern, it appears that the prefrontal excludes the lacrimal from the orbital margin, an edopoid synapomorphy (Sequeira, 2004). The skull table (portion of the skull behind the orbits) is partially preserved but it is evident that it was quite narrow (Figure 2.1). There is no evidence of a pineal foramen. The intertemporal bone is seemingly absent (Milner and Sequeira, 1998) which is an apomorphy of this taxon, as other known edopoids possess

Figure 2.2. Outline of cranial elements preserved in ventral view on the counterpart of *Macrerpeton* (AMNH 6834). A, Photograph of counterpart of specimen B, Photograph of cast of counterpart C, Outline of cast of ventral view with sutures.
Abbreviations: **art**, articular; **cp**, cultriform process; **dent**, denticles; **ex**, exoccipitals; **m**, maxilla; **psp**, parasphenoid; **pt**, pterygoid Scale bar equals 2 cm.

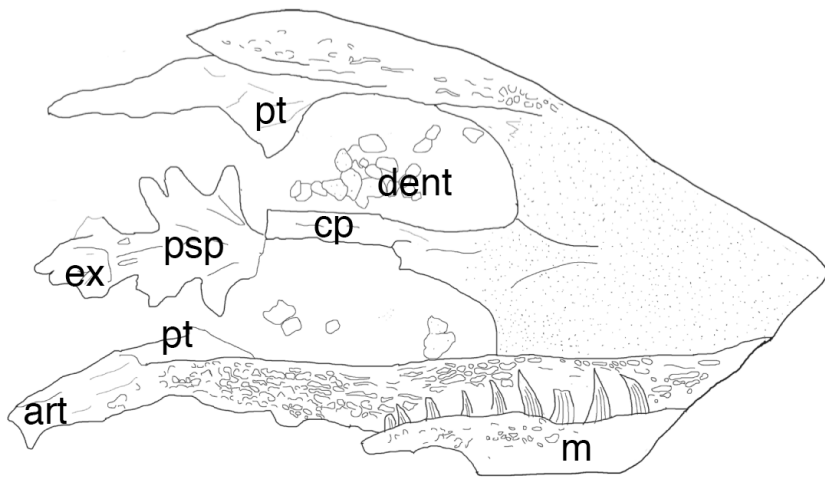
A



B



C



an intertemporal. The postorbital exhibits a raised posteriorly oriented flange as is seen in taxa such as *Cochleosaurus bohemicus* (Sequeira, 2004). A portion of the left otic notch is visible. It is a narrow, shallow embayment relative to that of other more anatomically derived stereospondyl amphibians (Yates and Warren, 2000).

A distinct postparietal lappet is present on the left side of the skull. The postparietal lappet is ornamented with shallow pits and ridges like the rest of the skull. Postparietal lappets are otherwise known only in *Cochleosaurus* among edopoids. The postparietal lappet of *Macrerpeton* is relatively small and weakly ornamented, as in *Cochleosaurus florensis* (as opposed to the larger, highly ornamented lappets of *C. bohemicus* [Sequeira, 2004]). However, in general shape the postparietal lappet of *Macrerpeton* is similar to that of *C. bohemicus*: transversely narrow with a distinct ‘neck’, terminating in a rounded, expanded posterior region (as opposed to the short, stubby lappets of *C. florensis* [Rieppel, 1980; Godfrey and Holmes, 1995]).

Palate

The palate is visible on the counterslab to the skull roof. It is crushed, with the mandibles obscuring the lateral edges of the palate. The most prominent features are the two rounded, semi-circular interpterygoid vacuities (Figure 2.2). Small ossicles filling the interpterygoid vacuity indicate there was a plate of denticles in the vacuities as in *Chenoprosopus* (Hook, 1993), which extended into a shagreen of denticles covering the ventral side of the anterior portion of the palate. The parasphenoid and cultriform process are visible but fragmented. The cultriform process is shorter and wider in *Macrerpeton* than in other macrerpetids such as *Adamanterpeton*. A thin medial ridge runs up the

parasphenoid and cultriform process. The main parasphenoid body bears a triangular patch of denticles, as in *Cochleosaurus bohemicus*.

The basisphenoid, basioccipital, and exoccipitals are preserved at the posterior of the skull. The sphenethmoid is not preserved. Like *Saharastega* (Damiani et al., 2006) and edopoid temnospondyls, there are two clear sharp-rimmed crests (tubera parasphenoidales) bordering linear grooves on either side of the midline ridge on the parasphenoid. The basioccipital and foramen magnum are visible but do not have fine detail preserved. Two exoccipital condyles are clearly visible in the posterior-most portion of the parasphenoid. Unlike other edopoids with well-preserved braincases, no sutures are clearly visible. Only fragments of the pterygoid are visible as they mostly have been crushed and obscured. The pterygoid bone appears to be triradiate with a poorly preserved narrow quadrate ramus.

Mandible

There are visible fragments of both right and left mandibles, but the right mandible is better exposed. It is strongly textured with elongated pits and ridges. There are no in-situ teeth exposed in the mandible. Although the entire mandible is not visible, it is clear it is posteriorly elongated and shallow, similar to *C. bohemicus*, *Adamanterpeton*, and *Nigerpeton*. In the posterior-most portion of the specimen, the articular is clearly visible. It appears quite narrow, but it is most likely due to the fact the surangular is no longer present. No foramina, sutures, or sulci are visible on the exposed medial surface of the right mandible.

Dentition

Only seven maxillary teeth are visible on the crushed right maxilla. The maxilla is only visible on the ventral counterslab. The conical teeth are all posteriorly curved and extremely pointed, clearly indicating a carnivorous diet. Longitudinal striations are preserved on the surface of the teeth, illustrating a characteristic temnospondyl labyrinthodont dentition. There is a pronounced increase in size of the dentition towards the maxillary-premaxillary suture, a characteristic that is ubiquitous in all edopoids. *Macrerpeton* has exceptionally pronounced peaking of the maxillary dentition, which is indicated as an autapomorphy by Milner and Sequeira (1998).

Discussion

Phylogenetics

The object of this phylogenetic analysis is to discover the placement of *Macrerpeton* within edopoids, as it has never been included in a cladistic analysis until now. It is presupposed that *Macrerpeton* is an edopoid temnospondyl because it possesses characteristics that have been used as diagnostic edopoid characteristics: exclusion of lacrimal from orbital margin and possession of a posteriorly oriented process of the postorbital (Sequeira, 2004). *Macrerpeton huxleyi* was coded into a revised version of the edopoid character matrix of Steyer et al. (2006) (see Appendix A). Character 40 of Sidor et al. (2005) and Steyer et al. (2006) was removed due to ambiguous codings in previous analyses. Additionally, two new characters were added for a total of 43 characters included in the matrix (Appendix A). The matrix was assembled using Mesquite v. 2.74 (Maddison and Maddison, 2010).

The character matrix was analyzed using TNT v. 1.1 (Goloboff et al., 2008) utilizing the New Technology Search, ratchet, and drift options (1000 random addition sequences). Bootstrap values were calculated using a traditional search with 100 replicates. Two versions of the character matrix were analyzed: one in which *Macrerpeton* was coded solely based on the holotype and one in which *Macrerpeton* was coded including additional information from the two referred specimens. The results of both analyses were identical: four most parsimonious trees of length 97. Presented in Figure (2.3) is the strict consensus of these 4 trees. Edopoidea is a monophyletic group containing *Edops* and the macrerpetids (Sequeira, 2004; Steyer et al., 2006), and is characterized by four synapomorphies (character 9, 15, 25, 30). Only character 25, enlargement of upper marginal teeth towards premaxillary-maxillary suture, is preserved in *Macrerpeton*. Macrerpetidae, formerly known as Cochleosauridae, is a node-based family containing *Procochleosaurus* to *Chenoprosopus* and all descendants of their last common ancestor, and is characterized by three synapomorphies (character 3, 10, 39). Again, the specimen of *Macrerpeton* preserves only character 39, presence of subdued dermal ornament adjacent to midline suture. Other taxa excluding *Macrerpeton* are recovered in the same positions as in previous analyses (Steyer et al., 2006).

Within Edopoidea, *Macrerpeton* is deeply nested within a clade usually known as Cochleosauridae (Milner and Sequeira, 1998; Sequeira, 2004; Steyer et al., 2006). However, with the placement of *Macrerpeton* within this clade, the valid name for this taxon becomes Macrerpetidae Moodie, 1909, which has priority over Cochleosauridae Broili, 1923. We circumscribe this clade as the last common ancestor of

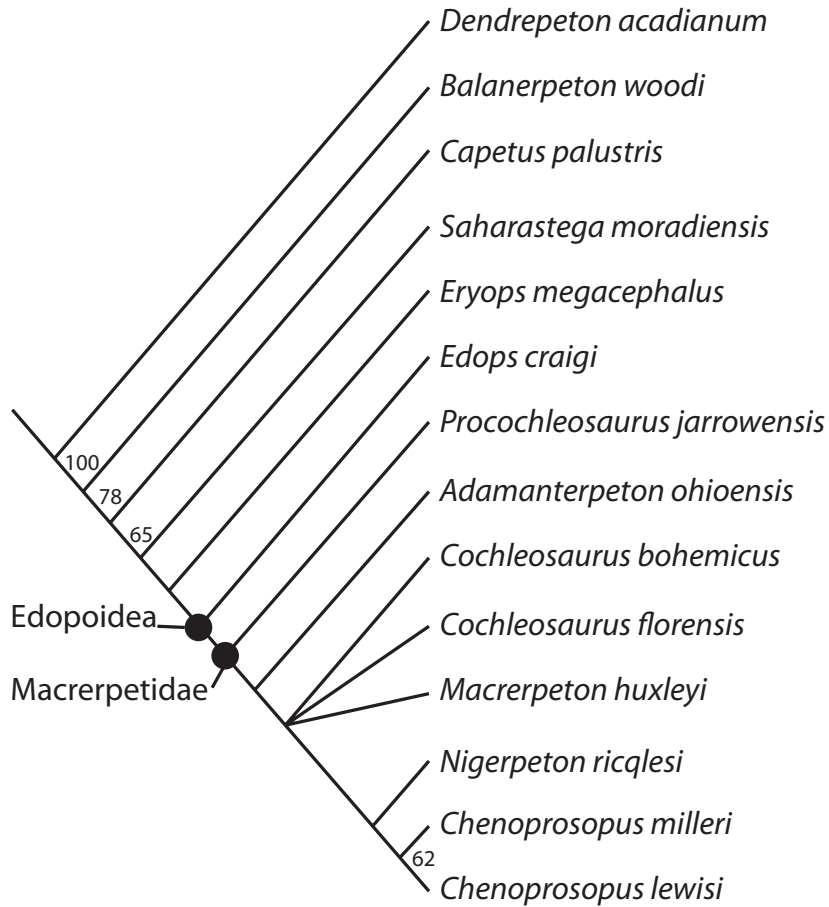


Figure 2.3. The strict consensus tree of 4 MPTs, length of 97 steps, retrieved from the phylogenetic analysis. CI=0.515; RI=0.618. Edopoidea and Macrerpetidae are indicated with circles and labels. Bootstrap values are labeled on each node where the value is over 50. Those nodes not labeled have a bootstrap value under 50.

Procochleosaurus jarrowensis Sequeira, 1996 and *Macrerpeton huxleyi* Cope, 1874 and all of its descendants, making it equivalent in composition to Cochleosauridae *sensu* Steyer, 2007 (with the addition of *Macrerpeton*). Within macrerpetids, *Macrerpeton* is the sister taxon of *Cochleosaurus* in the subclade Macrerpetinae (taking priority over Cochleosaurinae, and defined as the last common ancestor of *Macrerpeton huxleyi* and *Chenoprosopus milleri* and all of its descendants).

Paleoecology of Macrerpeton

Various temnospondyls are presumed to be aquatic rather than terrestrial, but the life traits of edopoids remain somewhat of a mystery. Most edopoids do not have lateral line sulci, canals for sensory organs, which are assumed to be indicative of an aquatic lifestyle due to their presence ancestrally in finned stem tetrapods (Witzmann et al., 2010). *Macrerpeton* and *Nigerpeton* are the only edopoids that show any indication of lateral line sulci, so other macrerpetids such as *Cochleosaurus* are interpreted to be semi-terrestrial. Although, it is important to note that not all aquatic taxa have lateral line sulci on the ossified skull roof even though the lateral line sensory organ is present, so it is debatable whether its presence or absence is indicative of lifestyle (Witzmann et al., 2010). *Macrerpeton* was presumably semi-aquatic and fed on other small freshwater animals. The position of *Macrerpeton* and the other taxon with lateral line sulci, *Nigerpeton*, on the tree indicate that an aquatic lifestyle potentially evolved twice in Macrerpetidae. This taxon is unique in the fact it is a more gracile predator than the other edopoid living in the same environment, *Adamanterpeton*. Additionally, *Macrerpeton* seems to have a smaller size overall than other macrerpetids, meaning it was uniquely adapted to a different lifestyle than its close relatives.

This specimen, AMNH 6834, is the only one of three known specimens attributed to *Macrerpeton huxleyi*. Despite the fact that in certain macrerpetid fossil localities some species are extremely common, like *C. bohemicus*, it does not necessarily mean that the existence of only a few specimens of a taxon means it was rare in its habitat. Milner and Sequeira (1998) argue that the lack of *Adamanterpeton* remains from the Linton coal measure locality can be attributed to the fact that taxon was a rare, mostly terrestrial amphibian and was swept into the oxbow lake where it was subsequently preserved. The Linton coal mine locality is notably limited in area; the bulk of the fossil organisms preserved in cannel coal are restricted to small, localized patches (Hook and Baird, 1986). Since the Linton coal measures most likely represent a stranded oxbow lake that was subsequently filled in with organic matter, the ecosystem preserved is probably a small time slice of a larger flood plain habitat, so care must be taken when using abundance data to infer terrestriality. Discovered over a century ago, the details of the fauna of the coal measures of Linton, Ohio still are ambiguous and more taxa need to be examined once again to provide a descriptive and more rigorously analytical picture of a rich Paleozoic ecosystem. Finding out more about the anatomy and life history traits of species like *Macrerpeton huxleyi* will also help us understand the early evolution of temnospondyls and amphibians.

References

- Cope, E. D. 1874. Supplement to the extinct Batrachia and Reptilia of North America. I. Catalogue of the air-breathing Vertebrata from the coal-measures of Linton, Ohio. Transactions of the American Philosophical Society 25:261–278.
- Damiani, R., C. A. Sidor, J. S. Steyer, R. M. H. Smith, H. C. E. Larsson, A. Maga, and O. Ide. 2006. The vertebrate fauna of the Upper Permian of Niger. V. The primitive temnospondyl *Saharastega moradiensis*. Journal of Vertebrate Paleontology 26:559–572.
- Godfrey, S. J., and R. Holmes. 1995. The Pennsylvanian temnospondyl *Cochleosaurus florensis* Rieppel, from the lycopsid stump fauna at Florence, Nova Scotia. Breviora 500:1–25.
- Goloboff, P. A., J. S. Farris, and K.C. Nixon. 2008. TNT, a free program for phylogenetic analysis. Cladistics 24:774–786.
- Hook, R. W. 1983. *Colosteus scutellatus* (Newberry), a primitive temnospondyl amphibian from the Middle Pennsylvanian of Linton, Ohio. American Museum Novitates 2770:1–41.
- Hook, R. W. 1993. *Chenoprosopus lewisi*, a new cochleosaurid amphibian (Amphibia: Temnospondyli) from the Permo-Carboniferous of north-central Texas. Annals of Carnegie Museum 62:273–291.
- Hook, R. W., and D. Baird. 1986. The diamond coal mine of Linton, Ohio, and its Pennsylvanian-age vertebrates. Journal of Vertebrate Paleontology 6:174–190.
- Hook, R. W., and D. Baird. 1988. An overview of the Upper Carboniferous fossil deposit at Linton, Ohio. The Ohio Journal of Science 88:55–60.
- Langston, W. 1953. Permian amphibians from New Mexico. University of California Press, Berkeley, California, 416 pp.
- Maddison, W. P., and D. Maddison. 2010. Mesquite: a modular system for evolutionary analysis, Version 2.74.
- Milner, A. R., and S. E. K. Sequeira. 1998. A cochleosaurid temnospondyl amphibian from the Middle Pennsylvanian of Linton, Ohio, USA. Zoological Journal of the Linnean Society 122:261–290.
- Moodie, R. L. 1909. New or little known forms of Carboniferous Amphibia in the American Museum of Natural History. Bulletin of the American Museum of Natural History 26:347–357.

- Moodie, R. L. 1916. The coal measures Amphibia of North America. Publications of the Carnegie Institution of Washington. 238:1–222.
- Rieppel, O. 1980. The edopoid amphibian *Cochleosaurus* from the Middle Pennsylvanian of Nova Scotia. *Palaeontology* 23:143–149.
- Romer, A. S. 1930. The Pennsylvanian tetrapods of Linton, Ohio. *Bulletin of the American Museum of Natural History* 59:77–147.
- Romer, A. S. 1945. *Vertebrate Paleontology*. 2nd Edition. The University of Chicago Press, Chicago, Illinois, 687 pp.
- Romer, A. S. 1947. Review of the Labyrinthodontia. *Bulletin of the Museum of Comparative Zoology* 99:1–368.
- Romer, A. S. 1968. Notes and comments on vertebrate paleontology. The University of Chicago Press, Chicago, Illinois, viii + 304 pp.
- Romer, A. S., and R. V. Witter. 1942. *Edops*, a primitive rhachitomous amphibian from the Texas red beds. *The Journal of Geology* 50:925–960.
- Ruta, M., D. Pisani, G. T. Lloyd, and M. J. Benton. 2007. A supertree of Temnospondyli: cladogenetic patterns in the most species-rich group of early tetrapods. *Proceedings of the Royal Society B: Biological Sciences* 274:3087–3095.
- Sequeira, S., and A. Milner. 1993. The temnospondyl amphibian *Capetus* from the Upper Carboniferous of the Czech Republic. *Palaeontology* 36:657–680.
- Sequeira, S. E. K. 1996. A cochleosaurid amphibian from the Upper Carboniferous of Ireland; pp. 65–80 in A. R. Milner (ed.), *Studies on Carboniferous and Permian Vertebrates*. Special Papers in Palaeontology 52.
- Sequeira, S. E. K. 2004. The skull of *Cochleosaurus bohemicus* Fric, a temnospondyl from the Czech Republic (Upper Carboniferous) and cochleosaurid interrelationships. *Transactions of the Royal Society of Edinburgh: Earth Sciences* 94:21–43.
- Sidor, C. A., F. R. O'Keefe, R. Damiani, J. S. Steyer, R. M. H. Smith, H. C. E. Larsson, P. C. Sereno, O. Ide, and A. Maga. 2005. Permian tetrapods from the Sahara show climate-controlled endemism in Pangaea. *Nature* 434:886–889.
- Steen, M. C. 1931. The British Museum collection of Amphibia from the Middle Coal Measures of Linton, Ohio. *Proceedings of the Zoological Society of London* 1930:849–892.

- Steyer, J. S., R. Damiani, C. A. Sidor, F. R. O'Keefe, H. C. E. Larsson, A. Maga, and O. Ide 2006. The vertebrate fauna of the Upper Permian of Niger. IV. *Nigerpeton ricqlesi* (Temnospondyli: Cochleosauridae), and the edopoid colonization of Gondwana. *Journal of Vertebrate Paleontology* 26:18–28.
- Witzmann, F., H. Scholz, J. Muller, and N. Kardjilov. 2010. Sculpture and vascularization of dermal bones, and the implications for the physiology of basal tetrapods. *Zoological Journal of the Linnean Society* 160:302–340.
- Yates, A. M., and A. Warren. 2000. The phylogeny of the higher temnospondyls (Vertebrata: Choanata) and its implications for the monophyly and origins of the Stereospondyli. *Zoological journal of the Linnean Society* 128:77–121.
- Zittel, K. A. von. 1887-1890. *Handbuch der Palaontologie*. Abeteliung 1. Palaozoologie Band III. Vertebrata (Pisces, Amphibia, Reptilia, Aves). Oldenbourg, Munich and Leipzig, 900 pp.

CHAPTER III

VARIATION OF OSTEOCYTE LACUNAE SIZE WITHIN THE TETRAPOD SKELETON: IMPLICATIONS FOR PALAEOGENOMICS

(Adapted from Montanari, S., Brusatte, S.L., De Wolf, W., Norell, M.A. 2011. Variation of osteocyte lacunae size within the tetrapod skeleton: implications for palaeogenomics. *Biology Letters* 7, 751-754.)

Abstract

Recent studies have touted the ability to reconstruct genome sizes (C-values) of extinct organisms such as dinosaurs using correlations between known genome sizes and bone cell (osteocyte lacunae) volumes. Because of the established positive relationship between cell size, including red blood cells and osteocytes, and genome size in extant vertebrates, osteocyte lacunae volume is a viable proxy for reconstructing C-values in the absence of any viable genetic material. However, intra-skeletal osteocyte lacunae size variation, which could cause error in genome size estimation, has remained unexplored. Here, 11 skeletal elements of one individual from each of four different major clades (Mammalia, Amphibia, Aves, Reptilia) were examined histologically. Skeletal elements in all four clades exhibit significant differences in the average sizes of their lacunae. This variation, however, generally does not cause a significant difference in estimated genome size when common phylogenetic estimation methods are employed. On the other hand, the spread of the estimations illustrates that this method may not be precise. High variance in genome size estimations remains an outstanding problem. Additionally, a

suite of new methods is introduced to further automate the measurement of bone cells and other microstructural features on histological thin sections.

Introduction

There is a well-established positive correlation between genome size (C-value) and the sizes of many cells in living vertebrates [1]. Osteocytes are the most abundant cell type in mature bone and are contained within small holes (lacunae) in the bone tissue [2]. In fossil organisms, even though the osteocytes are absent, their size and shape are preserved because the lacunae remain. Although red blood cell size is the most frequent proxy for genome size, it has been demonstrated that in their absence, the size of osteocyte lacunae can also serve as a valuable proxy [3]. This allows for the estimation of genome size in extinct animals for which no preserved genetic material is available, and unlocks the once-intractable possibility of studying large-scale patterns of genome evolution over deep time [3,4,5,6].

The use of lacunae size to estimate genome size, and study genomic evolution, in long-extinct organisms is an emerging area of research. However, one potentially confounding problem has yet to be addressed. Published studies have been inconsistent in their choice of bones for lacunar measurements, and measurements from different types of bone shape (long, irregular, flat) have been included in the same datasets [3,4,5,6]. Previous work has hinted that there may be variation in the size of osteocyte lacunae across the skeleton of an individual, [6], and if true, this may compromise the integrity of genome size estimates based on measurements from different types of bone. Differences

in lacunae size among organisms could be due to the uneven sampling of disparate bones, and not reflect true variety in genome size.

Here, we provide the first rigorous examination of osteocyte lacunae size variation in living vertebrates, and show that although there are significant differences in lacunar size among different bones, genome size estimates are mostly accurate in the face of this variation. With this being said, however, the overwhelming amount of variation present in measurements made at each step in the genome estimation process renders the method imprecise. Therefore, caution is recommended when estimating traits based on highly variable biological features, in this case osteocyte lacunae.

Materials and methods

Four representative taxa were chosen for thin sectioning: woodchuck (*Marmota monax*), Chinese alligator (*Alligator sinensis*), tiger salamander (*Ambystoma tigrinum*), and rock pigeon (*Columba livia*). For each individual specimen, eleven bones were transversely sectioned: tibia, fibula, rib, ulna, femur, thoracic vertebra, caudal vertebra, metatarsal, humerus, skull, and radius. Long bones were transversely sectioned in the midshaft region. Histological thin sections were prepared according to established guidelines[7]. Bones were embedded in cold-setting resin, cut on a low speed diamond saw, and subsequently ground and polished until desired optical clarity was reached. High-resolution micrographs were taken with a Zeiss Evo 60 environmental scanning electron microscope at the American Museum of Natural History. Osteocyte lacuna area was measured using the free NIH program ImageJ [8]. The image was cropped and

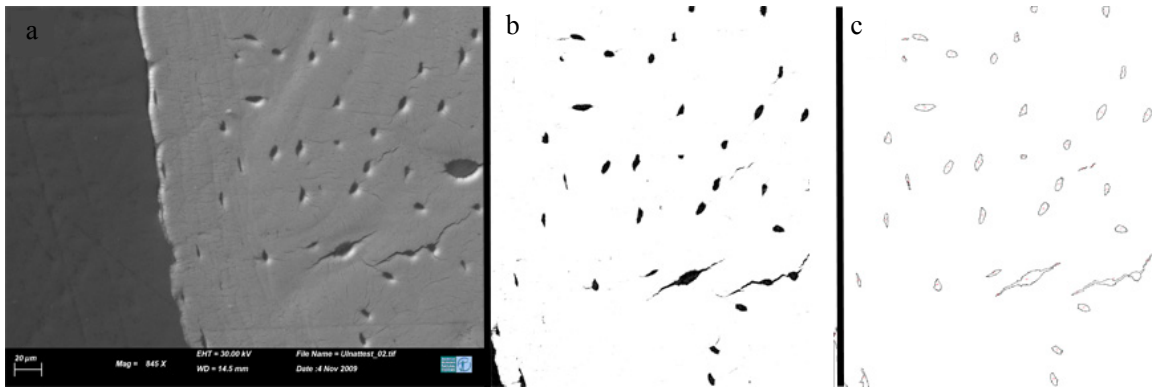


Figure 3.1. An illustration of the automated contrast-based thresholding measurement method. a) The raw photograph of a woodchuck ulna obtained from the SEM. b) The same image cropped with the threshold adjusted so the lacunae are highlighted. c) The image once the lacunae have been outlined and measured by the “Analyze Particles” feature in ImageJ. Certain cells with other features outlines, such as canaliculi seen in the bottom right of the image, can be manually excluded because each outlined cell is numbered on the image and in the resulting measurement output.

segmented based on contrast-based thresholding. The “Analyze Particles” feature was then used to automatically outline and calculate the area for all lacunae in the image area (Figure 3.1). The average lacunar areas from different bones within the same taxon were statistically compared using ANOVA in Microsoft Excel 2008. Volumes were also calculated (see Appendix B), as published datasets have used volumes to estimate genome size [3,4,5,6]. For genome size estimation, the mean natural log transformed osteocyte lacuna volume for each bone in each taxon was entered into a web-based program, PhyloPars, which uses a phylogeny and a maximum likelihood framework to estimate missing parameters [9]. Our calculated data were added to the dataset and phylogeny of Organ *et al.* [4]. Estimated genome sizes for our four taxa were compared to measured C-values from the Animal Genome Size Database [10]. Because there is variability in the measured C-values for individual taxa in the database, we performed a type of sensitivity analysis using the minimum, maximum, and average C-values for each species to determine the effect of variability on the genome size prediction (Appendix B).

Results

At $p < 0.05$, all four taxa have significantly different osteocyte areas and volumes across all bones sectioned (Table 3.1). No one type of bone consistently had higher or lower osteocyte size than other bones across the four taxa. When lacunar volumes were used to estimate genome size, and then compared to the empirically measured C-value for each taxon, every bone of the rock pigeon yielded a genome size estimate whose 95 percent confidence interval includes the measured value. All but two of the tiger

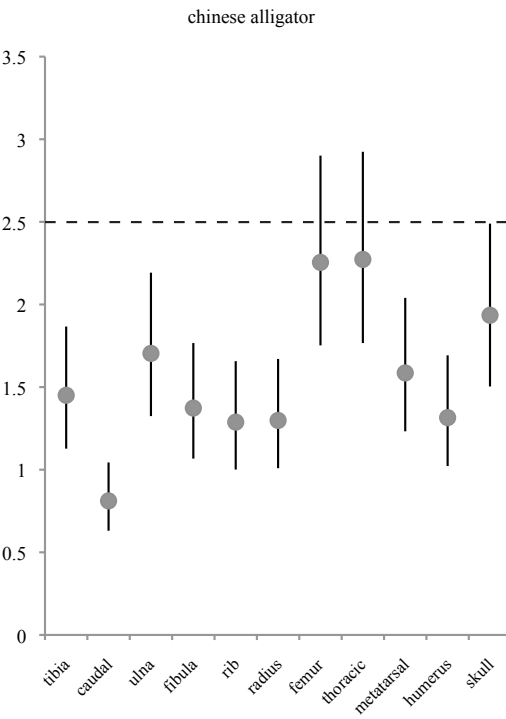
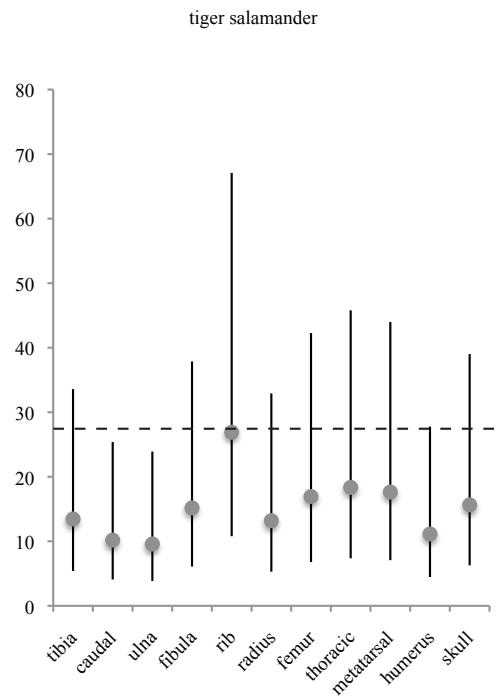
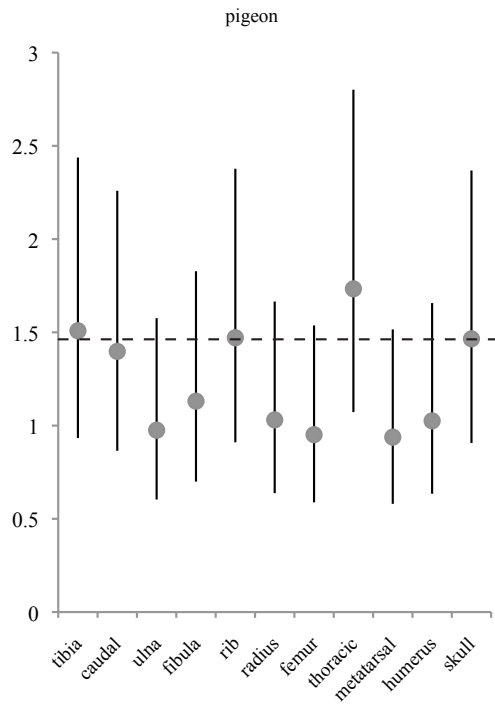
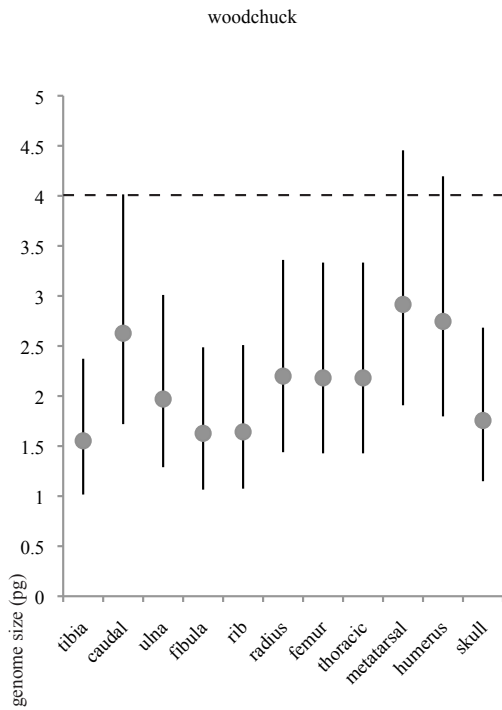
Table 3.1. ANOVA for Lacuna Area and Volume (a) ANOVA results for osteocyte lacuna areas (Bold P-value indicates significance at a level of 0.05)

Taxon	df	F	P-value
<i>Ambystoma tigrinum</i>	10	4.799	2.97E-05
<i>Marmota monax</i>	10	6.457	2.30E-09
<i>Columba livia</i>	10	2.031	0.04
<i>Alligator sinensis</i>	10	9.708	1.99E-13

(b) ANOVA results for osteocyte lacuna volumes

Taxon	df	F	P-value
<i>Ambystoma tigrinum</i>	10	3.95	0.00026
<i>Marmota monax</i>	10	8.92	1.72E-13
<i>Columba livia</i>	10	3.13	0.0015
<i>Alligator sinensis</i>	10	7.08	1.16E-09

Figure 3.2: A visual representation of estimated genome size measurements for all bones in each of the four taxa sampled. The filled in circle represents the mean estimated C-value in picograms (pg) and the lines extending from it represent a spread of 2 standard deviations around the mean. The horizontal dashed lines represent the average measured C-value for each taxon from the Animal Genome Size Database.



bone element

salamander bones (caudal, radius) contain the measured C-value within their 95 percent confidence intervals. Conversely, the C-values of both the woodchuck and the Chinese alligator fall within the 95 percent confidence intervals in only three out of 11 sampled elements (Figure 3.2). In both the tiger salamander and rock pigeon, the lacuna measurements from the rib resulted in the most accurate genome size estimation. The metatarsal was the best estimator of genome size in the woodchuck, whereas the thoracic vertebra was most accurate in the Chinese alligator.

Discussion

Although it was previously shown that the size and shape of osteocyte lacunae varies between compact and cancellous bone in one studied taxon [11], variation in osteocyte measurements between numerous different bones of the skeleton had remained unexplored until the present study. Furthermore, the measurement method employed here should be more accurate, and less prone to human error, than the techniques of previous studies, as areas of all lacunae are automatically calculated using a computer program rather than by measuring length and width by hand [3,4,5,6].

Our results unmistakably show that there is statistically significant variation in osteocyte lacuna size across the skeleton of extant vertebrates. With this established, the important question is: to what degree does this variation affect genome size estimates? Are C-value estimates relatively robust to variation in lacunar size among different bones, or is predicting genome size based on bone cell size doomed to intractable error? This is critical to answer because genome size is a correlate of many attributes of

organismal physiology, such as metabolic rate, that are notoriously difficult to assess in fossil organisms [12].

Although there is demonstrable variation in the volume and area of osteocyte lacunae in the four vertebrates sampled, genome size estimates are often accurate despite this variability. The tiger salamander and rock pigeon measurements performed the best, with the vast majority of skeletal elements, including all bones in the rock pigeon, predicting the measured C-value within two standard deviations of the mean. The genome size estimations for the woodchuck and the Chinese alligator, on the other hand, were not as accurate, as the majority of skeletal elements incorrectly predicted the genome size. This illustrates that genome size estimates based on osteocyte size may not always be accurate on a taxon-by-taxon basis, which raises serious doubts about the reliability of genome size reconstruction. This is not surprising, however, given that Organ *et al.* [3] found an overall significant correlation between osteocyte lacunae size and genome size in living vertebrates based on a large dataset of 26 species, but several cases of individual taxa in which this relationship does not hold. As a result, their regression analysis found that osteocyte size predicted only 32 percent of the variation in genome size, which means most of the variation is not described by this relationship at all. It is important to note, however, phylogenetic regressions still offer a vast improvement in accuracy of genome size estimations over simple linear regressions [3,6]

Variability in lacunar size is also a vexing problem. First, there is no systematic pattern in osteocyte lacuna size across the skeleton of all vertebrates. In other words, there is not one bone or bone type that always results in the smallest or largest osteocyte measurements in the four taxa sampled. Instead, it seems as if osteocyte size is essentially

randomly variable across the vertebrate skeleton. Therefore, consistently measuring osteocytes from the same bone would not be expected to improve resolution, standardize data collection, or reduce measurement error.

In addition, even within bones osteocyte size can be highly variable: each histological slide contains abundant osteocyte lacunae, so there will always be a standard deviation of measurement. Problematically, the commonly used phylogenetic estimation methods do not take this variability into account, because only one value for “measured osteocyte size” can be entered. This is clearly a quandary for genome estimations, because the standard deviations of the lacunar volume calculations are disproportionately large, often times more than 50 percent of the average calculated volume for that bone. Therefore, only using an average measure to estimate genome size effectively fails to propagate uncertainty by not taking standard deviations into account. We do find that average osteocyte size in many bones, despite their variability, still accurately predict genome size, at least in the sense that the 95% confidence interval of the estimation includes the measured value in the Animal Genome Size Database. Accuracy, however, must not be mistaken for precision, and this should be remembered when estimating genome size based on highly variable osteocyte sizes.

In summary, considerable variability in osteocyte lacunae measurements across the skeleton shows that lacunar size is an imperfect, but in some cases still useful, proxy for genome size estimation. We have found three important results: i) the size of osteocyte lacunae in compact bone do vary within an individual; ii) lacunar size measured on most bones is often an accurate method for predicting genome size, but this is not true for each individual taxon; iii) variability in osteocyte size is often large,

meaning that genome size estimations are imprecise. Together, these qualms mean that genome size estimates may not always be accurate, and are usually far from precise, but in the absence of genetic material in fossil organisms, they still prove our only means to trace the large-scale trends of genomic macroevolution in deep time. Coarse questions, such as whether Mesozoic theropod dinosaurs had relatively small genomes on par with those of avians [3], should be tractable with this method, but genome sizes estimates for individual taxa should not be considered accurate or precise.

References

1. Gregory, T. R. 2001 The Bigger the C-Value, the Larger the Cell: Genome Size and Red Blood Cell Size in Vertebrates. *Blood Cells Mol. Dis.* **27**, 830-843. (doi: 10.1006/bcmd.2001.0457)
2. Aarden, E. M., Burger, E. H. & Nijweide, P. J. 1994 Function of Osteocytes in Bone. *J. Cell. Biochem.* **55**, 287-299. (doi: 10.1002/jcb.240550304)
3. Organ, C. L., Shedlock, A. M., Meade, A., Pagel, M. & Edwards, S. 2007 Origin of avian genome size and structure in non-avian dinosaurs. *Nature* **446**, 180-184. (doi: 10.1038/nature05621)
4. Organ, C. L., Brusatte, S. L. & Stein, K. 2009 Sauropod dinosaurs evolved moderately sized genome unrelated to body size. *P. R. Soc. B* **276**, 4303-4308. (doi: 10.1098/rspb.2009.1343)
5. Organ, C. L. & Shedlock, A. 2009 Palaeogenomics of pterosaurs and the evolution of small genome size in flying vertebrates. *Biol. Letters* **5**, 47-50. (doi: 10.1098/rsbl.2008.0491)
6. Organ, C.L., Canoville, A., Reisz, R.R. & Laurin, M. 2011. Paleogenomic data suggest mammal-like genome size in the ancestral amniote and derived large genome size in amphibians. *Journal of Evolutionary Biology* **24**: 372-380.
7. Horner, J. R., Padian, K. & Ricqlés, A. 2001 Comparative osteohistology of some embryonic and perinatal archosaurs: developmental and behavioral implications for dinosaurs. *Paleobiology* **27**, 39-58. (doi: 10.1666/0094-8373(2001)027<0039:COOSEA>2.0.CO;2)
8. Abramoff, M.D., Magelhaes, P.J., Ram, S.J. 2004 Image Processing with ImageJ. *Biophotonics International* **11**, 36-42.
9. Bruggeman, J., Heringa, J. & Brandt, B. W. 2009 PhyloPars: estimation of missing parameter values using phylogeny. *Nucleic Acid Research* **37**, W179-W184. (doi: 10.1093/nar/gkp370)
10. Gregory, T.R., Nicol, J.A., Tamm, H., Kullman, B., Kullman, K., Leitch, I.J., Murray, B.G., Kapraun, D.F., Greilhuber, J., and Bennett, M.D. 2006 Eukaryotic genome size databases. *Nucleic Acids Research*. (doi: 10.1093/nar/gkl828)
11. Cané, V. & Marotti, G. 1982 Size and density of osteocyte lacunae in different regions of long bones. *Calcified Tissue Int.* **34**, 558-563.

12. Gregory, T. R. 2002 A Bird's-Eye View of the C-Value Enigma: Genome Size, Cell Size, and Metabolic Rate in the Class Aves. *Evolution* **56**, 121-130.
(doi: 10.1111/j.0014-3820.2002.tb00854.x)

CHAPTER IV

PLIOCENE PALEOENVIRONMENTS OF SOUTHEASTERN QUEENSLAND, AUSTRALIA INFERRED FROM STABLE ISOTOPES OF MARSUPIAL TOOTH ENAMEL

(Adapted from Montanari, S., Louys, J.C., Price, G. In preparation. Pliocene paleoenvironments of southeastern Queensland, Australia inferred from stable isotopes of marsupial tooth enamel. PLoS ONE.)

Abstract

The Chinchilla Local Fauna is a diverse assemblage of both terrestrial and aquatic Pliocene vertebrates from the Chinchilla Sand Formation of southeastern Queensland, Australia. This formation is a sequence of weakly consolidated grey to yellow/light brown sands, conglomerates, and sandy clays. Fossil remains are derived from fluvial sediments and are typically disarticulated. The age of the locality is based on biochronologic correlation with the Kanunka Local Fauna of the Tirari Desert in South Australia and the Bluff Downs Local Fauna of central-eastern Queensland. Prior inferences about the environment of this locality range from grassland to open woodland to wetland. Examining the carbon and oxygen isotopes in the tooth enamel of the marsupials from this site represents a quantitative method for discerning the paleoenvironments and paleoecology of the fossil fauna. Results from Chinchilla show that *Protemnodon* consumed both C3 and C4 photosynthesis plant types (mean $\delta^{13}\text{C} = -14.5 \pm 2.0\text{‰}$), and therefore probably occupied a mixed vegetation environment. *Macropus* spp. from the Chinchilla Sands also consumed a mixed diet of both C3 and C4 plants, with more of a tendency for C4 plant consumption (mean $\delta^{13}\text{C} = -10.3 \pm 2.3\text{‰}$).

Interestingly, their isotopic dietary signature is more consistent with tropical and temperate kangaroo communities than the sub-tropical communities found around Chinchilla today. Other genera sampled in this study include the extinct kangaroo *Troposodon* and the fossil diprotodontid *Euryzygoma*, each of which appear to have occupied distinct dietary niches. This study suggests that southeastern Queensland hosted a mosaic of tropical forests, wetlands and grasslands during the Pliocene and was much less arid than previously thought.

Introduction

The Chinchilla Local Fauna of Chinchilla, southeastern Queensland represents one of the few well studied and diverse Pliocene vertebrate assemblages in Australia. The age of this locality has been determined on the basis of biocorrelation with Kanunka, Bluff Downs, Spring Park, and Big Sink Local Faunas [1], at approximately 3.4 Ma. The vertebrate community at this locality is represented by an array of reptiles, fish, birds, rodents, and marsupials. This locality appears to represent a mosaic environment based on interpreted habitats of presumably sympatric taxa, such as a species of tree kangaroo (*Bohra*) that most likely lived in rainforests alongside kangaroos that usually feed on C3 plants and C4 grasses (e.g., *Macropus* spp.). Paleoenvironmental reconstructions made on the basis of this fauna have therefore ranged from equitable grasslands and wetlands (e.g., evidence from birds and turtles [2-5]) to more arid and strongly seasonal conditions (e.g., evidence from dasyurids and catfish [6]) to forested conditions similar to those found in Papua New Guinea (e.g., evidence from tree kangaroos and forest wallabies [7,8]).

Stable isotope geochemistry of fossil vertebrate tooth enamel is a well known method of discerning paleoecology, paleoenvironments, and paleoclimates e.g. [9-11]. The

carbon contained in plants consumed by herbivores is recorded in tooth enamel and does not change during the life of the animal once recorded [12]. Oxygen recorded in tooth enamel is from the animal's body water, which is mainly reflective of drinking water composition [13]. These methods have been shown to be useful in reconstructing diets and environments of marsupials from the Pleistocene of Australia in the southern part of the continent [14-16] but these methods have not yet been applied to fossils from this region or age.

This study is therefore the first to use quantitative paleoecological techniques to explore this region of the Australia and reconstruct the environments of the southeastern Queensland in the Pliocene. The Pliocene is a critical period for understanding the origins and evolution of Australia's unique modern biota. It is during this time that the Australian fauna first began to take on its modern appearance and distinctiveness, with many modern Australian groups and genera first appearing in Pliocene fossil deposits [17]. The Pliocene also documents the first paleobotanical evidence of grasslands [18], which in turn led to the diversification of many marsupial groups through increased use of this resource (e.g., vombatiforms (wombats) and macropodoids (kangaroos)). Our analyses will also allow us to develop better insights into the diets and niche partitioning of Pliocene fossil marsupials. In this study we plan to address the following questions:

- Is there evidence of pervasive grasslands in the Chinchilla Sand?
- How does the climate at the site during the Pliocene compare to what occurs in the area today?
- Do we observe dietary niche differentiation between taxa?

Pliocene localities are rare in Australia [19] and it is vital to determine the climate and environment of this time period in order to provide a basis of comparison with the Quaternary, when humans began changing the landscape and ecosystems of the continent in a more direct fashion.

Geology and age of formation

The name Chinchilla Sand was originally proposed by Woods (1960) for the predominantly sandy-clayey sequence of fluvial sediments exposed in the Condamine River and nearby gully systems, spanning a distance of roughly 65 km from Nangram Lagoon, situated about 20km northeast of Condamine, in the west and Warra in the east. The Chinchilla Sand Formation replaced the older Chinchilla Formation [20] and includes the Chinchilla Conglomerate of Ethridge [21]. The sediments are generally weakly consolidated, with clasts ranging in size from clay to pebbles, although the dominant lithology is sandy. Local lithification occurs as a result of calcium carbonate or iron oxide [22], with the most commonly encountered lithified materials being the conglomerate beds [21] and lithified calcareous sandstones. The quartzite material, including silcrete and ferruginous sandstone, are interpreted to be derived from the Mesozoic Orallo Formation and its lateritized profiles [23]. The Chinchilla Sand is thought to reach a maximum thickness of approximately 30m, on the basis of pits and wells sunk near Brigalow [22]. It is overlain unconformably by dark alluvial clays which are Quaternary in age [23].

Vertebrate fossils are found throughout the Chinchilla Sand, although are more commonly derived from the finer, clay-rich beds than the sandy, cross-bedded strata. The fauna from the Chinchilla Sand has been biocorrelated with the Kanunka Local Fauna of

the Tirari Dessert, South Australia [1]. This latter site has been interpreted to be approximately 3.4 Ma on the basis of magnetostratigraphy [1]. The Chinchilla Local Fauna is considered to postdate the Bluff Downs Local Fauna, which has been given a minimum age of 3.6 Ma [24]. Thus, the Chinchilla Local Fauna is conservatively dated as being late Early Pliocene in age. Direct dating of this site and more detailed stratigraphic analyses is currently in preparation.

Spread of grassland in Australia

During much of the first half of the Miocene in Australia, rainforests were widespread throughout Queensland [25], with forested conditions found more generally throughout the continent [18]. It was not until the late Miocene that aridity in the country increased and rainforests in Australia underwent a great reduction [18]. Central Australia became dry with open woodland and chenopod shrub dominated landscape. Although the beginning of the Pliocene began with warm, wet conditions, allowing the expansion of *Nothofagus* and other rainforest flora [18], it soon began to dry again.

The first paleobotanical evidence of grasslands in Australia appeared in the form of desert chenopod shrub phytoliths in northwestern Australia [18]. It has been thought that this represents the first major spread of grasslands, an assumption confirmed by the increase in grazing animals at the same time [26]. Additionally, there is evidence of phytoliths in oceanic cores on the Lord Howe Rise off the eastern coast that show there was a spread of grasslands on the eastern side of the continent at the same time [27]. Marine and pollen records illustrate a trend towards open woodland and grassland environments during the Pliocene, but there was still considerably more rain than today [18]. Wet sclerophyll forests became common near the eastern, southeastern and

northwestern coastal regions [28,29], with drier forests and woodlands present further inland [30]. Although rainforests persisted in eastern Australia during the Pliocene, the rise of herbaceous taxa during this time is correlated with increased seasonality [31]. By examining stable isotope geochemistry we can determine the proportions of grasslands and forests that were present during the Pliocene in southeastern Queensland, and compare these values with modern conditions in both tropical and subtropical zones to determine the most likely conditions present during this time.

Stable isotope ecology of mammals

Carbon isotopes

The carbon ($\delta^{13}\text{C}$) found in the carbonate phase of bioapatite is relative to the $\delta^{13}\text{C}$ of ingested organic material [9]. The different photosynthetic pathways, C3 (Calvin-Benson) and C4 (Hatch-Slack), are characterized by different $\delta^{13}\text{C}$ values and this is in turn reflected in the tooth enamel of mammalian herbivores. The carbon isotope ratios of plants change depending on their photosynthetic pathway and environmental conditions [32]. C3 plants have a $\delta^{13}\text{C}$ ranging from -32‰ in understory canopy conditions to -21‰ in drier environments [33]. Generally, the $\delta^{13}\text{C}$ of C3 plants increases as the climate gets drier. C4 plants, which are mainly grasses, can range from -15 to -9‰. C3 plants dominate cool, moist regimes. In Australia, abundances of C3 plants decline with increasing temperature and/or decreasing spring rains, while C4 grass is most abundant in areas where summer is hot and wet [34].

The isotopic fractionation between food (diet) and tissue (tooth enamel) has been studied in a variety of mammalian test systems. The fractionation constant between bulk diet and $\delta^{13}\text{C}$ of tooth enamel in wild herbivores is between +9 and 12‰ [35-37].

However, in more recent studies of marsupials, a ~12‰ fractionation between diet and enamel $\delta^{13}\text{C}$ was found in kangaroos and wombats [15,38]. This fractionation was used to examine diets of Pleistocene macropods in Forbes et al. (2010) and will be used in this study.

Also important to take into account is the effect of weaning on the $\delta^{13}\text{C}$ composition of tooth enamel. Early formed molars are ^{13}C depleted compared to late formed molars [16,38]. This is due to the shift from milk to grass in the diet of marsupials. It is either because of a change in internal physiological fractionation in the animal, or because the milk has more low $\delta^{13}\text{C}$ fat than plant fodder [38]. These ontogenetic changes must be taken into account when performing a study on fossil marsupials, so in our study we used only the third or fourth molars (the last erupting teeth) in our analysis wherever possible, so the $\delta^{13}\text{C}$ signal we interpreted was most likely from plant diet, not milk diet.

Oxygen isotopes

Oxygen isotopes in water vary due to temperature, evaporation, and source of air masses [39]. Terrestrial vertebrates do not directly ingest precipitation; instead, their water is primarily ingested from streams, ponds, lakes, and leaves. Each of these reservoirs typically have different $\delta^{18}\text{O}$ than precipitation due to preferential incorporation of the ^{18}O isotope into condensate during evaporation. The $\delta^{18}\text{O}$ of organisms with body water composed mainly of drinking water can be used to reconstruct the landscape hydrology in paleoenvironments e.g. [40].

Animals such as modern day kangaroos have low drinking water requirements, so the $\delta^{18}\text{O}$ of their tooth enamel mainly reflects that of leaf water (from food) and therefore,

relative humidity [41]. Plant leaf water is subject to evaporative enrichment of the heavy isotope ^{18}O at low humidity [42], and this $\delta^{18}\text{O}$ signature is passed on to the animals that consume these leaves, so it is possible fossil herbivores can be used as a paleohumidity proxy. Murphy (2007b) examined sources of $\delta^{18}\text{O}$ variation in kangaroo (*Macropus* spp.) tooth enamel. Relative humidity did explain a large proportion of the $\delta^{18}\text{O}$ tooth enamel variance, but they also uncovered a previously unreported correlation between mean annual temperature and relative humidity. Therefore, they recommended not using $\delta^{18}\text{O}$ of fossil teeth in herbivores to reconstruct relative humidity unless there is a reliable estimate of air temperature at the same locality [43]. Additionally, they also found no effect from weaning on the $\delta^{18}\text{O}$ of molars within individuals.

Methods

Collection

Fossils were collected from one of the Chinchilla Sand Formation localities, the Chinchilla Rifle Range, in Chinchilla, Queensland (Figure 4.1) by Ces and Doris Wilkinson over a more than 20 year period, and subsequently donated to the Queensland Museum. Most were recovered as surface finds uncovered by erosion of unconsolidated sediments in the main gully system, however some were excavated from Dig Site. All the fossils examined herein were recovered from the Chinchilla Sand Formation.

Stable isotopes

Bulk samples of enamel were obtained by using a Dremel drill to remove a flake of enamel, which was subsequently ground into fine powder using a ceramic mortar and pestle. For bioapatite samples, over 1000 μg was used to obtain an accurate result. Powdered samples of bioapatite were subsequently treated using 30% H_2O_2 and 0.1 N

acetic acid to remove organic material and surficial carbonates [44]. Analyses were run on a Thermo Electron Corporation Finnegan Delta plus XP mass spectrometer in continuous-flow mode via the Thermo Electron Gas Bench peripheral and a GC-PAL autosampler housed at the University of Rochester. Carbon and oxygen isotopic results are reported in per mil (‰) relative to VPDB (Vienna Pee-Dee Belemnite) with an allowable 2-sigma uncertainty of 0.12‰ and 0.20‰ for carbon and oxygen respectively. Statistical analyses, such as ANOVA and Tukey HSD were all performed on Microsoft Excel 2011 and PAST ver. 2.14.

Isotopic ratios of carbon are expressed using the permil notation, such as: $\delta^{13}\text{C}$ (permil, ‰) = $((R_{\text{sample}}/R_{\text{standard}}-1) \times 1000)$, where R = ratio of $^{13}\text{C}/^{12}\text{C}$ of an unknown sample relative to a known standard V-PDB [45]. Oxygen isotopes are expressed similarly to carbon isotopes: $\delta^{18}\text{O}$ (permil, ‰) = $((R_{\text{sample}}/R_{\text{standard}}-1) \times 1000)$, where R = ratio of $^{18}\text{O}/^{16}\text{O}$ of an unknown sample relative to a known standard, either V-PDB or V-SMOW [45]. In this paper, oxygen isotopes are reported with respect to V-PDB.

Modern stable isotope data in *Macropus* spp. from around Australia was obtained from Murphy et al. (2007). It is vital to note that there is a ~1.2 ‰ depletion in $\delta^{13}\text{C}$ in modern samples compared to pre-industrial $\delta^{13}\text{C}$ CO_2 of atmosphere due to the burning of fossil fuels (known as the Suess Effect) [46,47]. We therefore corrected for this enrichment by applying a correction of -1.2‰ to all Pliocene samples in order to allow for comparisons between carbon isotopes of modern and fossil marsupial tooth enamel [48]. We used specimens of *Macropus* spp. from Murphy et al. (2007a) that came from the following biogeographic regions noted in their supplementary information: CYP



Figure 4.1. Map of Chinchilla Sand locality Chinchilla is marked on this map, along with the shaded areas representing the biogeographic zones where modern kangaroo tooth enamel stable isotope values were taken from to compare to fossil values. Abbreviations for biogeographic zones are in the methods section.

(Cape York Peninsula), ARP (Arnhem Plateau), BBS (Brigalow Belt South), and SEQ (South East Queensland), SEH (South Eastern Highlands) and MGD (Miller Grass Downs). Regions are defined on the basis of Interim Biogeographic Regionalisation for Australia version 7 [49]. Climates of Australia are based on a Koppen classification system from the Australian Bureau of Meteorology [50].

Results

Carbon isotopes

Means and standard deviation of isotopes in each taxon group are presented in table 4.1. The overall range of $\delta^{13}\text{C}$ means over all taxa is -14.5 to -10.3‰, which corresponds to a diet of -26.5 to -22.3‰ when the ~12‰ enrichment is accounted for. The range of modern kangaroo $\delta^{13}\text{C}$ of enamel in the same region, taken from Murphy et al. (2007a), is -14.1 to -2.2‰, corresponding to a diet of -26.1 to -15.7‰. ANOVA shows significant differences in $\delta^{13}\text{C}$ between the 4 fossil taxa analyzed at Chinchilla ($p < 0.001$). For the comparisons between modern and fossil kangaroo (*Macropus* spp.) samples, $\delta^{13}\text{C}$ was different between the 6 tropical, subtropical, temperate, and desert zones and the fossil Chinchilla locality ($p < 0.001$). ANOVA results are summarized in Table 4.2.

The results of Tukey's HSD test from the carbon isotope ANOVAs are in Table 4.3a. *Protemnodon* $\delta^{13}\text{C}$ is significantly different than *Macropus*, but is not differentiated from the $\delta^{13}\text{C}$ of *Troposodon* or *Euryzygoma*. *Macropus* only shows differences from *Protemnodon*; there is no statistical difference between *Macropus* and *Euryzygoma* or *Macropus* and *Troposodon*.

Table 4.1. Stable isotope general statistics. Mean, n, and standard deviation (stdev) for both carbon and oxygen isotope values for all materials sampled. $\delta^{13}\text{C}$ Suess effect is the raw carbon isotope value with 1.2 per mil subtracted to account for the modern depletion in atmospheric $\delta^{13}\text{C}$. Isotope values are presented in per mil (‰)

Taxon	n	$\delta^{13}\text{C}$	$\delta^{13}\text{C}$ Suess effect	stdev	$\delta^{18}\text{O}$	stdev
<i>Euryzygoma</i>	12	-11.1	-12.3	2.8	-0.2	1.4
<i>Macropus</i>	24	-9.1	-10.3	2.3	-1.5	1.9
<i>Protemnodon</i>	8	-13.3	-14.5	2.0	-2.6	2.4
<i>Troposodon</i>	6	-11.6	-12.8	2.5	-1.5	1.0

Table 4.2. Summary of ANOVA results. Summary of the test statistics for each ANOVA, including degrees of freedom (dF), F-statistic, p (probability), and significance.

Variable	dF	F	p	significant
$\delta^{13}\text{C}$ fossils only	3	6.919	0.0006099	yes
$\delta^{13}\text{C}$ modern and Chinchilla <i>Macropus</i>	6	54.5	1.72E-33	yes
$\delta^{18}\text{O}$ fossils only	3	2.788	0.05108	no
$\delta^{18}\text{O}$ modern and Chinchilla <i>Macropus</i>	6	52.12	1.37E-32	yes

Table 4.3a and 4.3b. Summary of results from Tukey's HSD test from the $\delta^{13}\text{C}$ and $\delta^{18}\text{O}$ fossil and modern ANOVAs. Comparisons are pairwise and p values are in bold if significant ($p=0.05$)

4.3a. $\delta^{13}\text{C}$	<i>Macropus</i>	<i>Protemnodon</i>	<i>Troposodon</i>
<i>Euryzygoma</i>	0.2551	0.236	0.9759
<i>Macropus</i>		0.002533	0.1168
<i>Protemnodon</i>			0.4451

4.3b. $\delta^{18}\text{O}$	<i>Macropus</i>	<i>Protemnodon</i>	<i>Troposodon</i>
<i>Euryzygoma</i>	0.4172	0.03481	0.4397
<i>Macropus</i>		0.5884	1
<i>Protemnodon</i>			0.5641

Table 4.4a and 4.4b. Summary of results from Tukey's HSD test from the $\delta^{13}\text{C}$ and $\delta^{18}\text{O}$ ANOVAs of modern *Macropus* and fossil *Macropus* from Chinchilla.

Comparisons are pairwise and p values are bolded if significant ($p < 0.05$). Regional abbreviations: CYP (Cape York Peninsula), ARP (Arnhem Plateau), BBS (Brigalow Belt South), and SEQ (South East Queensland), SEH (South Eastern Highlands) and MGD (Miller Grass Downs).

4.4a. $\delta^{13}\text{C}$	BBS	CYP	ARP	MGD	SEH	Chinchilla
SEQ	0.5603	3.89E-05	9.06E-05	0.202	2.57E-05	2.57E-05
BBS		0.02532	0.06355	0.9965	2.57E-05	2.60E-05
CYP			0.9999	0.1371	2.57E-05	0.1927
ARP				0.2668	2.57E-05	0.09244
MGD					2.57E-05	3.74E-05
SEH						0.0004263

4.4b. $\delta^{18}\text{O}$	BBS	CYP	ARP	MGD	SEH	Chinchilla
SEQ	0.0008475	0.9964	0.06652	2.57E-05	0.001761	0.1508
BBS		7.36E-05	2.57E-05	0.4295	2.57E-05	2.57E-05
CYP			0.277	2.57E-05	0.01669	0.4729
ARP				2.57E-05	0.9375	0.9999
MGD					2.57E-05	2.57E-05
SEH						0.8069

When fossil Chinchilla *Macropus* are compared to modern *Macropus* from 6 different biogeographic regions of Australia using ANOVA, $\delta^{13}\text{C}$ is significantly different (Table 4.2). The *Macropus* from the modern region that contains the Chinchilla locality and the surrounding area, Brigalow Belt South (BBS) and South East Queensland (SEQ), have $\delta^{13}\text{C}$ values significantly higher than fossil *Macropus* when examined with Tukey's HSD test (Table 4.4a). *Macropus* from Miller Grass Downs (MGD) are similar to *Macropus* from all regions, including Chinchilla. Alternatively, there was no significant difference between fossil *Macropus* $\delta^{13}\text{C}$ from Chinchilla and modern *Macropus* from tropical regions Cape York Peninsula (CYP) and Arnhem Plateau (ARP).

Oxygen isotopes

Means and standard deviations of $\delta^{18}\text{O}$ from sample fossil taxa are in Table 4.1. The values of fossil taxa sampled range from -2.6 to -0.2‰. Regional modern *Macropus* have an enamel $\delta^{18}\text{O}$ range from -2.8 to 4.2‰. There is not a wide variation in the $\delta^{18}\text{O}$ between taxa; ANOVA of $\delta^{18}\text{O}$ values shows no significant differences between the four fossil genera ($p=0.051$). The ANOVA between $\delta^{18}\text{O}$ of modern *Macropus* from the six biogeographic zones compared with $\delta^{18}\text{O}$ from fossil Chinchilla *Macropus* show a significant difference. ANOVA results are summarized in Table 4.2.

The results of Tukey's HSD test from the oxygen ANOVAs are contained in table 4.3b. There is a significant difference in the pairwise comparisons between *Protemnodon* and *Euryzygoma*. When Chinchilla fossil *Macropus* $\delta^{18}\text{O}$ are compared to $\delta^{18}\text{O}$ of *Macropus* from subtropical (BBS, SEQ), tropical (ARP, CYP), temperate (SEH), and grassland (MGD) regions, Chinchilla fossil *Macropus* is only different from values from BBS and MGD; BBS is the region that contains modern-day Chinchilla (Table 4.4b).

Figure 4.2. Bivariate plot of carbon and oxygen for fossil and modern teeth. A. $\delta^{18}\text{O}$ vs. $\delta^{13}\text{C}$ values for *Macropus* spp. from six modern localities, grouped by their climatic region. Labels on axes indicate the boundary between a C3 dominated and a C3/C4 mixed environment. B. $\delta^{18}\text{O}$ vs. $\delta^{13}\text{C}$ values for *Troposodon*, *Protemnodon*, *Euryzygoma*, and *Macropus* from Chinchilla Sand. Each taxon is marked by a symbol as seen in the legend.

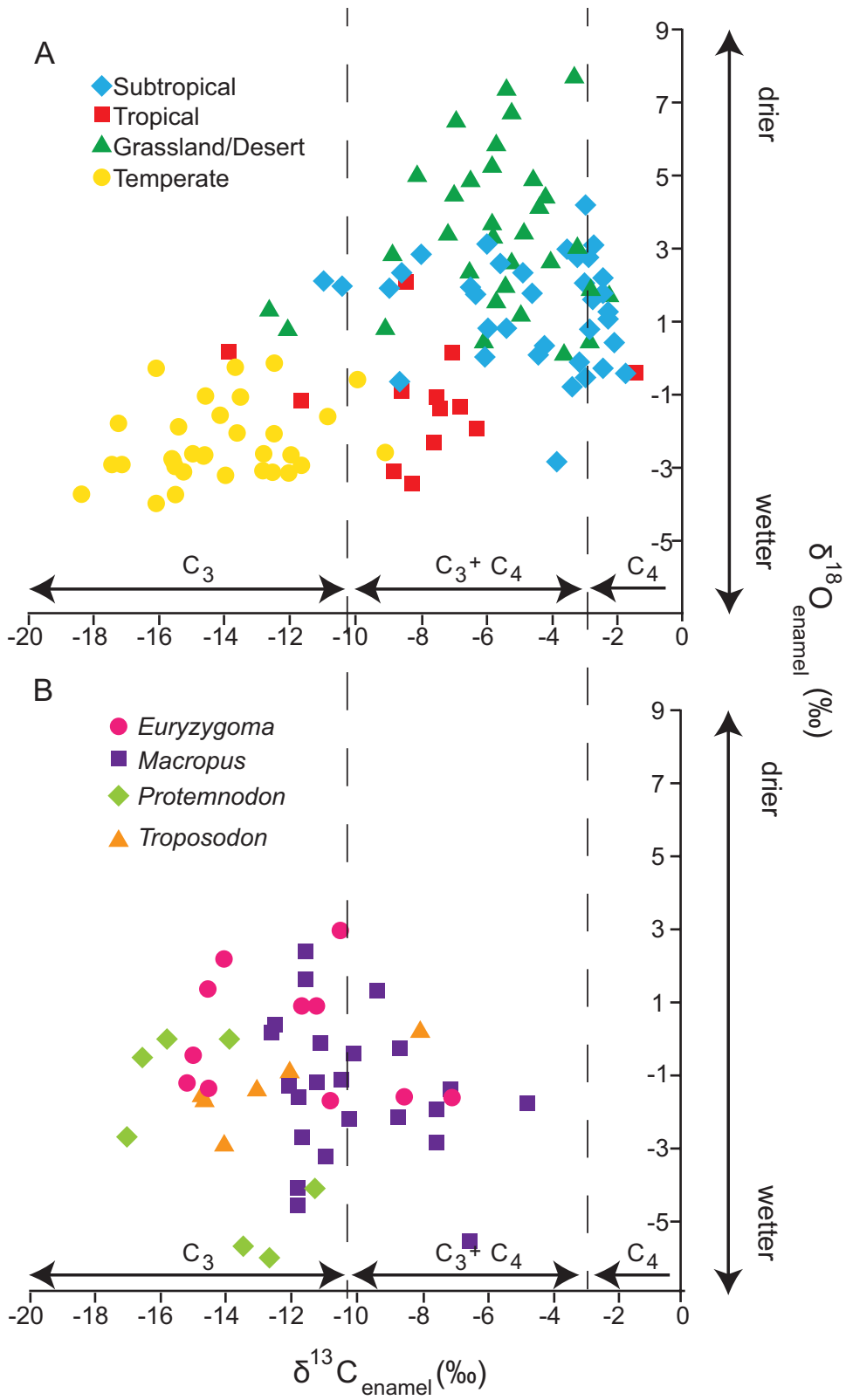


Table 4.5. $\delta^{13}\text{C}$ diet and %C3 diet of fossil and modern marsupials. $\delta^{13}\text{C}$ diet is obtained by taking the average $\delta^{13}\text{C}$ of enamel and subtracting the diet-enamel enrichment factor of 12‰ (Fraser et al. 2008). %C3 diet is calculated using equation 1 in Johnson et al. (1997) with 26.5‰ and 12.5‰ used as the average for C3 and C4 plants in the landscape.

Taxon	Locality	$\delta^{13}\text{C}$ diet	% C3 diet
<i>Euryzygoma</i>	Chinchilla	-24.3	84.3
<i>Macropus</i> spp. Fossil	Chinchilla	-22.3	70.0
<i>Protemnodon</i>	Chinchilla	-26.5	100.0
<i>Troposodon</i>	Chinchilla	-24.8	87.9
<i>Macropus</i> spp. Modern	SEQ	-15.7	22.8
<i>Macropus</i> spp. Modern	BBS	-17.3	34.2
<i>Macropus</i> spp. Modern	CYP	-20.1	54.4
<i>Macropus</i> spp. Modern	ARP	-19.8	52.4
<i>Macropus</i> spp. Modern	MGD	-17.8	38.1
<i>Macropus</i> spp. Modern	SHE	-26.1	96.9

Discussion

Dietary niches

Between the four taxon groups sampled here, we observe clear indications of unique dietary niche separation (Figure 4.2). *Euryzygoma*, *Macropus*, and *Troposodon* ate a mixed C3 and C4 diet, with average $\delta^{13}\text{C}_{\text{diet}} = -24.3\text{‰}$, -22.3‰ and -24.8‰ respectively (Table 4.5). These three taxa were eating a mixed diet, but the majority of it was comprised of C3 plants; the percentage of C3 plants in the diet was calculated using equation (1) in Johnson et al. (1997) [51]. *Euryzygoma* has a $\delta^{13}\text{C}_{\text{diet}}$ that indicates it primarily fed on C3 plants, which is in concordance with a previous estimate of diet from another diprotodontid, *Diprotodon* [52]. *Protemnodon*, thought to be a forest-dwelling marsupial based on morphological evidence [8], is unmistakably occupying a different niche than the other three taxa based on the fact it has the most negative mean $\delta^{13}\text{C}$ out of all four taxa sampled (-14.5‰). This indicates that *Protemnodon* could have subsisted primarily on C3 browse, such as would be found in a sclerophyll forest. Overall, there is evidence of a C4 grass signature in the diets of these animals, but C3 plants were the majority of the diet.

Due to the $\delta^{18}\text{O}$ of the fossil Chinchilla taxa not being enriched, the environment was most likely moist and mesic. This not only indicates an environment with moderate to high rainfall, but when combined with the carbon isotope data indicates the C3 plants present were more likely in forests rather than grasslands, as grasses are prevalent in drier environments. Other evidence, such as the presence of fossils like *Bohra* (tree kangaroo) and the dental morphology of taxa sampled like *Protemnodon* indicates the C3 plants consumed in this environment were most likely trees in an open forest. It appears that

although C4 grasslands had spread to this region, they were not the primarily dietary intake for any of these four taxa. Oxygen isotopes show no statistical differences, and we hypothesize that this is a result of drinking water from frequently replenished water sources that were connected without much evaporation.

Paleoenvironment of the Chinchilla Sand locality

To better understand the paleoenvironment of the Chinchilla Sand, it is useful to compare to modern day signatures found in *Macropus* to better understand how $\delta^{13}\text{C}$ and $\delta^{18}\text{O}$ naturally vary in a known landscape. The diet of *Macropus* in the modern region of Queensland around Chinchilla is statistically different than all of the $\delta^{13}\text{C}$ signatures in the tooth enamel of the Pliocene marsupials. It is apparent that the diets of kangaroos in this region today are dominated by C4 grasses with highly positive $\delta^{13}\text{C}$ values (Table 4.6). This suggests that the proportion of C4 grasses in the landscape today is far greater in this region than they were in the Pliocene.

When examining $\delta^{18}\text{O}$ in addition to $\delta^{13}\text{C}$, there is a significant difference between the oxygen isotopes of fossil Chinchilla marsupials and modern day *Macropus* from the BBS region. It appears that out of the two biogeographic zones in this area of Queensland, Pliocene fossil Chinchilla taxa are more similar to that of the modern SEQ zone than the BBS zone. When comparing the $\delta^{13}\text{C}$ of *Macropus* found in tropical biogeographic zones ARP and CYP, the Chinchilla fossil *Macropus* spp. are indistinguishable. The same pattern holds with the $\delta^{18}\text{O}$; at Chinchilla the $\delta^{18}\text{O}$ of *Macropus* tooth enamel is most similar to that in the tropical regions, SEQ and the temperate SEH. The fact that fossil Chinchilla *Macropus* are so similar to *Macropus* from

Table 4.6. Summary of general statistics for modern *Macropus* spp. values in different biogeographic and climatic regions from Murphy et al. (2007). Isotope values are presented in per mil (‰). See methods for acronyms of region names. Header labels are taxon, n (sample size), biogeographic region (region), climate, carbon isotope value ($\delta^{13}\text{C}$), oxygen isotope value ($\delta^{18}\text{O}$), and standard deviation (stdev).

Taxon	n	Region	Climate	$\delta^{13}\text{C}$	stdev	$\delta^{18}\text{O}$	stdev
<i>Macropus</i> spp.	14	SEQ	Subtropical	-2.2	1.9	-0.1	1
<i>Macropus</i> spp.	24	BBS	Subtropical	-3.8	2.6	2.3	0.8
<i>Macropus</i> spp.	9	CYP	Tropical	-8.1	3.1	-0.4	1.1
<i>Macropus</i> spp.	6	ARP	Tropical	-7.8	0.9	-1.7	1.6
<i>Macropus</i> spp.	32	MGD	Grassland/Dese rt	-5.8	2.4	3.4	2.1
<i>Macropus</i> spp.	31	SHE	Temperate	-14.1	2.2	-2.3	1.1

SEH in $\delta^{18}\text{O}$ could indicate a similar hydrologic regime, and therefore a similar plant structure of C3 forests. It can be useful to compare areas of modern average rainfall and compare them to fossil values to get an indication of what paleorainfall could have been [14]. Average rainfall in Chinchilla (BBS) region today is 600-800mm, while SEQ has a range from 600 up to 1200mm in small patches near the coast. The Miller Grass Downs (MGD) has 200-500mm of rainfall per year. In contrast, the CYP and ARP regions receive 1000-2000mm of rain per year. SEH in southeastern Australia can have mean annual precipitation ranging from 500 up to 1600mm per year. It is clear that *Macropus* from Chinchilla group with those from CYP and ARP, tropical regions of Australia, in both carbon and oxygen values. This suggests that rainfall in this locality during the Pliocene was much higher than it is today, and that it was possibly closer to a tropical level of rainfall (over 1000mm). It also suggests the environment at the locality was forested due to its dissimilarity from grassland environments sampled (MGD).

It is difficult to determine the precise mean annual rainfall during the Pliocene based on these results because there is a possibility that the $\delta^{18}\text{O}$ of precipitation was significantly different than it is today. But, with the combined evidence we have, it appears that Chinchilla in the Pliocene represented a mosaic environment that included forest and mixed C3/C4 grassland. There is no specific isotopic evidence of a closed canopy, but the dietary signature of the browser *Protemnodon* and the presence of taxa such as tree kangaroo *Bohra* [7] and forest wallaby *Silvaroo* [8] indicates that this could have been present. The presence of many aquatic taxa, such as ducks, pelicans, turtles, lungfish and crocodiles, indicates the presence of extensive long-term water bodies in the region, while the thick fluvial deposits indicate extensive river systems. Also, our

results do not preclude the reconstruction of the Chinchilla paleoenvironment as riparian forests surrounded by tropical grasslands. Our results suggests that tropical conditions, that today are restricted only to northern Queensland and the Northern Territory, could have extended significantly southwards through Queensland during the Pliocene, but further isotopic sampling on a greater range of taxa is needed. Although C4 grasslands were spreading across Australia at this time, our results suggest they were not the primary habitat type present in this locality.

Conclusion

Despite the fact the Pliocene marks the spread of grasses around Australia [18], the locality of Chinchilla Sand was not dominated by C4 grasslands. Instead, the environment was more mixed, with a clear indication of abundant C3 plants, potentially a wet tropical sclerophyll forest. The Pliocene *Macropus* spp. at Chinchilla were consuming both C3 and C4 plants. The proportion of C4 grasses in their diets can be confirmed in the future through dental microwear analyses. Both *Euryzygoma* and *Troposodon* were mixed feeders with a tendency towards C3 plants, while the purported forest wallaby *Protemnodon* subsisted almost entirely on C3 plants, indicating the probable presence of trees. These inferences are confirmed by our comparison of fossil isotopic values with those of modern *Macropus* spp. from different regions of Australia. Therefore, we reconstruct the Chinchilla Sand locality as significantly wetter and more vegetated during the Pliocene than today, potentially representing an environment with some forests and tropical grasslands and wetlands. Further exploration at this site and neighboring Pleistocene localities will give us a better indication of paleoecology and shifts in paleoenvironments in relation to climate change in the region.

References

- 1 Tedford RH, Wells RT, Barghoorn SF (1992) Tirari Formation and contained faunas, Pliocene of the Lake Eyre Basin, South Australia. *Beagle: Records of the Museums and Art Galleries of the Northern Territory*, The 9: 173.
- 2 Gaffney ES (1981) A review of the fossil turtles of Australia. *American Museum Novitates* : 1-38.
- 3 Gaffney ES, Bartholomai A (1979) Fossil trionychids of Australia. *Journal of Paleontology* : 1354-1360.
- 4 Olson SL (1975) The fossil rails of CW De Vis, being mainly an extinct form of *Tribonyx mortierii* from Queensland. *Emu* 75: 49-54.
- 5 Olson SL (1977) The identity of the fossil ducks described from Australia by CW De Vis. *Emu* 77: 127-131.
- 6 Wroe S, Mackness BS (2000) A new genus and species of dasyurid from the Pliocene Chinchilla Local Fauna of south-eastern Queensland. *Alcheringa* 24: 319-326.
- 7 Dawson L (2004) A new Pliocene tree kangaroo species (Marsupialia, Macropodinae) from the Chinchilla Local Fauna, southeastern Queensland. *Alcheringa* 28: 267-273.
- 8 Dawson L (2004) A new fossil genus of forest wallaby (Marsupialia, Macropodinae) and a review of *Protemnodon* from eastern Australia and New Guinea. *Alcheringa* 28: 275-290.
- 9 Koch PL, Hoppe KA, Webb SD (1998) The isotopic ecology of late Pleistocene mammals in North America.: Part 1. Florida. *Chemical Geology* 152: 119-138.
- 10 Kohn MJ (1999) You are what you eat. *Science* 283: 335.
- 11 Cerling TE, Harris JM, Leakey MG (1999) Browsing and grazing in elephants: the isotope record of modern and fossil proboscideans. *Oecologia* 120: 364-374.
- 12 Hillson S (1996) *Dental anthropology*. Cambridge University Press Cambridge.
- 13 Longinelli A (1984) Oxygen isotopes in mammal bone phosphate: a new tool for paleohydrological and paleoclimatological research? *Geochimica et Cosmochimica Acta* 48: 385-390.
- 14 Prideaux GJ, Long JA, Ayliffe LK, Hellstrom JC, Pillans B, et al (2007) An arid-adapted middle Pleistocene vertebrate fauna from south-central Australia. *Nature* 445: 422-425.

- 15 Fraser RA, Grün R, Privat K, Gagan MK (2008) Stable-isotope microprofiling of wombat tooth enamel records seasonal changes in vegetation and environmental conditions in eastern Australia. *Palaeogeography, Palaeoclimatology, Palaeoecology* 269: 66-77.
- 16 Forbes MS, Kohn MJ, Bestland EA, Wells RT (2010) Late Pleistocene environmental change interpreted from $\delta^{13}\text{C}$ and $\delta^{18}\text{O}$ of tooth enamel from the Black Creek Swamp Megafauna site, Kangaroo Island, South Australia. *Palaeogeography, Palaeoclimatology, Palaeoecology* 291: 319-327.
- 17 Black KH, Archer M, Hand SJ, Godthelp H (2012) The Rise of Australian Marsupials: A Synopsis of Biostratigraphic, Phylogenetic, Palaeoecologic and Palaeobiogeographic Understanding. *Earth and Life* : 983-1078.
- 18 Martin HA (2006) Cenozoic climatic change and the development of the arid vegetation in Australia. *Journal of Arid Environments* 66: 533-563.
- 19 Tedford RH, Wells RT, Prideaux GJ (2006) Pliocene and earlier Pleistocene marsupial evolution in southeastern Australia. *Alcheringa: An Australasian Journal of Palaeontology* 30: 313-322.
- 20 Woods JT (1956) The skull of *Thylacoleo carnifex*. *Memoirs of the Queensland Museum* 13: 125-140.
- 21 Jack RL, Etheridge R (1892) The geology and paleontology of Queensland and New Guinea: with sixty-eight plates and a geological map of Queensland. JC Beal, Government Printer.
- 22 Woods JT (1960) Fossiliferous fluvial and cave deposits. *Journal of the Geological Society of Australia* 7: 393-403.
- 23 Bartholomai A, Woods JT (1976) Notes on the vertebrate fauna of the Chinchilla Sand. Bureau of Mineral Resources, Geology and Geophysics, Bulletin 166: 151-152.
- 24 Mackness BS, Whitehead PW, McNamara GC (2000) New potassium--argon basalt date in relation to the Pliocene Bluff Downs Local Fauna, northern Australia. *Australian Journal of Earth Sciences* 47: 807-811.
- 25 Travouillon KJ, Legendre S, Archer M, Hand SJ (2009) Palaeoecological analyses of Riversleigh's Oligo-Miocene sites: implications for Oligo-Miocene climate change in Australia. *Palaeogeography, Palaeoclimatology, Palaeoecology* 276: 24-37.

- 26 Archer M, Hand SJ, Godthelp H (1994) Patterns in the history of Australia's mammals and inferences about palaeohabitats. *History of the Australian vegetation: Cretaceous to Recent* (ed. Hill RS) : 80-196.
- 27 Locker S, Martini E (1986) Phytoliths from the southwest Pacific Site 591. *Initial Reports of the Deep Sea Drilling Program 90*: 1079-1084.
- 28 Hill RS (1992) Australian vegetation during the Tertiary: macrofossil evidence. *Beagle: Records of the Museums and Art Galleries of the Northern Territory*, The 9: 1.
- 29 Hill RS (1994) *History of the Australian vegetation: Cretaceous to Recent*. Cambridge Univ Pr.
- 30 McGowran B, Archer M, Bock P, Darragh TA, Godthelp H, et al (2000) Australasian palaeobiogeography: the Palaeogene and Neogene record.
- 31 Greenwood DR, Christophel DC, Bermingham E, Dick CW, Moritz C (2005) The origins and tertiary history of Australian "tropical" rainforests. *Tropical rainforests: past, present and future* : 336-373.
- 32 O'Leary MH (1988) Carbon isotopes in photosynthesis. *Bioscience* 38: 328-336.
- 33 Tieszen LL (1991) Natural variations in the carbon isotope values of plants: implications for archaeology, ecology, and paleoecology. *J Archaeol Sci* 18: 227-248.
- 34 Hattersley PW (1983) The Distribution of C₃ and C₄ Grasses in Australia in Relation to Climate. *Oecologia* 57: 113-128.
- 35 DeNiro MJ, Epstein S (1978) Influence of diet on the distribution of carbon isotopes in animals. *Geochimica et Cosmochimica Acta* 42: 495-506.
- 36 Lee-Thorp JA, Van Der Merwe NJ, Brain CK (1989) Isotopic evidence for dietary differences between two extinct baboon species from Swartkrans. *Journal of Human Evolution* 18: 183-189.
- 37 Bocherens H, Koch PL, Mariotti A, Geraads D, Jaeger JJ (1996) Isotopic biogeochemistry (13 C, 18 O) of mammalian enamel from African Pleistocene hominid sites. *Palaios* : 306-318.
- 38 Murphy BP, Bowman DM, Gagan MK (2007) Sources of carbon isotope variation in kangaroo bone collagen and tooth enamel. *Geochimica et Cosmochimica Acta* 71: 3847-3858.

- 39 Dansgaard W (1964) Stable isotopes in precipitation. *Tellus* 16: 436-468.
- 40 Sponheimer M, Lee-Thorp JA (1999) Oxygen isotopes in enamel carbonate and their ecological significance. *J Archaeol Sci* 26: 723-728.
- 41 Ayliffe LK, Chivas AR (1990) Oxygen isotope composition of the bone phosphate of Australian kangaroos: potential as a palaeoenvironmental recorder. *Geochimica et Cosmochimica Acta* 54: 2603-2609.
- 42 Epstein S, Thompson P, Yapp CJ (1977) Oxygen and hydrogen isotopic ratios in plant cellulose. *Science* 198: 1209.
- 43 Murphy BP, Bowman DM, Gagan MK (2007) The interactive effect of temperature and humidity on the oxygen isotope composition of kangaroos. *Functional Ecology* 21: 757-766.
- 44 MacFadden BJ, Higgins P (2004) Ancient ecology of 15-million-year-old browsing mammals within C3 plant communities from Panama. *Oecologia* 140: 169-182.
- 45 Coplen TB (1994) Reporting of stable hydrogen, carbon, and oxygen isotopic abundances. *Pure and Applied Chemistry* 66: 273-273.
- 46 Friedli H, Löttscher H, Oeschger H, Siegenthaler U, Stauffer B (1986) Ice core record of the $^{13}\text{C}/^{12}\text{C}$ ratio of atmospheric CO_2 in the past two centuries. *Nature* 324: 237-238.
- 47 Leuenberger M, Siegenthaler U, Langway C (1992) Carbon isotope composition of atmospheric CO_2 during the last ice age from an Antarctic ice core. Carbon isotope composition of atmospheric CO_2 during the last ice age from an Antarctic ice core .
- 48 Yeakel JD, Bennett NC, Koch PL, Dominy NJ (2007) The isotopic ecology of African mole rats informs hypotheses on the evolution of human diet. *Proc Biol Sci* 274: 1723-1730.
- 49 Interim Biogeographic Regionalisation for Australia. National Reserve System Section, Australian Government Department of Sustainability, Environment, Water, Population and Communities, Canberra, May 2012.
<http://www.environment.gov.au/parks/nrs/science/pubs/bioregions.pdf>
- 50 Australian Climate Zones. Commonwealth of Australia. 2005.
http://reg.bom.gov.au/climate/environ/other/kpn_group.shtml

- 51 Johnson BJ, Miller GH, Fogel ML, Beaumont PB (1997) The determination of late Quaternary paleoenvironments at Equus Cave, South Africa, using stable isotopes and amino acid racemization in ostrich eggshell. *Palaeogeography, Palaeoclimatology, Palaeoecology* 136: 121-137.
- 52 Gröcke DR (1997) Distribution of C3 and C4 plants in the Late Pleistocene of South Australia recorded by isotope biogeochemistry of collagen in megafauna. *Australian Journal of Botany* 45: 607-617.

CHAPTER V

CRACKING THE EGG: THE USE OF MODERN AND FOSSIL EGGS FOR ENVIRONMENTAL AND ECOLOGICAL INTERPRETATION

Abstract

A myriad of extant and extinct vertebrates produce eggs. These eggs are a useful tool for reconstructing environments and ecologies over a range of time scales. In this review, methods for analyzing and understanding stable isotope ecology of egg products are presented. It is shown that this area of stable isotope ecology deserves further research and can potentially be a powerful way to interpret environments in deep time.

Introduction

It has become commonplace to use tooth enamel and bone with stable isotope analysis to answer paleoenvironmental questions, but eggs provide another biogenically created material that can be used to elucidate specific information about modern and fossil ecosystems. In the past decade, using stable isotope analysis on eggshells and other egg products to reconstruct environments and ecology has proven to be a useful tool for both modern and fossil ecological analyses. It is well-established that stable isotopes of carbon ($\delta^{13}\text{C}$), nitrogen ($\delta^{15}\text{N}$), and oxygen ($\delta^{18}\text{O}$) of biogenic materials such as teeth, bone, collagen, feathers, hair, and eggshells can yield information about ecology, diets, migration patterns, and behavior of animals (see Hobson 1999; Koch 2007). Here, the use of eggshell and other egg products in stable isotope research will be examined in detail in order to provide a holistic overview of established research in this field, and will allow the identification of potential areas for future research.

Eggshells are frequently found as remains in archaeological and paleontological sites, and exist in well-cataloged historical museum collections. These well-preserved records allow us to trace changes in environment and ecology over time (Green and Scharlemann 2003). Eggshells are a suitable substrate for testing because they are often fragmented and sampling does not require destruction of a large amount of material, which causes only small amounts of damage to collections. Often times it is possible to identify eggshells to a species level when found in an archaeological site, and even sometimes in paleontological sites, making any isotopic inferences even more powerful. This is even true with dinosaurs, as there are instances where eggs and adult dinosaur remains can be identified and associated (Norell et al. 1995) (Figure 5.1). Ostrich eggshell is frequently found at archaeological sites as beads, decorations, or water carriers in northern China, Mongolia (Janz, Elston and Burr 2009), southern Africa (Orton 2008), northern Africa (Friedman et al. 1999) and India (Badam 2005), which provides a dateable substrate for isotopic analysis. These can provide direct evidence of what environments were like at the time of human inhabitation in localities where we would not normally be able to glean this information. Eggshells have both an organic and inorganic fraction that can be preserved in the environment for 1000s (organic) to millions (inorganic) of years. Additionally, eggshells from archaeological localities that preserve the organic portion can be dated using C-14, allowing for strong environmental change over time interpretations.



Figure 5.1. Dinosaur eggs as they are found in the field. IGM 100/1125. These paired macroelongatoolithid type eggs are from the Gobi Desert of Mongolia. They were laid by an oviraptorid dinosaur. Photo: Mick Ellison, AMNH.

Stable isotope ecology

Pioneering work in the late 1970s through the 1980s established a firm foundation for understanding how the stable isotopes of nitrogen and carbon contained in animal diets were reflected in the tissues of an individual (DeNiro and Epstein 1978; Schoeninger and DeNiro 1984). Around the same time, work to determine the sources and controls of oxygen isotopes in animal tissues was completed (Luz and Kolodny 1985). These papers laid the groundwork for our understanding of how stable isotopes interact with live organisms both in modern ecology and paleoecology. Carbon and nitrogen isotopes reflect the diet of the animals while oxygen isotopes in animal tissues have been shown to be primarily sourced from ingested environmental water. Only a short review on stable isotopes in biology and ecology will be provided here, for a more detailed review see Koch (1998, 2007).

The carbon isotopic ratio ($\delta^{13}\text{C}$) found in the inorganic and organic portions of the egg is relative to the $\delta^{13}\text{C}$ of ingested organic material (Koch, Hoppe and Webb 1998). In herbivores, this is ingested plant material, but in omnivores and carnivores their $\delta^{13}\text{C}$ value also carries the $\delta^{13}\text{C}$ signal of their prey, and in turn the primary producers at the bottom of the food web. The different photosynthetic pathways, C3 (Calvin-Benson) and C4 (Hatch-Slack), are characterized by different $\delta^{13}\text{C}$ values. This is reflected in the $\delta^{13}\text{C}$ value of the egg materials. C3 plants have a $\delta^{13}\text{C}$ ranging from -32‰ in understory canopy conditions to -21‰ in drier environments (Tieszen 1991). Generally, the $\delta^{13}\text{C}$ of C3 plants increases as the climate gets drier. C4 plants, which are mainly grasses, can range from -21 to -9‰. C3 plants dominate in cool, moist regimes. In omnivorous animals, the $\delta^{13}\text{C}$ values of their tissues will reflect the $\delta^{13}\text{C}$ values of their prey.

Variations in the $\delta^{13}\text{C}$ of primary producers (phytoplankton) in the marine realm from offshore to near shore also provide a way to determine the habitat and land use of a species that could travel between environments. In both cases of herbivores and omnivores, stable isotope mixing models can be used to determine the relative contribution of different plants or prey sources to diet.

Nitrogen isotopes ($\delta^{15}\text{N}$) can be measured in organic fractions of animal remains, and for analyses can be measured in egg yolk, albumen, membrane and organic shell matrix. The nitrogen in animal protein is almost entirely composed from nitrogen in the diet of the organism. It appears nitrogen fractionation in both biogenic materials such as bone collagen and hair is similar to that in organic portions of eggs. The enrichment of $\delta^{15}\text{N}$ between diet and organic tissue in vertebrates is generally thought to be between 3-5‰ (Schoeninger and DeNiro 1984). The basis of the nitrogen cycle for consumption by egg-laying vertebrates is in plants; plants take up nitrogen from the soil, and this $\delta^{15}\text{N}$ signature will vary geographically. There is a marked negative correlation between rainfall abundance and plant $\delta^{15}\text{N}$ (Heaton 1987), which can be useful for reconstructing environments using eggshell samples. Trophic level can also be traced using $\delta^{15}\text{N}$. Each consumer's $\delta^{15}\text{N}$ will become enriched relative to the food they consume, which will continue up the food web with an enrichment between 3 – 4‰ at each trophic level (Post 2002).

Oxygen isotopes in water vary due to temperature, evaporation, and source of air masses (Dansgaard 1964). Terrestrial vertebrates do not directly ingest precipitation; instead, their water is primarily ingested from streams, ponds, lakes, and leaves. These reservoirs typically have different $\delta^{18}\text{O}$ than precipitation due to preferential

incorporation of the ^{18}O isotope into condensate during evaporation. The $\delta^{18}\text{O}$ of organisms with body water composed mainly of drinking water can be used to reconstruct the landscape hydrology in paleoenvironments. Organisms that obtain most of their body water from evaporatively enriched leaf water will have high $\delta^{18}\text{O}$ values that differ more than expected from just meteoric water values. Oxygen isotopes can be a useful tool in determining habitat, terrestrial land use, diet, and physiology in little known extant and extinct species (Koch 2007).

Eggshell structure

In both reptiles and avian eggs, the structures of the egg are essentially similar. A basic egg consists of a yolk, surrounded by albumen, which is contained in a shell membrane all held in by a crystalline shell on the outside (Figure 5.2). Bird eggshells are composed of columnar calcite crystals with an organic matrix of collagen fibers throughout. The inner surface of the calcite shell has radiating cones (mammillae) that are anchored at their tip to an organic membrane that encases the yolk and albumen. Eggshell pores are present along calcite crystal boundaries that provide a mechanism for gas exchange while the eggs are incubating. There is a transparent cuticle on the outside of the shell that protects matter from entering the pores. In general, a bird egg is approximately 95% inorganic matter, 3.5% organic matter and 1.5% water (Von Schirnding, Van Der Merwe and Vogel 1982).

Hirsch (1983) describes in detail the structure of chelonian eggshell in comparison to avian, dinosaurian, and other reptilian eggshell. Chelonian eggshells are the only eggshells composed of aragonite as opposed to calcite (Hirsch 1983). Hirsch

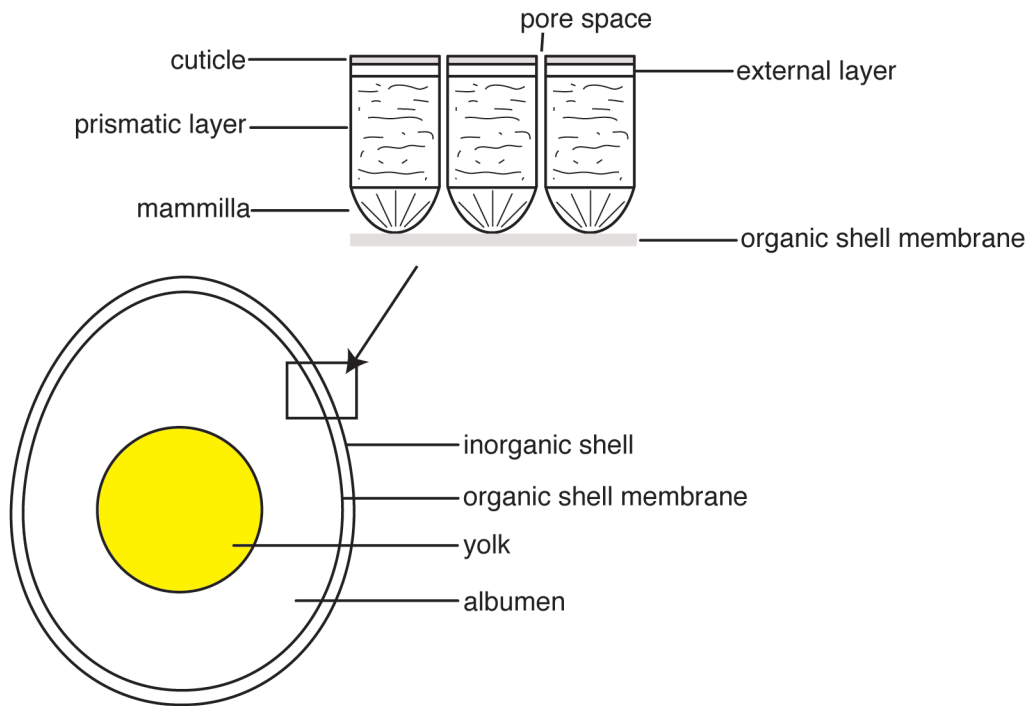


Figure 5.2. Schematic of egg and eggshell based on avian model. A diagram of the general structure of an avian egg. The microstructure of the eggshell depicted is based on ostrich eggshell but is similar to any vertebrate with the rigid-shelled egg type. Based on a similar drawing of eggshell microstructure seen in Mikhailov (1991).

(1983) also noted that there are three ‘types’ of eggshells, soft-, pliable-, and rigid-shelled, and that chelonians have both pliable and rigid-shelled eggs. Soft-shelled eggs seen in snakes, lizards, and the tuatara have a ‘shell’ made primarily of organic membrane, with no organized calcareous layer. There are only unorganized, small floating crystals or a calcareous ‘crust’ on the outside of the egg. This egg type is very unlikely to fossilize, although there is one instance of an exceptionally preserved egg of this type from a Cretaceous choristoderan reptile (Hou et al. 2010).

Pliable-shelled eggs are seen in sea turtles and other types of turtles. While their shells are still pliable, they have a thicker, more organized calcareous shell than seen in soft-shelled eggs (Hirsch 1983). Compared to other sorts of turtles with this eggshell type, sea turtles have the thinnest calcareous layer, and their chances of fossilization are poor. Rigid-shelled eggs are most commonly preserved in the fossil record due to their thick calcareous layers composed of interlocking crystals that will not easily dissociate. Some turtles, such as tortoises, some gekkos, all crocodiles, birds, and dinosaurs have this type of eggshell. When compared to soft-shelled eggs, they have a far smaller organic component, reduced only to a thin membrane inside the shell and a delicate network of collagen fibers in the calcareous layers. Currently, we have a poor knowledge of the detailed structure of squamate, sphenodontian, and monotreme eggs. For a detailed look at eggshell parataxonomy, see Hirsch (1996) and Mikhailov (1997).

Captive and laboratory tests

The first published experiment on stable isotopic fractionation in eggshells was in Folinsbee et al. (1970). They completed controlled diet and water experiments with chickens to investigate the timing of diet turnover in both organic and inorganic portions

of the eggshell. They found a linear relationship between $\delta^{18}\text{O}$ in water and inorganic eggshell carbonate, and saw this as a useful proxy for reconstructing paleoenvironments. Consequently, they also tested fossil dinosaur and bird eggshells. Later, Johnson (1998) would find that the linear relationship between $\delta^{18}\text{O}$ of eggshell carbonate and water source did not hold true in wild ostriches, indicating that this relationship might not be a reasonable assumption to make in open ecosystems where body water is obtained from other sources such as plants.

The first paper explicitly exploring the sources and variation of carbon isotopes in eggshells was von Schirnding et al. (1982). They examined captive ostriches in South Africa to understand relationships between diet and $\delta^{13}\text{C}$ of the inorganic and organic portion of the eggshell. In addition, they recognized that ostrich and other bird eggshells are frequently found at archaeological sites, so it would be useful to ascertain how long the organic portion of the eggshell was viable for isotopic testing. At the end of their captive experiment it was shown that ostriches in different environments with different food sources had a remarkably consistent $\delta^{13}\text{C}$ diet to tissue fractionation of 2.1‰ (organic portion) and 16.2‰ (inorganic portion) and this meant eggs could be a very useful substrate for stable isotope analysis.

Schaffner and Swart (1991) conducted a similar study to understand fractionation between diet and tissue in eggs, but using seven species of wild seabirds: Caspian tern (*Sterna caspia*), elegant tern (*Sterna elegans*), laughing gulls (*Larus atricilla*), sooty tern (*Sterna fuscata*), white tailed tropicbird (*Phaethon lepturus*) and red billed tropicbird (*Phaethon aethereus*). They collected the majority of their samples from spent or broken eggs, which reduced the need for invasive methods of dietary study. This was the first

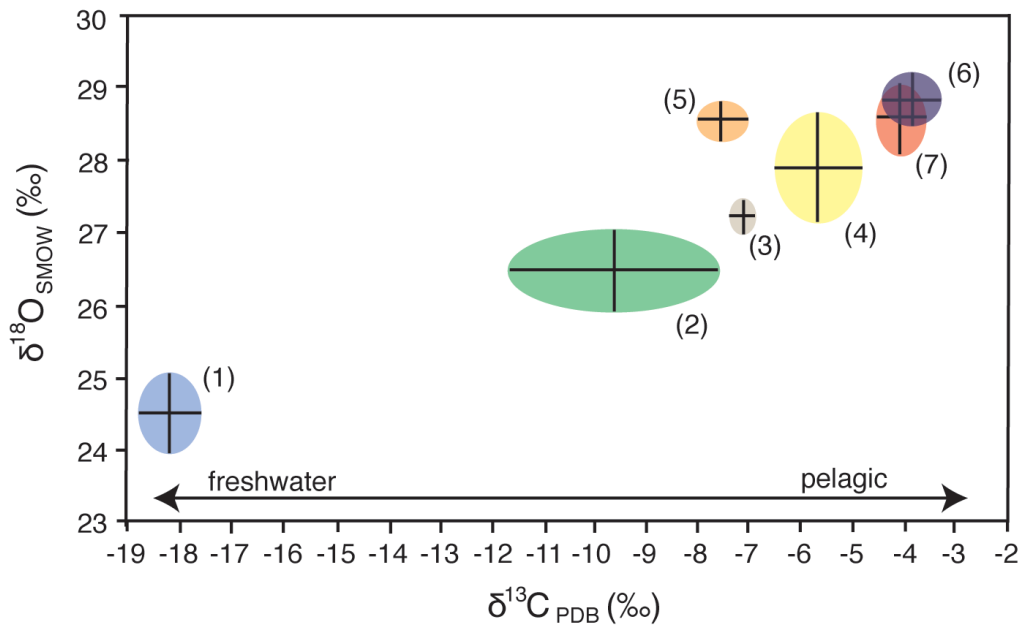


Figure 5.3. Bivariate plot of carbon versus oxygen from eggshell carbonate for seven species of seabird (Schaffner and Swart 1991). A clear separation between freshwater and pelagic feeders is evident on both carbon and oxygen axes. (1), western grebes, primarily feed in estuarine, while (2) caspian terns, (3) elegant terns, (4) laughing gulls, (5) sooty terns, (6) white-tailed tropicbirds, and (7) red-billed tropic birds feed in pelagic environments.

instance of a dietary study on bird eggshells using both carbon and oxygen isotopes. They found the enrichment between diet, which in this case was often fish as the birds were piscivores, and tissue was less than the previously recorded 16.2‰ in ostriches from the inorganic portion of the eggshell (Von Schirnding, Van Der Merwe and Vogel 1982). Instead, it was between 14- 15‰. What was evident was a gradient between freshwater, estuarine, offshore, and pelagic species in both oxygen and carbon isotopes (Figure 5.3). It was also noted that the $\delta^{18}\text{O}$ of the eggshell was enriched by 28.5‰ relative to the water source, which meant there was an additional approximately 2-4‰ enrichment based on the expected precipitation of calcite at a body temperature of 39-40 degrees C. They concluded that remains of eggshells would be a reliable, noninvasive method for determining diet in environments where continuous invasive collection would not be possible.

There remains a paucity of captive experiments that definitively determine the sources of isotopic variation in each egg material (e.g., yolk, organic membrane, inorganic component). These experiments are a necessity to understanding enrichment (fractionation) between diet and environment and the egg products. These enrichment factors need to be understood to properly reconstruct historical or paleoenvironments, and must be done for multiple species and groups, as they can vary. It was not until 1995 that egg products other than the organic and inorganic portions of the shell were examined; yolk and albumen were tested in this manner in Japanese quail (*Coturnix japonica*), wild-strain mallards (*Anas platyrhynchos*), prairie falcon (*Falco mexicanus*), peregrine falcons (*Falco peregrinus*) and gyrfalcons (*Falco rusticolis*) (Hobson 1995). In this study, it was shown that there were relatively consistent dietary fractionations in the same material

between species in both $\delta^{13}\text{C}$ and $\delta^{15}\text{N}$. Enrichment in yolk for $\delta^{13}\text{C}$ is $\sim 0\text{‰}$, while $\delta^{15}\text{N}$ enrichment ranges from 3.1 - 3.6‰. In albumen, the range of $\delta^{13}\text{C}$ is 0.8-1.6‰ and $\delta^{15}\text{N}$ is 2.4- 3.1‰. In these species tested, enrichment of eggshell carbonate was less than what was seen in ostriches by von Schirnding et al. (1982), ranging from 11.1-15.6‰. In this experiment a diet switch was also used, so it was shown that albumen, shell carbonate, and shell membrane $\delta^{13}\text{C}$ values indicate a diet integrated over 3-5 days, while the yolk is closer to 8 days.

Using gentoo penguins, Polito et al. (2009) were able to illustrate the different enrichment factors between diet (whole fish) and each portion of the egg: eggshell organics, carbonates, shell membrane, albumen, and yolk. Their results showed that the enrichment factor of $\delta^{13}\text{C}$ in the inorganic carbonate of the eggshell was far lower than in previously recorded birds. Gentoo penguins have a fractionation constant of approximately 7‰ between diet and eggshell carbonate, while fractionation between diet and shell membrane is 2.9‰ which is concordant with values from Hobson (1995). The $\delta^{13}\text{C}$ and $\delta^{15}\text{N}$ enrichment in yolk is 0.0 and 3.5‰ respectively, and in albumen it is 0.8 and 4.7‰. This experiment represented the first data on isotopic discrimination in penguins or any captive seabird. They showed that it is possible to reconstruct diet of these penguins when proper fractionations are taken into account; without their experiments, estimations of past environments and ecologies of these penguins would have been grossly misinformed. There is a comprehensive table organizing these data in Polito et al. (2009).

Most studies of fossil and modern eggs using stable isotope analysis are predominantly about birds, but there are a handful of studies that have used reptile eggs.

In 1986, Burleigh and Arnold looked at a small number of island tortoise eggshells to understand niche partitioning between extinct species. A few papers that have mainly focused on dinosaur eggshells have also included some samples of turtle and/or crocodile eggs (e.g., Erben, Hoefs and Wedepohl 1979; Sarkar, Bhattacharya and Mohabey 1991). Beyond that, there has been no stable isotopic research done on reptile eggshells, and as of 2012, there are no captive feeding experiments to test diet-tissue fractionations.

Alteration and preservation of eggshell

Digenesis in eggshells has primarily been studied in fossil aves and non-avian dinosaurs. While it appears that the organic portion of eggshell may only persist for 1000s of years (Johnson, Fogel and Miller 1998), the inorganic portion, if it is not severely altered, may contain useful paleoenvironmental and paleobiological information for millions of years. Diagenesis can alter the physical crystal structure and/or the chemical signature in calcium carbonate. If a fossil is composed of aragonite, it will commonly alter to calcite, but if it is originally calcite, as in archosaur eggshells, the status of alteration may be more difficult to assess. X-ray diffraction (XRD) is commonly used to visualize alteration of aragonite to calcite, i.e., in corals (Cusack et al. 2008), but this will not help distinguish between primary and secondary calcite alteration. A suite of methods must be used to assess alteration and determine if fossil eggshell remains are suitable for stable isotope analysis.

Cathodoluminescence (CL) is a method for assessing digenesis that has been commonly used to examine patterns of alteration in calcite shells (Barbin et al. 1995). It is a method employed using a CL detector attached to a scanning electron microscope (SEM). The CL detector measures the wavelengths of the photons being emitted from the

mineral while it is being bombarded with high energy electrons in the SEM. Commonly, manganese (Mn) and iron (Fe) will replace calcium (Ca) in a crystal lattice. There is bright fluorescence in CaCO_3 if there is substitution of Mn^{2+} in the crystal lattice in place of Ca; the presence of Fe^{2+} will quench luminescence (Barbin 2000). Unaltered CaCO_3 only fluoresces lightly under CL, and the biogenic calcite of eggshells does not contain Mn and Fe, so CL can be used as a determinate of alteration in these fossils (Grellet-Tinner, Corsetti and Buscalioni 2010). This method can also help visualize where alteration is, such as if it is pervasive throughout the shell or if it is localized to pores or outer surfaces of the shell (Figure 5.4).

Transmitted light microscopy using a petrographic microscope (TLM) and scanning electron microscopy (SEM) can also provide clues about the alteration of fossil eggshells. Examining a thin section of an eggshell through TLM gives a strong indication of the preservation of original crystal eggshell structures and layers. Intrusive pore waters can dissolve crystals of eggshells after burial, and these waters can also imprint a different chemical signature on the eggshells if they are dissolved. Not being able to identify specific layers such as the mammillae may indicate the eggshell has been recrystallized (Figure 5.5). SEM analysis can also help visualize crystal structure and layers of eggshell in order to assess alteration. While using the SEM, different modes such as electron back-scatter diffraction (EBSD) and energy-dispersive x-ray spectroscopy (EDS) can be used to understand in greater detail specific zones of alteration and their elemental composition.

As previously mentioned, iron will quench luminescence, so EBSD can be used to determine where in the fossil iron might be present if it does not luminesce under CL.

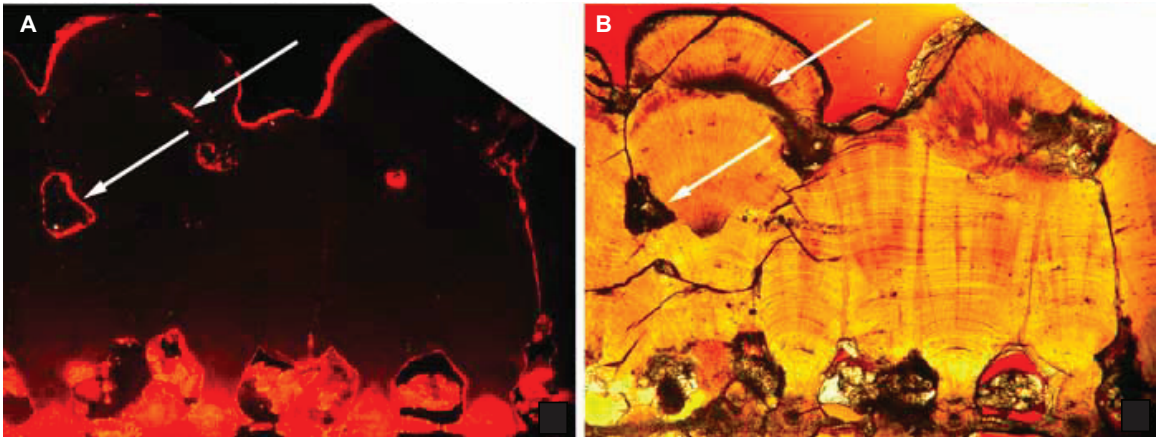


Figure 5.4. CL and TLM photos of megaloolithid eggshell from Auca Mahuevo, Argentina (Grellet-Tinner et al. 2010). A. Red luminescence in the CL image indicates this eggshell has been altered chemically on the exposed surfaces and in interior pockets. The white arrows point to a dissolution edge where two eggshells were fused together, most likely through dissolution. B. The same view of the eggshell in TLM with arrows pointing to the same dissolution fronts. Images and interpretation from Grellet-Tinner et al. (2010).

The backscatter detector in an SEM measures the number of electrons that reach it, and this number is inversely proportional to the size of the atom the electrons collided with; atoms with a low atomic number will show up as a dark area in the BSE image, while atoms with a high atomic number will show up lighter in the BSE image. EBSD has been used to study crystallographic patterns in avian eggshell in order to understand mineralization and behavior of trace elements (Dalbeck and Cusack 2006). This method is often used in conjunction with EDS integrated into the SEM to fine-tune elemental maps of a specimen. The EDS x-ray detector detects characteristic elemental x-rays and the software then analyzes the resulting energy spectrum to determine the types and abundances of elements. This technique can be useful when creating an elemental map of a fossil specimen to determine zones of alteration, and is helpful in identifying elements that are not typically present in biogenic calcite, which will indicate alteration has taken place. EDS has shown to be effective in looking at mineral and elemental alteration in fossil dinosaur eggshells (Grellet-Tinner et al. 2010, Montanari et al. In review).

In addition to the above-mentioned methods, other methods such as electron microprobe and x-ray absorption near-edge spectroscopy analyses have been used to look at eggshell alteration in birds with good success (Dauphin et al. 2006). Grellet-Tinner et al. (2010) provides a useful flow chart for determining the best combination of methods to use in assessing diagenesis and alteration in fossil eggshells. They note that most studies only use one of these methods to determine if alteration has taken place, when clearly due to the strengths and weaknesses of each method, a combination of two or more visualization and microscopy techniques would be most effective.

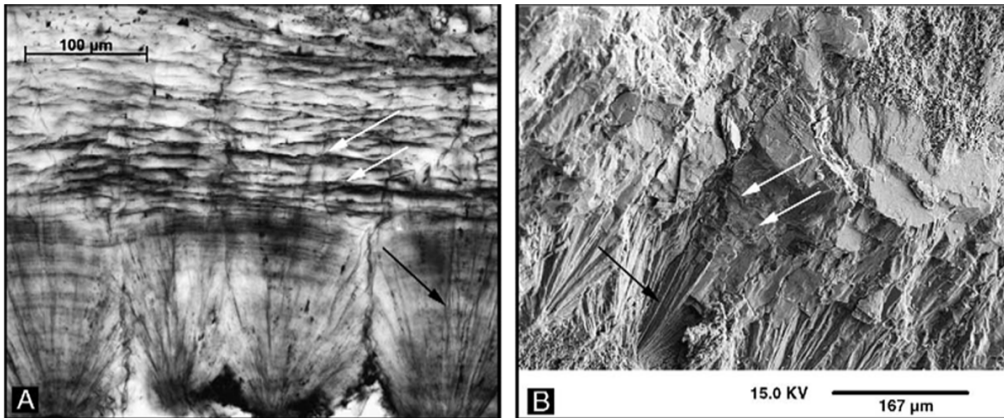


Figure 5.5. TLM and SEM images of dinosaur eggshell from *Deinonychus antirrhopus* (Grellet-Tinner et al. 2006). A. TLM view of a thin section of eggshell carbonate. White arrows point to organic material reflecting growth lines in the prismatic layer. The black arrow points to acicular calcite crystals in the mammillae. B. SEM view of the same egg where the same features are labeled with black and white arrows. This illustrates a lack of recrystallization in this portion of the eggshell. Images and interpretation from Grellet-Tinner et al. (2006).

Fossil eggshell studies

After the work of Folinsbee (1970) on stable isotopes in eggshell, dinosaur paleontologists picked up on the potential utility of this tool for determining more information on the environments dinosaurs lived in. This first paper specifically focused on dinosaur eggshell chemistry was that of Erben (1979), who attributed the decline of dinosaur species to pathologies in their eggshells. He included dinosaur shells from fossil sites in Utah, Spain, France, and Mongolia, along with comparisons to a variety of bird and reptile shells to verify the conclusion drawn in Folinsbee et al. (1970). He purportedly identified eggs with specific dinosaur species, but this was merely conjecture and weakened some of his assumptions. Sarkar et al. (1991) showed that eggshell carbonate from the Lameta beds of India showed a semi-arid environment with a definite C3 signal and evaporated pools for drinking water.

More detailed dinosaur eggshell stable isotopic research surfaced in the 2000s with Cojan et al. (2003) work on sampling changes in $\delta^{13}\text{C}$ and $\delta^{18}\text{O}$ in eggshell carbonate throughout a stratigraphic section in France. They were able to determine, due to accurate stratigraphic sampling, that the dinosaur eggshells showed a change in evaporation rates in the locality when compared with associated soil carbonates. Zhao and Yan (2000) were able to sample across the Cretaceous-Paleogene transition in China (Zhao and Yan 2000). They noticed a trend towards more negative values in $\delta^{13}\text{C}$, and therefore diet, towards the boundary. This could potentially indicate variable local environmental signals in the Nanxiong basin in southern China. They also found additional information in the eggshells, such as pathologies and $\delta^{18}\text{O}$ anomalies, which they suggested indicated that stress was being put on the dinosaurs from the environment

(Zhao et al. 2009). In Central Asia, dinosaur eggshells from Gobi Desert Late Cretaceous localities have been analyzed and indicate clear variation in the paleoenvironments within one region during the same time period, and also over different time periods (Montanari et al. In review). Dinosaur eggshells from the Late Cretaceous of Romania indicated the environment there had humid micro-habitats where the dinosaurs were laying their eggs (Bojar, Csiki and Grigorescu 2010).

Work on fossil bird eggshell has been greatly enhanced by the ability to do modern experiments on closely related species to determine more specific controls on the enrichment of carbon, nitrogen, and oxygen. The groundwork for this research was laid by the pioneering work on controls of carbon and oxygen isotopes by Johnson (1998). They were able to use controlled feeding experiments in zoos and farms to test previous assumptions on stable isotope fractionations in bird eggs. It was shown that the carbon isotopes of the organic and inorganic fractions of the eggshell were enriched 2 and 16‰ respectively relative to diet, almost identical to what was shown in von Schirnding et al. (1982). The $\delta^{15}\text{N}$ of the organic fraction of the eggshell was found to be enriched by 3‰ relative to diet and correlate inversely with mean annual precipitation. Contra Folinsbee et al. (1970), Schirnding et al. (1982) found that while ostrich $\delta^{18}\text{O}$ of eggshell carbonate varied linearly with drinking water in the captive based experiments, in the wild the same pattern was not seen, leading them to conclude this variation was due to leaf water being the primary water source of ostrich body water. Johnson (1998) illustrated the possibility of fossil ratite eggshells to be a viable source of information for paleoenvironmental reconstruction, and since then numerous studies have been able to unveil a picture of terrestrial climate that had never been seen before. Emu eggshells were used to illustrate

the strength of the Australian monsoon over the last 65,000 years based on the prevalence of C4 grass in their diet (Johnson 1999). An archive of the change from a C3 dominated ecosystem to one with both C3 and C4 mosaic vegetation was discovered in ratiite (ostrich) eggshells of northern Pakistan and India (Stern, Johnson and Chamberlain 1994).

Studies utilizing eggshells have become more popular in the last decade and have been able to provide detailed climatic information about certain landscapes. Fossil ratiite bird eggshells have proved most useful for these sorts of analysis due to the fact they are robust and are present in the fossil record from at least the Neogene to present. The change in the composition of grasslands from the Early Miocene until the present was tracked using eggshells from species of *Diamantornis*, *Namornis*, and *Stuthio*, both fossil and recent (Segalen et al. 2002). The $\delta^{13}\text{C}$ of the eggshells indicate a shift from a mainly C3 plant dominated diet to one dominated by C4 plants in the present, which indicates concordant environmental and climate shifts. Both $\delta^{18}\text{O}$ and $\delta^{13}\text{C}$ of extinct elephant bird *Aepyornis* indicate it ate primarily C3 vegetation in the Holocene landscape of Madagascar, and also had a $\delta^{18}\text{O}$ less influenced by evaporation than modern ostriches (Clarke et al. 2006). This allows us to better understand potential environmental mechanisms that could have caused the extinction of this species.

Newsome et al. (2011) examined the $\delta^{15}\text{N}$ in extant and fossil *Dromaius novaehollandiae* eggshells and fossil *Genyornis newtoni* eggshells over a 130 ka timescale to better understand the causes of megafaunal extinction in the last Pleistocene of Australia. They found a significant rise in $\delta^{15}\text{N}$ of the eggshell values from the Last Glacial Maximum to the Holocene, documenting more frequent arid conditions. The $\delta^{13}\text{C}$

values decreased in *Dromaius* but not in *Genyornis* prior to the megafauna extinctions, and additionally other differences in the ecology of these two sympatric species were noted (Newsome et al. 2011). Carbon isotopic composition of Adélie penguin (*Pygoscelis adeliae*) eggshells illustrated a recent shift to lower trophic level prey in the last 200 years when compared with the previous 38,000 years (Emslie and Patterson 2007). Also, oxygen isotope record of Adélie penguin eggshells over a span of 8,000 years can help reconstruct the paleoenvironment of Terra Nova Bay, Antarctica (Lorenzini et al. 2012). It is apparent that this method of examining stable isotopes in eggshells is increasingly gaining popularity in Holocene records.

Future directions

The variety of studies detailed above illustrates how useful eggs and egg products can be as a proxy for environment, diet, and ecology in modern and deep time. Despite how useful this tool is, there are still a number of areas untouched by stable isotopic research. For example, there has been little to no work done on the stable isotope ecology of fossil and modern turtle, squamate, or monotreme eggs. It is also important to note that there are techniques that have been developed in other fields that may be useful to determining alteration in eggshells, such as laser ablation inductively coupled mass spectroscopy, which is able to analyze the elemental compositions in different layers of biogenic minerals on the order of micron size resolution (Castro et al. 2010). With recent work on penguins that illustrated different fractionation constants between egg materials and diet, it is clear we need to focus more time on experiments with controlled feeding and captive birds and reptiles. Additionally, new methods of determining diagenesis in fossil eggshells are being developed, with the recent use of tools such as EDS (Montanari

et al. In review). Developments of methods for understanding carbonate diagenesis are critical to the success of stable isotope analyses on fossil eggshells. Due to the availability of eggs and egg products in museum collections, modern ecosystems, and fossil deposits, any future research on this subject will allow us a better and fuller understanding of the biology and ecology of egg-laying vertebrates.

References

- Badam, Gyani L. 2005. A note on the ostrich in india since the miocene. *Man and Environment* 30 (2): 97-104.
- Barbin, Vincent. 2000. Cathodoluminescence of carbonate shells: Biochemical vs diagenetic process. In *Cathodoluminescence in Geosciences*. Ed. M Page, V Barbin, P Blanc, and D Ohnenstetter. Springer.
- Barbin, Vincent, Uwe Brand, Roger A Hewitt, and Karl Ramseyer. 1995. Similarity in cephalopod shell biogeochemistry since carboniferous: Evidence from cathodoluminescence. *Geobios* 28 (6): 701-710.
- Bojar, Ana-Voica, Zoltan Csiki, and Dan Grigorescu. 2010. Stable isotope distribution in maastrichtian vertebrates and paleosols from the hațeg basin, south carpathians. *Palaeogeography, Palaeoclimatology, Palaeoecology* 293 (3-4): 329-342.
- Castro, Waleska, Jurian Hoogewerff, Christopher Latkoczy, and José R Almirall. 2010. Application of laser ablation (LA-ICP-SF-MS) for the elemental analysis of bone and teeth samples for discrimination purposes. *Forensic Science International* 195 (1): 17-27.
- Clarke, Simon J, Gifford H Miller, Marilyn L Fogel, Allan R Chivas, and Colin V Murray-Wallace. 2006. The amino acid and stable isotope biogeochemistry of elephant bird (aepyornis) eggshells from southern madagascar. *Quaternary Science Reviews* 25 (17-18): 2343-2356.
- Cusack, Maggie, J England, P Dalbeck, A W Tudhope, A E Fallick, and N Allison. 2008. Electron backscatter diffraction (EBSD) as a tool for detection of coral diagenesis. *Coral Reefs* 27 (4): 905-911.
- Dalbeck, Paul and Maggie Cusack. 2006. Crystallography (electron backscatter diffraction) and chemistry (electron probe microanalysis) of the avian eggshell. *Crystal Growth & Design* 6 (11): 2558-2562.
- Dansgaard, Willi. 1964. Stable isotopes in precipitation. *Tellus* 16 (4): 436-468.
- Dauphin, Yannicke, Jean-Pierre Cuif, Murielle Salomé, Jean Susini, and C Terry Williams. 2006. Microstructure and chemical composition of giant avian eggshells. *Anal Bioanal Chem* 386 (6): 1761-71.
- DeNiro, Michael J and Samuel Epstein. 1978a. Influence of diet on the distribution of carbon isotopes in animals. *Geochimica Et Cosmochimica Acta* 42:495-506.

- Emslie, Steven D and William P Patterson. 2007. Abrupt recent shift in $\delta^{13}C$ and $\delta^{15}N$ values in adélie penguin eggshell in antarctica. *Proceedings of the National Academy of Sciences* 104 (28): 11666.
- Erben, Heinrich K, J Hoefs, and K H Wedepohl. 1979. Paleobiological and isotopic studies of eggshells from a declining dinosaur species. *Paleobiology* 5 (4): 380-414. <http://www.jstor.org/stable/2400319>.
- Friedman, Renee F, Amy Maish, Ahmed G Fahmy, John C Darnell, and Edward D Johnson. 1999. Preliminary report on field work at hierakonpolis: 1996-1998. *Journal of the American Research Center in Egypt* 36:1-35.
- Green, Rhys E and Jorn P W Scharlemann. 2003. Egg and skin collections as a resource for long-term ecological studies. *Bulletin-British Ornithologists Club* 123:165-176.
- Grellet-Tinner, Gerald, Frank Corsetti, and Angela D Buscalioni. 2010. The importance of microscopic examinations of eggshells: Discrimination of bioalteration and diagenetic overprints from biological features. *Journal of Iberian Geology* 36 (2): 181-192.
- Heaton, Tim H E. 1987. The $^{15}N/^{14}N$ ratios of plants in south africa and namibia: Relationship to climate and coastal/saline environments. *Oecologia* 74 (2): 236-246.
- Hirsch, Karl F. 1983. Contemporary and fossil chelonian eggshells. *Copeia* 1983 (2): 382-397. <http://www.jstor.org/stable/1444381>.
- . 1996. Parataxonomic classification of fossil chelonian and gecko eggs. *Journal of Vertebrate Paleontology* 16 (4): 752-762. <http://www.jstor.org/stable/4523772>.
- Hobson, Keith A. 1999. Tracing origins and migration of wildlife using stable isotopes: A review. *Oecologia* 120 (3): 314-326.
- Hobson, Keith A. 1995. Reconstructing avian diets using stable-carbon and nitrogen isotope analysis of egg components: Patterns of isotopic fractionation and turnover. *The Condor* 97 (3): 752-762. <http://www.jstor.org/stable/1369183>.
- Hou, Lian-Hai, Pi-Peng Li, Daniel T Ksepka, Ke-Qin Gao, and Mark A Norell. 2010. Implications of flexible-shelled eggs in a cretaceous choristoderan reptile. *Proceedings of the Royal Society B: Biological Sciences* 277 (1685): 1235-1239.
- Janz, Lisa, Robert G Elston, and George S Burr. 2009. Dating north asian surface assemblages with ostrich eggshell: Implications for palaeoecology and extinction. *J Archaeol Sci* 36 (9): 1982-1989.

- Johnson, Beverly J, Gifford H Miller, Marilyn L Fogel, John W Magee, Michael K Gagan, and Allan R Chivas. 1999. 65,000 years of vegetation change in central australia and the australian summer monsoon. *Science* 284 (5417): 1150-1152.
- Johnson, Beverly J, Marilyn L Fogel, and Gifford H Miller. 1998. Stable isotopes in modern ostrich eggshell: A calibration for paleoenvironmental applications in semi-arid regions of southern africa. *Geochimica Et Cosmochimica Acta* 62 (14): 2451-2461.
- Koch, Paul L. 2007. Isotopic study of the biology of modern and fossil vertebrates. In *Stable Isotopes in Ecology and Environmental Science*. 2nd ed. Boston: Blackwell Publishing .
- Koch, Paul L, Kathryn A Hoppe, and S David Webb. 1998. The isotopic ecology of late pleistocene mammals in north america:: Part 1. Florida. *Chemical Geology* 152 (1-2): 119-138.
- Lorenzini, Sandra, Ilaria Baneschi, Anthony E Fallick, Maria C Salvatore, Giovanni Zanchetta, Luigi Dallai, and Carlo Baroni. 2012. Insights into the holocene environmental setting of terra nova bay region (ross sea, antarctica) from oxygen isotope geochemistry of adelic penguin eggshells. *The Holocene* 22 (1): 63-69.
- Luz, Boaz and Yehoshua Kolodny. 1985. Oxygen isotope variations in phosphate of biogenic apatites, IV. Mammal teeth and bones. *Earth and Planetary Science Letters* 75 (1): 29-36.
- Mikhailov, Konstantin E, Emily S Bray, and Karl E Hirsch. 1996. Parataxonomy of fossil egg remains (veterovata): Principles and applications. *Journal of Vertebrate Paleontology* 16 (4): 763-769. <http://www.jstor.org/stable/4523773>.
- Montanari, Shaena, Pennilyn Higgins, Mark A Norell. In review. Dinosaur eggshell and tooth enamel geochemistry as an indicator of Central Asian Cretaceous paleoenvironments. *Palaeogeography, Palaeoclimatology, Palaeoecology*.
- Newsome, Seth D, Gifford H Miller, John W Magee, and Marilyn L Fogel. 2011. Quaternary record of aridity and mean annual precipitation based on $\delta^{15}\text{N}$ in ratite and dromornithid eggshells from lake eyre, australia. *Oecologia* 167 (4): 1151-62.
- Norell, Mark A, Jim M Clark, Luis M Chiappe, and Demberlyn Dashzeveg. 1995. A nesting dinosaur. *Nature* 378 (6559): 774-776.
- Orton, Jayson. 2008. Later stone age ostrich eggshell bead manufacture in the northern cape, south africa. *J Archaeol Sci* 35 (7): 1765-1775.

- Post, David M. 2002. Using stable isotopes to estimate trophic position: Models, methods, and assumptions. *Ecology* 83 (3): 703-718.
- Sarkar, A, S.K. Bhattacharya, and D.M. Mohabey. 1991. Stable-isotope analyses of dinosaur eggshells: Paleoenvironmental implications. *Geology* 19:1068-1071.
- Schoeninger, Margaret J and Michael J DeNiro. 1984. Nitrogen and carbon isotopic composition of bone collagen from marine and terrestrial animals. *Geochimica Et Cosmochimica Acta* 48 (4): 625-639.
- Segalen, Loic, Maurice Renard, Martin Pickford, Brigitte Senut, Isabelle Cojan, Laurence Le Callonnec, and Pierre Rognon. 2002. Environmental and climatic evolution of the namib desert since the middle miocene: The contribution of carbon isotope ratios in ratite eggshells. *Comptes Rendus Geoscience* 334 (12): 917-924.
- Stern, Libby A, Gary D Johnson, and C. Page Chamberlain. 1994. Carbon isotope signature of environmental change found in fossil ratite eggshells from a south asian neogene sequence. *Geology* 22:419-422.
- Tieszen, Larry L. 1991. Natural variations in the carbon isotope values of plants: Implications for archaeology, ecology, and paleoecology. *J Archaeol Sci* 18 (3): 227-248.
- Von Schirnding, Y, N J Van Der Merwe, and J C Vogel. 1982. Influence of diet and age on carbon isotope ratios in ostrich eggshell. *Archaeometry* 24 (1): 3-20.
- Zhao, Zikui and Zheng Yan. 2000. Stable isotopic studies of dinosaur eggshells from the nanxiong basin, south china. *Science in China Series D: Earth Sciences* 43 (1): 84-92.

CHAPTER VI

DINOSAUR EGGSHELL AND TOOTH ENAMEL GEOCHEMISTRY AS AN INDICATOR OF CENTRAL ASIAN CRETACEOUS PALEOENVIRONMENTS

(Adapted from Montanari, S. Higgins, P., and Norell, M.A. In review. Dinosaur eggshell and tooth enamel geochemistry as an indicator of Central Asian Cretaceous paleoenvironments. *Palaeogeography, Palaeoclimatology, Palaeoecology*)

Abstract

The Late Cretaceous fossiliferous beds of Mongolia's Gobi Desert have yielded spectacular articulated remains of an extraordinary diversity of fossil mammals, lizards, turtles, birds, and nonavian dinosaurs. Paleoenvironmental interpretations of the deposits at these localities have ranged from arid wind-blown dune fields to more mesic, moist environments. Among the diversity of fossils, dinosaur eggshells and teeth are commonly found at these localities. Dinosaur eggs, like modern avian eggs, are constructed of biomineralized calcite (CaCO_3) allowing carbon and oxygen stable isotopes to be quantified to provide information about the environment in which the egg-laying animals were living. Here we show that dinosaur eggshell and teeth from the Djadokhta and Nemegt Formations have not been significantly altered and reflect an environment of dry dunes during deposition of the Djadokhta Formation and a more mesic stream environment for conditions in the Nemegt Formation. Carbonate nodules from the same eggshell-bearing layers also independently reflect a similar environmental signal. This study represents the first geochemical analysis of dinosaur remains from the Cretaceous of Mongolia and illustrates the potential of utilizing dinosaur fossil geochemistry of both eggs and teeth to reconstruct Mesozoic environments.

Introduction

Geochemical analysis of biological materials in fossils, such as tooth enamel, bone, and eggshell is a commonly used method for discerning paleoenvironments and paleobiology of extinct organisms and ecosystems (Koch, 1998, 2007). Typically these types of studies are done on mammalian tooth enamel, but it has been shown that these methods can be used on dinosaur teeth and eggshells for paleoecological reconstruction (e.g., Cojan et al., 2003; Amiot et al., 2004; Fricke et al., 2008, 2009). Carbon in the carbonate phase of bioapatite ($[\text{Ca}_5(\text{PO}_4, \text{CO}_3)_3(\text{OH}, \text{CO}_3)]$), the material making up both teeth and bone, is reflective of organic material ingested by the organism. Oxygen in bioapatite is primarily influenced by the oxygen isotopic composition of the water an organism drinks (Longinelli, 1984; Luz and Kolodny, 1985).

Southern Mongolia is made up of flat-lying, non-marine, Late Cretaceous rock formations. During the Late Cretaceous, the Gobi Desert region was a completely terrestrial interior continental setting, as it is 2800 km from the nearest known Cretaceous marine outcrops in Kazakhstan (Averianov, 1997). This location provides a unique window into Central Asian Cretaceous paleoclimates that cannot be obtained anywhere else. Terrestrial paleoclimate records from the Mesozoic are especially limited, and vertebrate fossils can provide a useful proxy.

Experiments on modern bird eggshell over the past four decades clearly show that carbon and oxygen isotopes of the calcite shells record the environmental conditions the female was experiencing immediately prior to egg laying (Folinsbee et al., 1970; Johnson et al., 1997). Using this information, paleoenvironmental archives have been obtained from ostrich eggshell (e.g., Johnson et al. 1998), and dinosaur eggshell from India (Sarkar

et al., 1991), France (Cojan et al., 2003), China (Zhao et al., 2009) and Romania (Bojar et al., 2010), illustrating the potential of this proxy. Oxygen isotopes in eggshell have been well correlated with the isotopic composition of drinking water, while carbon isotopes of the eggshell carbonate strongly reflect stable isotopic composition of ingested food material (Folinsbee et al., 1970; Erben et al., 1979; Von Schirnding et al., 1982; Schaffner and Swart, 1991).

It can be difficult to use dinosaurs for stable isotope investigation because, unlike mammals, we are unable to do any experimentation on living non-avian dinosaurs to measure isotopic fractionations between diet, drinking water and isotopes in eggshells and bioapatite. With eggshell, it is assumed that the fractionation of oxygen and carbon isotopes in dinosaur eggshell is fundamentally similar to what occurs in extant bird eggshell (Cojan et al., 2003). But in studies of dinosaur teeth, absolute isotopic values of tooth enamel cannot be attributed to true environmental signal because the exact fractionation constant is not known, an issue that has been showcased in numerous publications.

Fricke et al. (2008) states that if certain well-founded assumptions are made, then we can compare relative differences in isotopic values among taxa from the same and/or different localities to glean important environmental information. The first assumption is that dinosaurs utilize and incorporate carbon like all extant homeothermic vertebrates do. The second assumption is that dinosaurs were homeothermic, which has been illustrated numerous times (e.g., Fricke and Rodgers, 2000). In this paper, we look at eggshells and teeth from two different species of dinosaur from three different localities. If our data show distinct differences or similarities in isotope values when compared to between

localities and species, then we may be able to characterize the ancient environment with general reference to vegetation and precipitation. One would expect distinct differences in isotopic values between species that occupy different dietary niches. Additionally, there would be isotopic differences between species inhabiting environments with different climate regimes. Similarities in isotope values could mean the animals ate similar food and occupied similar dietary niches, or that diagenesis has overwhelmed all signal and reset isotope values to be homogenous.

Background on isotopes and environment

There are numerous detailed reviews on the systematics of carbon and oxygen isotopes in ecosystems (e.g., Koch, 2007), and how they are preserved in fossils so only a brief review will be presented here. Plants utilize one of three metabolic pathways: C3, C4, and CAM. Grasses and succulents utilize the C4 and CAM pathways. Since there is no evidence for widespread C4 or CAM plants until the Cenozoic we will be operating under the assumption only C3 plants occur in the Late Cretaceous (Sage, 2004). Carbon isotope ratios of plants depend on both photosynthetic pathways and environmental conditions (O'Leary, 1988). Isotopic ratios of carbon are expressed using the permil notation, such as: $\delta^{13}\text{C}$ (per mil, ‰) = $((R_{\text{sample}}/R_{\text{standard}}-1) \times 1000)$, where R = ratio of $^{13}\text{C}/^{12}\text{C}$ of an unknown sample relative to a known standard V-PDB (Coplen, 1994).

There is a large discrimination between the C-12 and C-13 of atmospheric CO₂ and the organic matter of C3 plants, with the average $\delta^{13}\text{C}$ of C3 plants ranging from -32 to -21‰ compared to an atmospheric $\delta^{13}\text{C}$ of -8‰ (Tieszen, 1991). The lowest values represent C3 plants exposed to high respiration and decomposition rates, such as forest floor cover (Cerling et al., 2004). Conversely, $\delta^{13}\text{C}$ values of organic matter in the

neighborhood of -24‰ and higher are indicative of a semi-arid environment with low relative humidity (Kohn, 2010). As a rule, C3 plants with more positive $\delta^{13}\text{C}$ concentrations are adapted to environments that are semi-arid and water stressed. It is notable that the $\delta^{13}\text{C}$ of atmospheric CO_2 can also change over time, which in turn affects the $\delta^{13}\text{C}$ of organic plant matter (Fricke et al., 2008). The $\delta^{13}\text{C}$ of atmospheric CO_2 can differ by $\sim 1\text{‰}$ depending on glaciation, so care must be taken in interpreting results from times when the extent of glacial cover is not known (Koch, 1998).

Oxygen isotopes are expressed similarly to carbon isotopes: $\delta^{18}\text{O}$ (per mil, ‰) = $((R_{\text{sample}}/R_{\text{standard}} - 1) \times 1000)$, where R = ratio of $^{18}\text{O}/^{16}\text{O}$ of an unknown sample relative to a known standard, either V-PDB or V-SMOW (Coplen, 1994). In this paper, oxygen isotopes are reported with respect to V-PDB. Oxygen isotopic ratios in water vary because of temperature, evaporation, and source of the precipitation's air mass (Dansgaard, 1964). The cause of $\delta^{18}\text{O}$ variation is the preferential incorporation of ^{18}O into condensate as water is precipitated and removed from the cooling air mass. The same is true in terrestrial bodies of water; ^{16}O is preferentially evaporated concentrating the ^{18}O in the water body.

Typically, terrestrial vertebrates do not ingest precipitation directly. Instead, most water ingestion comes from leaves, streams, ponds, and lakes that will have a different $\delta^{18}\text{O}$ than precipitation (Fricke et al., 2008). In humid areas, there may not be a large discrepancy between $\delta^{18}\text{O}$ of precipitation and $\delta^{18}\text{O}$ of water on land, but in arid regions the increased evaporation will lead to a large difference in these $\delta^{18}\text{O}$ values. Another important factor is that not all animals (e.g., desert dwelling vertebrates) are obligate water drinkers, meaning they either get most of their water from plants and seeds, or they

create metabolic water from the breakdown of proteins (Chew, 1961; Johnson et al., 1997; Johnson et al., 1998). Metabolic water is formed in all organisms, but rarely does it contribute substantially to body water. Animals such as kangaroo rats never need to drink free water because their entire water budget is met by metabolic water, but larger organisms need water from other sources (Chew, 1961). It has been shown that non-passerine birds such as ostriches produce metabolic water, but the majority of their body water needs are met by drinking surface water and water contained in the plants they eat (Wither, 1983). It is likely that the physiology of dinosaurs functioned similarly to extant birds like ostriches, so the $\delta^{18}\text{O}$ of their body water reflects ingested water from plants and surface reservoirs. Leaf water of plants in water stressed areas can be ^{18}O enriched relative to $\delta^{18}\text{O}$ of meteoric water because of the preferential evapotranspiration of ^{16}O (Gonfiantini et al., 1965). Yet again, because we do not know if the dinosaurs in question were obligate drinkers or not, all of these scenarios must be taken into account when interpreting the data.

Geology and stratigraphy

The stratigraphy of Mongolia's Late Cretaceous Nemegt Basin is divided into three formations: Djadokhta, Barun Goyot, and Nemegt (from stratigraphically oldest to youngest). (Jerzykiewicz and Russell 1991; Hasegawa et al. 2008). Evidence from geochronological studies shows the lithologic sequence of the Nemegt Basin is essentially a semi-continuous section from Cenomanian to Maastrichtian (Jerzykiewicz and Russell 1991; Shuvalov 2000; Hasegawa et al. 2009). All three of the formations in this basin are known to have produced a vast array of fossil vertebrates, such as dinosaurs (e.g., Norell et al. 1994; Clark et al. 2001), mammals (e.g., Wible et al., 2007), crocodiles

(e.g., Pol and Norell, 2004), turtles (e.g., Mlynarski and Narmandach, 1972), and lizards (e.g., Gao and Norell, 2000).

The localities of Ukhaa Tolgod (43° 32' N; 101° 31' E) and Bayn Dzak (44° 09' N; 103° 41' E) (Fig. 6.1) are assigned to the Djadokhta Formation, which is Campanian in age (Loope et al., 1998; Dashveg et al., 2005; Dingus et al., 2008). The formation was first described in 1927 at the Bayn Dzak locality (Berkey and Morris, 1927). The fossil locality of Bayn Dzak, also known as the Flaming Cliffs and Shabarak Usu, was discovered by the Central Asiatic Expeditions of the American Museum of Natural History in the 1920s (Andrews, 1932). Dinosaurs such as *Velociraptor*, *Saurornithoides*, and *Oviraptor* were discovered in the red beds of Bayn Dzak (Osborn, 1924). Ukhaa Tolgod, discovered in 1993 by the Mongolian Academy of Sciences-American Museum of Natural History Expedition (MAE), has yielded an unprecedented diversity of extremely well-preserved specimens of birds, dinosaurs, mammals, and lizards reviewed by Dashzeveg et al., (1995). This locality is correlated to the Djadokhta Formation based on lithofacies and biostratigraphic evidence and is assigned a Campanian age (Dingus et al., 2008).

The rocks of the Djadokhta Formation at Bayn Dzak are reddish-orange medium to fine grained sandstones (Fig. 6.2). Some of the strata contain calcareous nodules and pockets of silty clay (Dashzeveg et al., 2005). The fossiliferous unit of the Djadokhta Formation exposed at Bayn Dzak is reddish colored structureless medium grained sandstone that varies between 2m and 14m in thickness. There is evidence of migrating dunes, with cliffs of consolidated sandstones with 5-7m high crossbed sets. Calcareous nodules are found in both the crossbedded and structureless sandstone layers, and these

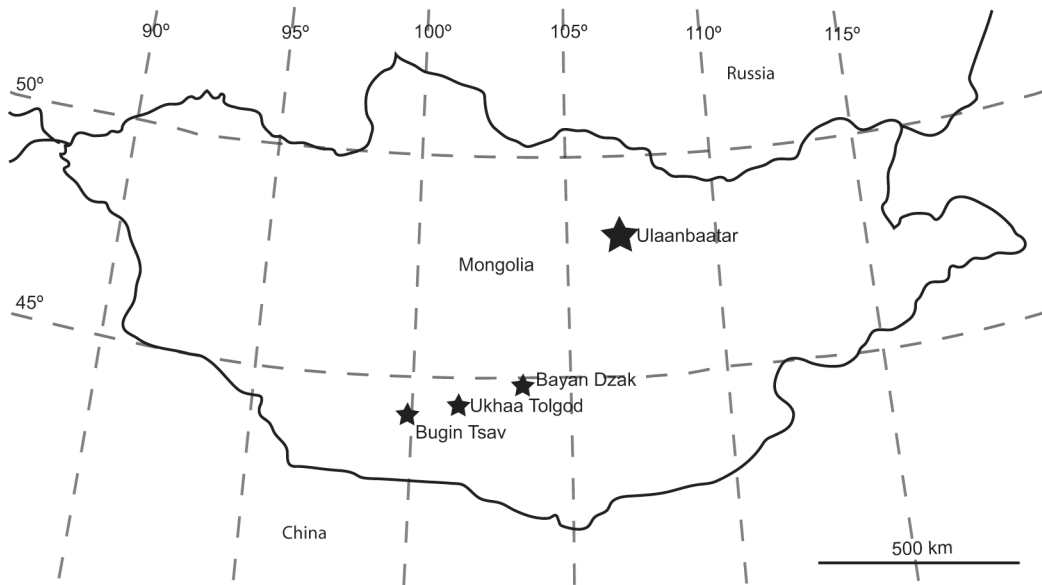
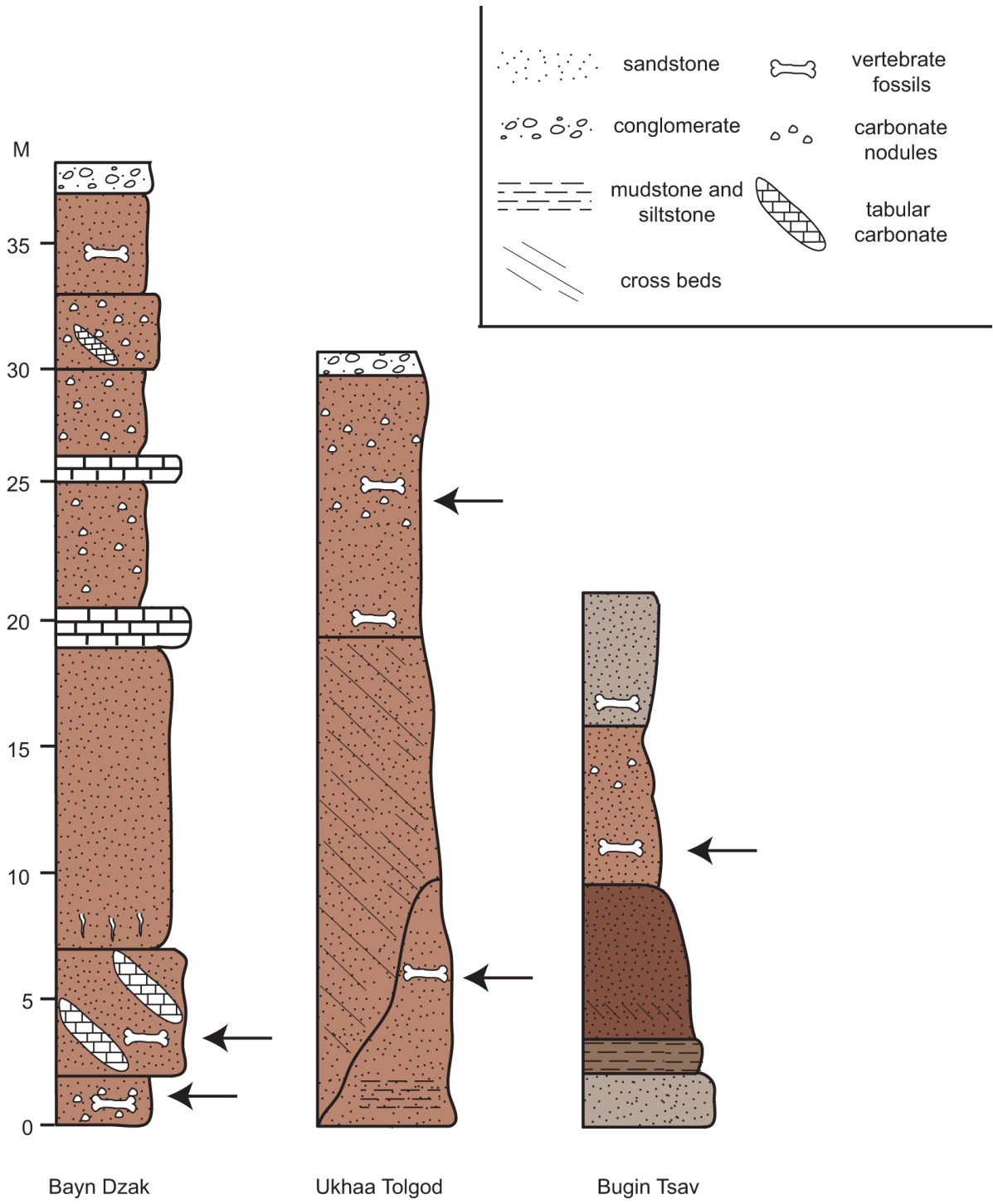


Figure 6.1. Map of Mongolia. The locations of the localities are marked with stars.

white nodules often contain the bones of mammals, multituberculates, and lizards (Dashzeveg et al., 2005). There are thin beds of concretionary calcite and lenses of siltstone and mudstone within the sandstone units, indicating an arid to semi-arid depositional environment.

At Ukhaa Tolgod, lithology similar to that seen at Bayn Dzak is observed (Fig. 6.2). The outcrops of fossiliferous rock are also reddish fine-grained structureless sandstones. There are also cross-stratified dune deposits and siltstone deposits that are not laterally continuous (Dingus et al., 2008). The vertebrate fossils preserved at Ukhaa Tolgod often appear to be in death positions, which seem to indicate the animals were rapidly buried in sandslides off of superhydrated collapsing dunes while they were still alive (Loope et al., 1998; Dingus et al., 2008). Calcite sheets and nodules are also present at this locality, which indicates the dunes were stable for a period of time. There are indications of small ponds in the interdune corridors during times of dune stabilization, but these were mostly ephemeral (Dingus et al., 2008). Based on these lithographic and faunal similarities, Ukhaa Tolgod is assigned to the Bayn Dzak Member of the Djadokhta Formation proposed by Dashzeveg et al. (2005) (Dingus et al., 2008). The Bugin Tsav locality (43° 52' N; 100° 01' E) (Fig. 6.1) is located in the southern portion of the central Gobi Desert of Mongolia and is assigned to the Nemegt Formation and overlies the Barun Goyot Formation (Gradzinski 1969). The Nemegt Formation is considered late Campanian (Weishampel et al., 2008) to Maastrichtian (Kielan-Jaworoska and Barsbold, 1972) in age.

Figure 6.2. Generalized stratigraphic columns. Stratigraphic columns showing the general structural and lithologic successions at each locality. The prevalence of aeolian and structureless sandstones indicates the Djadokhta Formation localities, Baynz Dzak and Ukhaa Tolgod, were far drier than the Nemegt Formation locality, Bugin Tsav. The stratigraphy at Bugin Tsav indicates the presence of a fluvatile system. Columns are compiled from Dashzeveg et al., 2005 (Bayn Dzak), Dingus et al., 2008 (Ukhaa Tolgod), and Kielan-Jaworowska and Sochava, 1969 (Bugin Tsav). Arrows indicate where analyzed fossils were found in each section.



The Nemegt Formation differs from the Djadokhta Formation in that it consists mainly of fluvial sediments deposited by braided or meandering river systems (Gradzinski and Jerzykiewicz, 1974; Jerzykiewicz and Russell, 1991). Fossiliferous sediments at the Bugin Tsaav locality are yellowish-brown sands that range in grain size from very fine to very coarse. Additionally, there are thin-bedded conglomerates and sandy siltstones (Gradzinski, 1969). Features such as climbing ripples, flaser structures, and scoured surfaces are present providing additional evidence that the Nemegt Formation was deposited on an alluvial plain with a low-flow regime (Gradzinski, 1969). Remains of dinosaurs and other vertebrates like turtles (sometimes found in mass death assemblages) are commonly found in point bar deposits without much obvious reworking, so death appears to have been close to the location of burial (Weishampel et al., 2008) (Fig. 6.2).

Bioattribution of eggshell

Mongolian dinosaur eggs have been studied on the basis of microstructure (Grellet-Tinner et al., 2002; Grellet-Tinner et al., 2006; Balanoff et al., 2008), nesting behavior (Norell et al., 1995; Weishampel et al., 2008), and embryonic associations (Norell et al., 1994; Balanoff et al., 2008), but never have stable isotopes been utilized in the analyses of these eggshells. Unfortunately, dinosaur eggshells are usually found separate from any identifiable skeletal remains, so taxonomic assignment is in most cases problematic. This has led to the development of an eggshell parataxonomic scheme (Mikhailov et al., 1997), which is used for identifying “ootaxa”. Eggshell types are characterized by a combination of size, shape, ornamentation, and microstructure (Mikhailov et al., 1997). Recent discoveries of dinosaur nests with associated remains of parents or embryos have allowed association of certain eggshell morphotypes with

distinct species or groups of dinosaurs and in many cases we no longer have to rely entirely on the parataxonomic scheme (Norell et al. 1994, Grellet-Tinner et al., 2006).

At Ukhaa Tolgod, the oviraptorid taxon known to belong to an egg morphotype is *Citipati osmolskae*. They certainly belong to the oofamily Elongatoolithidae (Grellet-Tinner et al., 2006). At Bugin Tsav, we do not know the exact identity of the egg-layer, but the microstructural and ultrastructural similarities between the eggshells from Ukhaa Tolgod and Bugin Tsav seem to indicate they are both from oviraptorids (Weishampel et al. 2008). Because this egg type has only been found associated with this group of dinosaurs in the Late Cretaceous of Central Asia, this allows us to parataxonometrically categorize them as elongatoolithid, and for this egg type to be preliminarily assigned to oviraptorids. This eggshell morphotype is characterized by the elongate egg shape and lineartuberculate ornamentation on the surface of the eggshell. In this study, only elongatoolithid type eggshell fragments were used, to provide for taxonomic control in interpreting the palaeoenvironments of these localities. These fragments were mostly collected *in situ* weathering out of rocks or as nearly complete eggs in float.

Diagenesis in biogenic materials

All fossilized material is affected by diagenesis, even soon after burial (Trueman and Tuross, 2002). Alteration occurs when there is isotopic exchange between bioapatite and surrounding fluids at a significantly different temperature and isotopic composition than formation; alteration can also occur when there is dissolution or addition of secondary apatite or carbonate (Zazzo et al., 2004). Because diagenesis is nearly universal, it needs to be shown that the primary signal in the fossil material has not been completely obscured by secondary diagenetic alteration. The highly porous bioapatite

constructed of small apatite crystals (with more surface area) found in bone seem to be more susceptible to alteration, whereas tooth enamel is more resistant due to its tightly packed, large bioapatite crystals (Kohn and Cerling, 2002).

While there is no way to prove definitively that diagenesis has not obscured primary signal, a suite of methods, such as cathodoluminescence and comparison of signals in biogenic carbonate to signals in authigenic carbonates, can be used to best illustrate that alteration is not completely pervasive (Cojan et al., 2003; Fricke et al., 2008; Fricke et al., 2009). One such method is comparison of the isotopic signal of the material in question, in this case eggshell calcite and tooth enamel, with an independent proxy, such as bulk organic carbon or carbonate nodules in the same formation. If the carbon and oxygen isotopic compositions of the two substrates differ, then overall diagenetic forces, such as hydrothermal alteration or burial, have not significantly impacted the locality and erased the primary environmental signal (Sarkar et al., 1991; Cojan et al., 2003; Fricke et al., 2008). We apply this method, and when eggshells were collected, carbonate nodules weathering out from the same sedimentary layer were also collected if available.

Additionally, cathodoluminescence (CL) is used on polished thin sections of the eggs to check for zones of chemical and mineral alteration. Authors using fossil shells for geochemical analysis commonly use CL as a diagenetic indicator (Barbin et al., 1995). Pure CaCO_3 has very little luminescence; unaltered CaCO_3 is essentially non-luminescent under CL, but has slight changes in luminescence when there are ionic substitutions in the crystal lattice (Grellet-Tinner et al., 2010). Iron and manganese most commonly replace calcium in the crystal lattice and typically diagenetic pore waters are enriched in

these two elements relative to biological host fluid (Grellet-Tinner et al., 2010). Finding signs of alteration under CL gives an indication that diagenesis has occurred. Energy-dispersive spectroscopy (EDS) can also be used to create an element map of the eggshell in the SEM and obtain qualitative elemental abundance data. If there is suspicion of diagenesis under CL, EDS can be used to determine where the secondary elements have infiltrated the eggshell. If luminescence is absent, it provides evidence there has been little or no diagenetic alteration of biogenic carbonate.

Methods

Between 5-19 eggshell fragments from each locality were analyzed. Carbonate nodules from Ukhaa Tolgod were also analyzed as comparative samples, providing a test of diagenesis. Across all materials, a total of 60 samples were analyzed. Samples of eggshell were manually abraded to remove adhered sediment and subsequently crushed with a mortar and pestle. The carbonate nodules were prepared by drilling out material from each nodule with a Dremel tool. Bulk samples of protoceratopsian tooth enamel were obtained by crushing or drilling enamel flakes after they were separated from the underlying dentin. For carbonate samples (nodules and eggshell) approximately 250 μg of sample was obtained, and for bioapatite samples over 1000 μg was used to obtain an accurate result. Powdered samples of bioapatite were subsequently treated using 30% H_2O_2 and 0.1 N acetic acid to remove organic material and surficial carbonates; carbonate samples were treated only with H_2O_2 (see MacFadden and Higgins (2004) for detailed methods). Analyses were run on a Thermo Electron Corporation Finnegan Delta plus XP mass spectrometer in continuous-flow mode via the Thermo Electron Gas Bench peripheral and a GC-PAL autosampler housed at the University of Rochester. Carbon and

oxygen isotopic results are reported in per mil (‰) relative to VPDB (Vienna Pee-Dee Belemnite) with an allowable 2-sigma uncertainty of 0.12‰ and 0.20‰ for carbon and oxygen respectively. Statistical analyses, such as t-tests, F-tests, Hotelling's pairwise comparisons, and MANOVA were all performed on Microsoft Excel 2011 and PAST ver. 2.14.

Thin sections made of eggshell fragments from each locality were examined under both SEM and transmitted light microscopy. Using transmitted light to view the thin sections illustrates preservation of the two distinct layers seen in unaltered oviraptorid-type eggshell. The sections were viewed under 50x magnification on a Nikon polarizing microscope. Photographs of the slide were captured using a Sony CCD-Iris camera with UltraTV software. These thin sections were also viewed with CL in a Hitachi S-4700 SEM equipped with a Gatan MonoCL cathodoluminescence detector. Eggshells were examined under the Zeiss EVO 60 variable pressure SEM to look at crystal structure and make elemental maps with the equipped Bruker AXS Quantax 4010 EDS. Eggshells were cleaved manually, and the freshly broken side was examined under extended pressure in the SEM chamber to see if the two eggshell layers were visible. Then, these same freshly broken shells, along with the thin sections of the same eggshell, were used to create elemental maps to discern whether secondary elements had infiltrated the eggshells. The EDS maps were made using Bruker Esprit 1.9.3 software with a wavelength between 15-20 kV and a collection time 5 minutes for element maps. Some images were refined in Adobe Photoshop CS5 to improve contrast and visibility of fine-scale structures.

Results and discussion

Eggshell microscopy

Under transmitted light, distinct structures can be seen in the eggshell thin sections. Oviraptorid eggshell is unique in that it consists of two distinct aprismatic layers of biogenic calcite as opposed to the tri-layered avian and mono-layer crocodilian eggshell (Grellet-Tinner et al., 2006). The base inorganic eggshell layer consists of acicular calcite crystals arranged in a fan-like pattern. The distinct second layer consists of calcite crystals arranged with their C crystalline axis oriented 90 degrees in respect to the first layer (Grellet-Tinner et al., 2006). The outer surface of the shell appears wavy due to the lineartuberculate orientation of the shell. The preservation of these fine-scale structures in the shell helps strengthen the case the calcite crystals have not been significantly altered by outside diagenetic sources (Fig. 6.3A). Often times, the eggshell surface can appear very eroded, which most likely means it was exposed to some acidic environment that degraded its structure and composition. Under variable pressure SEM, the same crystal layers are seen. On freshly broken dinosaur eggshells, the radiating acicular fan-like crystals can be seen forming a separate layer (Fig 6.3B). Additionally, the underside of the eggshell still clearly shows mammillary cones, all adding to the argument that these eggshells have not been severely altered (Fig. 6.3C).

The CL and EDS elucidated the elemental compositions of the eggshells. Under CL, the thin sections did not exhibit bright luminescence. This could indicate that there is a large amount of iron in the eggshell, so the same eggs were placed under the SEM to examine their elemental composition through EDS. A fresh ostrich egg was also placed in

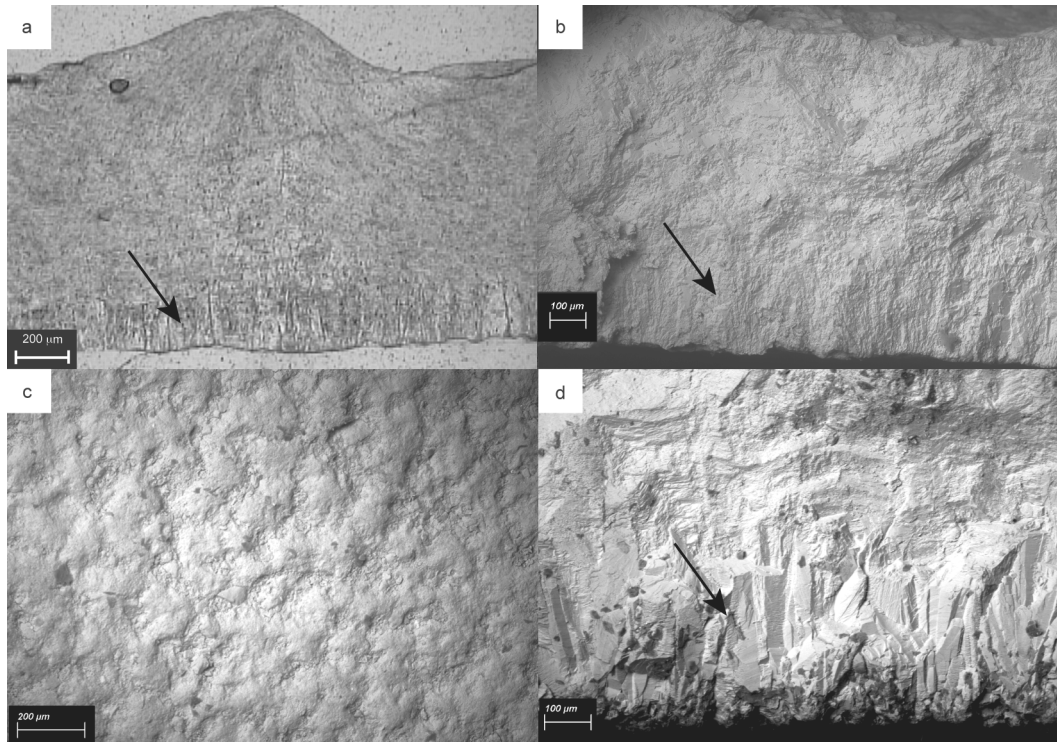


Figure 6.3. Photomicrographs of dinosaur eggshell. Black arrows point to the layer of radial calcite crystals in a,b, and d. a. Transmitted light radial view of an elongatoolithid eggshell thin section (specimen IGM 100/1189) from Bugin Tsav. Note the clear delineation of the radiating acicular calcite layer from the second layer. b. Radial SEM view of IGM 100/1189 with both eggshell layers also visible. c. SEM view of IGM 100/1189 illustrating the bottom of the eggshell's mammillary cones. d. Radial SEM view of a modern ostrich eggshell that depicts the similarities in appearance of eggshell layers to the dinosaur eggshell fragments utilized in this study.

the SEM for comparison purposes. The ostrich eggshell showed similar structure features, like the fan-like calcite base layer, and reflected a pure calcium carbonate elemental composition with only a small amount of sodium detected in the shell, as a replacement for calcium. In the dinosaur eggshells, on the other hand, more elements appear in some EDS spectra, such as magnesium, iron, and strontium. Silica and aluminum are present, but that is clearly due to adhered sand grains on the eggshell (see images in supplement). The amount of other elements besides Ca, C, and O in the dinosaur eggshell total <1% in each shell sampled. We maintain that this supports the conclusion that there are no major elemental changes in the eggshell since burial, and their composition remains relatively pure and appropriate for stable isotopic testing.

Stable isotope paleoecology

The mean $\delta^{13}\text{C}$ and $\delta^{18}\text{O}$ values, number of samples, and standard deviations for each material in each locality are provided in Table 6.1. The Hotelling's pairwise comparisons of these means between materials and localities are presented in Table 6.2. F-tests and t-tests were also performed for pairwise comparisons of carbon and oxygen between substrates tested (Table 6.3).

Carbon isotopes and reconstructing vegetation

At Ukhaa Tolgod and Bayn Dzak, both of the Djadokhta Formation localities, the $\delta^{13}\text{C}$ of eggshell ($\delta^{13}\text{C}_{\text{egg}}$) values are high with a mean of $-5.2 \pm 1.1\text{‰}$ and $-4.6 \pm 0.9\text{‰}$ respectively. These means of $\delta^{13}\text{C}_{\text{egg}}$ from both Djadokhta Formation sites are not significantly different (Table 6.3). At Bugin Tsav, the younger Nemegt Formation locality, the mean of $\delta^{13}\text{C}_{\text{egg}}$ is similarly high ($-5.6 \pm 0.65\text{‰}$) (Fig. 6.4). Across avian groups, eggshell calcite is enriched by $\sim 16.0\text{‰}$ relative to ingested plant fodder (Von

Schirnding et al., 1982; Schaffner and Swart, 1991). If we assume non-avian dinosaurs, as extinct relatives of birds, had a similar method of fractionation, then the vegetation of the paleoenvironment may be characterized. With the enrichment factor of 16.0‰ subtracted from the measured $\delta^{13}\text{C}$, the average plant $\delta^{13}\text{C}$ is found to be -21.2‰ at Ukhaa Tolgod and -20.6‰ and -21.6‰ at Bayn Dzak and Bugin Tsav respectively.

The closest modern day environmental analog to the calculated plant $\delta^{13}\text{C}$ from the eggshells in both formations is a semi-arid desert ecosystem that supports gymnosperms (*Pinus* sp.) and small shrubs (DeLucia and Schlesinger, 1991). Among modern C3 plants, it is noted that gymnosperms often have the highest $\delta^{13}\text{C}$ values (Tieszen, 1991). It is quite probable that gymnosperms like pine trees and small shrubs dominated the Cretaceous ecosystems of Mongolia, as they are well adapted to water stress, and the seeds from gymnosperms could have served as a food source for nesting dinosaurs. Without actual remains of Cretaceous gymnosperms, this is only an assumption and cannot yet be directly tested. It is notable that the $\delta^{13}\text{C}$ of the dinosaur enamel in this study and others (Stanton-Thomas and Carlson 2003, Fricke et al. 2008, Fricke and Pearson 2008) is high when compared to enamel values of modern mammals that forage on C3 plants. The $\delta^{13}\text{C}$ of enamel ($\delta^{13}\text{C}_{\text{enam}}$) of the protoceratopsian teeth from Ukhaa Tolgod has an average of $-5.39 \pm 1.53\%$. This mean is similar to what was found in Fricke and Pearson (2008) for the $\delta^{13}\text{C}_{\text{enam}}$ of herbivorous dinosaurs of the Hell Creek Formation, which was -5.9‰. The diet-tissue fractionation in mammalian herbivores has been fairly well established (DeNiro and Epstein, 1978). For wild herbivorous mammals, the fractionation between bulk diet and $\delta^{13}\text{C}$ of enamel apatite is

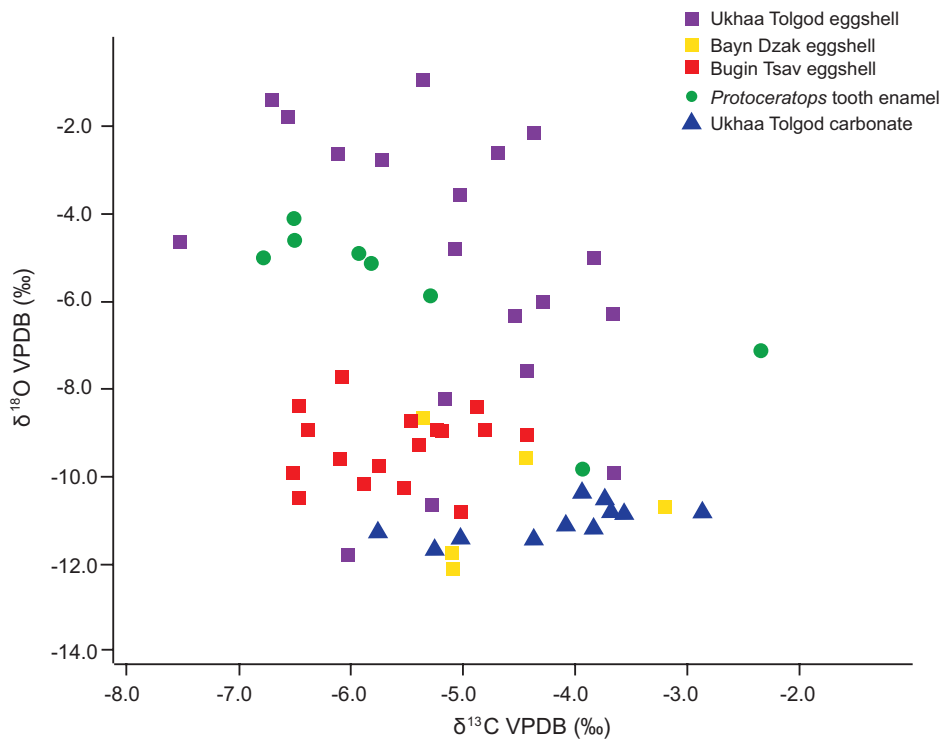


Figure 6.4. Bivariate plot of oxygen and carbon. $\delta^{18}\text{O}$ vs. $\delta^{13}\text{C}$ values for eggshell, tooth enamel, and soil carbonate. Samples are marked by colored squares, circles, and triangles.

Table 6.1. Stable isotope results and statistics. Mean, n (sample number), standard deviation (SD), and variance for both carbon and oxygen isotope values for all materials sampled. Isotope values are presented in per mil (‰)

Material	n	$\delta^{13}\text{C}$			$\delta^{18}\text{O}$		
		mean	SD	var	mean	SD	var
Ukhaa Tolgod eggshell	19	-5.2	1.1	1.2	-5.2	3.2	10.5
Ukhaa Tolgod carbonate nodule	11	-4.2	0.9	0.7	-11.0	0.4	0.2
Bayn Dzak eggshell	5	-4.6	0.9	0.8	-10.5	1.5	2.1
Ukhaa Tolgod <i>Protoceratops</i> teeth	8	-5.4	1.5	2.3	-5.8	1.9	3.5
Bugin Tsav eggshell	17	-5.6	0.7	0.4	-9.3	0.8	0.7

Table 6.2. Pairwise comparisons of all materials and localities. Post-hoc Hotelling's pairwise comparisons of eggshell and carbonate nodules within the same environment illustrate significantly different isotopic values between Ukhaa Tolgod eggshell and carbonate nodules. Significant p-values are shown in bold.

	UT Eggshell	UT Carb Nodes	<i>Protoceratops</i> Enamel	BD Eggshell
Ukhaa Tolgod Eggshell				
Ukhaa Tolgod Carbonate Nodes	0.000000258			
<i>Protoceratops</i> Enamel	0.619286	0.000193258		
Bayn Dzak Eggshell	0.000206455	0.712936	0.00955824	
Bugin Tsav Eggshell	0.00000092	0.00303766	0.00149165	0.159946

Table 6.3. Results from t-tests. F-tests were first performed to see if the variances between samples were equal or unequal. Depending on that result, the appropriate t-test for equal or unequal variance was performed. These t-tests show at Ukhaa Tolgod, there is a significant difference between the $\delta^{13}\text{C}$ of the carbonate nodules and eggshell. This also holds true for the $\delta^{18}\text{O}$ for the same materials. Eggshell $\delta^{13}\text{C}$ composition from all three localities is indistinguishable, but $\delta^{18}\text{O}$ is different. Abbreviations: UT= Ukhaa Tolgod, BD=Bayn Dzak, BT= Bugin Tsav.

Variable 1	Variable 2	test	p value	significant?
UT eggshell carbon	UT carbonate carbon	t-equal var.	0.02	yes
UT eggshell carbon	BD eggshell carbon	t-equal var.	0.33	no
UT eggshell carbon	BT eggshell carbon	t-equal var.	0.14	no
UT eggshell oxygen	UT carbonate oxygen	t-unequal var.	0	yes
UT eggshell oxygen	BT eggshell oxygen	t-unequal var.	0	yes
UT eggshell oxygen	BD eggshell oxygen	t-equal var.	0.002	yes
BT eggshell oxygen	BD eggshell oxygen	t-equal var.	0.03	yes

obviously more difficult to physically test because the living relatives of dinosaurs do not have teeth. This 'high' $\delta^{13}\text{C}$ in dinosaurs could be indicative of diagenesis or, as has been suggested by Fricke et al. (2008), indicative of a different physiological fractionation in dinosaurs relative to ingested matter than mammals. Fricke et al. (2008) compared hadrosaur tooth enamel to bulk organic sediments from two different sites and consistently found an -18‰ offset between the $\delta^{13}\text{C}$ of organic sediment matter (diet) and the $\delta^{13}\text{C}$ of the dinosaurian tooth enamel.

If this offset holds true at our localities, then the *Protoceratops* diet had an average value of $\sim -23.4\text{‰}$. This value is not only concordant with the average value calculated from eggshell fractionation at the same locality (-21.2‰) but with plants from water-stressed environments. C3 plants exposed to a high amount of sunlight have higher $\delta^{13}\text{C}$ values than those that are constantly shaded (Lockheart et al., 1998). It is also critical to understand that the absolute values of $\delta^{13}\text{C}$ of organic plant matter will be higher during the Cretaceous because the $\delta^{13}\text{C}$ of atmospheric CO_2 at the time was 1-2‰ higher than it is today, so the $\delta^{13}\text{C}$ of plants would also be higher (Hasegawa et al., 2003; Foreman et al., 2011).

Oxygen isotopes and paleoenvironmental signal

The oxygen isotope composition of the eggshell fragments should reflect the drinking water that was in the environment of the nesting mother (assuming she was an obligate drinker). The $\delta^{18}\text{O}$ of eggshell ($\delta^{18}\text{O}_{\text{egg}}$) values at Ukhaa Tolgod are highly variable with a mean of $-5.2 \pm 3.2\text{‰}$ and a variance of 10.5. This is the highest variance of isotope values recorded in any of the materials sampled in this study. The $\delta^{18}\text{O}_{\text{egg}}$ reflects the organism's drinking water days before the egg was laid (Folinsbee et al.,

1970; Johnson et al., 1998). When precipitation falls, its $\delta^{18}\text{O}$ signature is relatively uniform, but once it collects on the surface, it will be subject to evaporative enrichment in ^{18}O .

Additionally, it is possible that the $\delta^{18}\text{O}_{\text{egg}}$ signature is due to physiological needs of the organisms in question. Ostriches are not obligate water drinkers - that is, they obtain enough water to survive purely through vegetation consumed. Leaf water in warm, dry regions can be ^{18}O -enriched relative to the $\delta^{18}\text{O}$ of meteoric water ($\delta^{18}\text{O}_{\text{mw}}$) because of preferential evapotranspiration of ^{16}O (Gonfiantini et al., 1965). In this instance, the $\delta^{18}\text{O}_{\text{egg}}$ may be reflecting the $\delta^{18}\text{O}$ of leaf water in the plant, which can vary upwards of 14‰ over the course of a single day (Johnson et al., 1998). Therefore, the large range of oxygen isotope values in the eggshells from this locality is probably reflective of a combination of evaporative enrichment of the water source and evapotranspiration within the leaves of food.

The $\delta^{18}\text{O}_{\text{egg}}$ from the Bayn Dzak locality of the Djadokhta Formation has a mean of $-10.5 \pm 1.5\text{‰}$ with a variance of 2.10. At the Bugin Tsav locality of the Nemegt Formation, the mean $\delta^{18}\text{O}_{\text{egg}}$ is $-9.3 \pm 0.8\text{‰}$ and has a variance of 0.7, the lowest variance of all eggshell isotopic values. The mean $\delta^{18}\text{O}_{\text{egg}}$ from Ukhaa Tolgod is significantly higher than that seen at Bayn Dzak and Bugin Tsav. While this could indicate diagenesis, the earlier findings with the structural and elemental purity of the eggshell make this less likely. In fact, this sort of difference between localities and formations would be expected because there are clearly differing environments represented between an arid environment like Ukhaa Tolgod and the more mesic environment, Bugin Tsav. $\delta^{18}\text{O}$ of surface waters in areas subject to evaporative water loss are high, while in more mesic

environments there is not as much variance (Sternberg et al., 1989). The mean $\delta^{18}\text{O}_{\text{enam}}$ of the protoceratopsian teeth is also high, like that from the eggshell in Ukhaa Tolgod, but less variable. It appears as though the protoceratopsians were drinking from evaporated pools, just as is indicated in the oviraptorid eggshells, but whatever they were eating and/or drinking was not as water stressed. More samples of the tooth enamel from different species at these localities are needed to confirm the microhabitat differentiation between species. The difference between the eggshell stable isotopes in oxygen values at both Djadokhta localities is most likely explained by regional variation, primarily in hydrology as reflected by $\delta^{18}\text{O}_{\text{egg}}$.

Carbonate nodules

The carbonate nodules from Ukhaa Tolgod do not appear to be traditional paleosol carbonates. Hasegawa et al. (2008) calls the carbonate pebbles “reworked calcrete” at the Bayan Dzak locality. The fabric of the nodules is micritic, pointing to early diagenetic groundwater calcite. Eberth (1993) notes that there are similar groundwater calcrete nodules in the structureless sandstones of the contemporaneous Djadokhta Formation Bayan Mandahu locality of China’s Gobi Desert. Calcite cements like those found in the Djadokhta Formation are common in sandstones and are formed during long periods of non-deposition in semi-arid localities with less than ~760 mm per year of precipitation (Birkeland, 1999; Royer, 1999; Dingus et al., 2008).

At Ukhaa Tolgod, the carbonate nodule $\delta^{13}\text{C}$ ($\delta^{13}\text{C}_{\text{carb}}$) mean is $-4.1 \pm 0.9\%$. These carbonate nodules appear to be contemporaneous with the fossils at Ukhaa Tolgod. Quade and Roe (1999) state that these sorts of calcretes represent ground-water cements and can potentially be used in the same way paleosol carbonates are to reconstruct

paleoclimate, but the fractionation and source of $\delta^{13}\text{C}$ found in the nodules are not well defined. The source of carbon in the carbonate nodules and the eggs are most likely not exactly the same, so a difference between $\delta^{13}\text{C}_{\text{carb}}$ and $\delta^{13}\text{C}_{\text{egg}}$ is expected. In this case, we are using the isotopic values of the carbonate nodules to compare to the other carbonate at the site (eggshell) to see if there was any mixing of the isotopic values, indicating diagenesis. There is no linear mixing of the isotopic values from different materials (Fig. 6.4) and the carbonate nodules and eggshells are significantly different despite the fact they are from the same site (Table 6.2). This fact strengthens the assertion that the palaeoenvironmental reconstruction is not affected by diagenesis.

The $\delta^{18}\text{O}_{\text{carb}}$ from Ukhaa Tolgod does not show as much scatter (mean -11.0 ± 0.4 ‰) in the data as the eggshell fragments from the same locality. An F-test shows the variances of $\delta^{18}\text{O}_{\text{carb}}$ and $\delta^{18}\text{O}_{\text{egg}}$ are not equal. Generally, the $\delta^{18}\text{O}$ of soil carbonates is determined mainly by the meteoric water $\delta^{18}\text{O}$ (precipitation), soil temperature, and soil water evaporation (Levin et al., 2004). The fact that $\delta^{18}\text{O}_{\text{carb}}$ has such a low variance (0.2) also makes logical sense because it is from early-diagenetic ground-water calcrete which would not be subject to as much evaporative enrichment as more exposed water sources.

Comparing lithology and isotopic paleoenvironment reconstructions

A qualitative verification of our stable isotope inferences of environment is in concordance with paleoenvironmental information we can glean from the rock record. The Djadokhta Formation is largely composed of cross-bedded sandstones, representing large dunes, and structureless sandstone facies. The scarcity of small channel cuts and mud or silt stones leads one to believe the environment on a whole was devoid of abundant water sources. Our isotopic data from Ukhaa Tolgod strongly support this

assumption. The high $\delta^{13}\text{C}_{\text{egg}}$ and $\delta^{13}\text{C}_{\text{enam}}$ are indicative of dinosaurs feeding on vegetation adapted to a dry environment. The oviraptorid eggshells from Ukhaa Tolgod show a great range in oxygen isotopic values, but the *Protoceratops* teeth from the same locality tell a different story with much less $\delta^{18}\text{O}$ variation, perhaps due to differences in microhabitats of oviraptors versus protoceratopsians. It is fairly apparent from both lithological and isotopic evidence that dinosaurs at Djadokhta localities were not drinking running water from frequently replenished sources. The eolian dunes had minimal drainage, with runoff collecting in interdune ponds and streams undergoing evaporation. Similar lithologies at the contemporaneous Bayn Dzak locality give us a similar paleoenvironmental interpretation from the rocks. The stable isotope values of the eggshell from Bayn Dzak are different from that at Ukhaa Tolgod; the $\delta^{13}\text{C}_{\text{egg}}$ means are statistically similar, but there is a substantial difference in the $\delta^{18}\text{O}_{\text{egg}}$ at these Djadokhta Formation localities. The $\delta^{18}\text{O}_{\text{egg}}$ at Bayn Dzak is less enriched than at Ukhaa Tolgod, which illustrates that the environment could have been less dry at Bayn Dzak representing regional hydrological variation.

On the other hand, the lithology of Bugin Tsav and the younger Nemegt Formation is most certainly representative of a more mesic environment than the Djadokhta Formation Ukhaa Tolgod locality. In the Nemegt Formation, there are clear features in the sandy siltstones, such as ripples and flaser structures, that indicate the environment there was a braided stream system. Most of the fossils there are preserved in laterally discontinuous deposits of sandstone, which are indicative of point bars. The lack of carbonate nodules at this locality, which generally only form in dry conditions, also reinforces the notion these two formations represent different types of environments. The

stable isotopic evidence presented in this paper also strengthens this interpretation. The distinct variances and means between the $\delta^{18}\text{O}_{\text{egg}}$ of Ukhaa Tolgod and $\delta^{18}\text{O}_{\text{egg}}$ of Bugin Tsav (Table 6.3) suggests that the smaller variance of $\delta^{18}\text{O}_{\text{egg}}$ at Bugin Tsav means the oviraptorids were drinking from less evaporated bodies of water, such as streams. Interestingly, there is no statistical difference when Hotelling's post-hoc comparison (Table 6.2) is performed between eggshell from Bayn Dzak (Djadokhta) and Bugin Tsav (Nemegt), indicating that perhaps Ukhaa Tolgod was an unusually dry environment in the Late Cretaceous in this region. This unique quality of the environment at Ukhaa Tolgod could be part of the reason we see such unprecedented exceptional fossil preservation at this locality when compared to other Gobi localities (Dashzeveg et al. 1995). The consumed vegetation $\delta^{13}\text{C}$ for both formations is calculated to be $\sim -22\text{‰}$, which indicates that the type and physiological qualities of the plants present in both sorts of environments were the same. Further discovery and sampling of organic plant material from these localities is needed to confirm our isotopic inferences about the plants these dinosaurs were eating.

Overall, when stable isotopes are examined in dinosaur remains, environmental heterogeneity becomes apparent in both plants and surface waters when compared within the same formation and time slice (Bayn Dzak and Ukhaa Tolgod) and also between localities from two different formations potentially spanning millions of years (Ukhaa Tolgod/Bayn Dzak versus Bugin Tsav). Comparing within and between formations and time scales helps us test the viability of our methods for reconstruction environmental change in a basin over time. While this reconstruction cannot particularly reveal whether the Mongolian fauna fell victim to either a mass-wasting event like a landslide (Loope et

al., 1998) or were buried in a sudden sandstorm (Jerzykiewicz, 1998), it shows the Gobi Desert was still a dry, harsh environment ~80 Ma. Even before the uplift of the Tibetan plateau and the Himalayas during the Cenozoic, which currently deprive the Gobi of rainfall, this ecosystem probably was only able to support sheltered areas of biodiversity where organisms could thrive and reproduce.

References

- Amiot, R., Lécuyer C., Buffetaut E., Fluteau F., Legendre S., Martineau F., 2004. Latitudinal temperature gradient during the Cretaceous Upper Campanian–Middle Maastrichtian: $\delta^{18}\text{O}$ record of continental vertebrates. *Earth and Planetary Science Letters* 226, 255-272.
- Andrews, R.C., Nelson, N.C., Hillhouse, C., Granger, W., 1932. The new conquest of central Asia: A narrative of the explorations of the Central Asiatic Expeditions in Mongolia and China, 1921-1930. American Museum of Natural History.
- Averianov, A.O., 1997. New late Cretaceous mammals of southern Kazakhstan. *Acta Palaeontologica Polonica* 42, 243-256.
- Balanoff, A.M., Norell M.A., Grellet-Tinner G., Lewin M.R., 2008. Digital preparation of a probable neoceratopsian preserved within an egg, with comments on microstructural anatomy of ornithischian eggshells. *Die Naturwissenschaften* 95, 493-500.
- Barbin, V., Brand U., Hewitt R.A., Ramseyer K., 1995. Similarity in cephalopod shell biogeochemistry since Carboniferous: evidence from cathodoluminescence. *Geobios* 28, 701-710.
- Berkey, C.P., Morris, F.K., 1927. Geology of Mongolia: a reconnaissance report based on the investigations of the years 1922-1923. 2. The American Museum of Natural History.
- Birkeland, P.W., 1999. Soils and geomorphology. 372. Oxford University Press New York.
- Bojar, A.-V., Csiki Z., Grigorescu D., 2010. Stable isotope distribution in Maastrichtian vertebrates and paleosols from the Hațeg Basin, South Carpathians. *Palaeogeography, Palaeoclimatology, Palaeoecology* 293, 329-342.
- Cerling, T.E., Hart J.A., Hart T.B., 2004. Stable isotope ecology in the Ituri Forest. *Oecologia* 138, 5-12.
- Chew, R.M., 1961. Water Metabolism of Desert-Inhabiting Vertebrates. *Biological Reviews* 36, 1-28
- Clark, J.M., Norell M.A., Barsbold R., 2001. Two new oviraptorids (Theropoda: Oviraptorosauria), Upper Cretaceous Djadokhta Formation, Ukhaa Tolgod, Mongolia. *Journal of Vertebrate Paleontology* 21, 209-213.

- Cojan, I., Renard M., Emmanuel L., 2003. Palaeoenvironmental reconstruction of dinosaur nesting sites based on a geochemical approach to eggshells and associated palaeosols (Maastrichtian, Provence Basin, France). *Palaeogeography, Palaeoclimatology, Palaeoecology* 191, 111-138.
- Coplen, T.B., 1994. Reporting of stable hydrogen, carbon, and oxygen isotopic abundances. *Pure & Applied Chemistry* 66, 273-276.
- Dansgaard, W., 1964. Stable isotopes in precipitation. *Tellus* 16, 436-468.
- Dashzeveg, D., Novacek M.J., Norell M.A., Clark J.M., Chiappe L.M., Davidson A., McKenna M.C., Dingus L., Swisher C., Altangerel P., 1995. Extraordinary preservation in a new vertebrate assemblage from the Late Cretaceous of Mongolia. *Nature* 374, 446-449.
- Dashzeveg, D., Dingus L., Loope D.B., Swisher III C.C., Dulam T., Sweeney M.R., 2005. New stratigraphic subdivision, depositional environment, and age estimate for the Upper Cretaceous Djadokhta Formation, southern Ulan Nur Basin, Mongolia. *American Museum Novitates* 1-31.
- DeLucia, E.H., Schlesinger W.H., 1991. Resource-Use Efficiency and Drought Tolerance In Adjacent Great Basin and Sierran Plants. *Ecology* 72, 51-58.
- DeNiro, M.J., Epstein S., 1978. Influence of diet on the distribution of carbon isotopes in animals. *Geochimica Et Cosmochimica Acta* 42, 495-506.
- Dingus, L., Loope D.B., Dashzeveg D., Swisher III C.C., Minjin C., Novacek M.J., Norell M.A., 2008. The geology of Ukhaa Tolgod (Djadokhta Formation, Upper Cretaceous, Nemegt Basin, Mongolia). *American Museum Novitates* 1-40.
- Eberth, D.A., 1993. Depositional environments and facies transitions of dinosaur-bearing Upper Cretaceous redbeds at Bayan Mandahu (Inner Mongolia, People's Republic of China). *Canadian Journal of Earth Sciences* 30, 2196-2213.
- Erben, H.K., Hoefs J., Wedepohl K.H., 1979. Paleobiological and Isotopic Studies of Eggshells from a Declining Dinosaur Species. *Paleobiology* 5, 380-414.
- Folinsbee, R.E., Fritz P., Krouse H.R., Robblee A.R., 1970. Carbon-13 and Oxygen-18 in Dinosaur, Crocodile, and Bird Eggshells Indicate Environmental Conditions. *Science* 168, 1353-1356.
- Foreman, B.Z., Fricke H.C., Lohmann K.C., Rogers R.R., 2011. Reconstructing paleocatchments by integrating stable isotope records, sedimentology, and taphonomy: A Late Cretaceous case study (Montana, United States). *Palaios* 26, 545.

- Fricke, H.C., Rogers R.R., 2000. Multiple taxon--multiple locality approach to providing oxygen isotope evidence for warm-blooded theropod dinosaurs. *Geology* 28, 799.
- Fricke, H.C., Pearson D.A., 2008. Stable isotope evidence for changes in dietary niche partitioning among hadrosaurian and ceratopsian dinosaurs of the Hell Creek Formation, North Dakota. *Paleobiology* 34, 534
- Fricke, H.C., Rogers R.R., Backlund R., Dwyer C.N., Echt S., 2008. Preservation of primary stable isotope signals in dinosaur remains, and environmental gradients of the Late Cretaceous of Montana and Alberta. *Palaeogeography, Palaeoclimatology, Palaeoecology* 266, 13-27.
- Fricke, H.C., Rogers R.R., Gates T.A., 2009. Hadrosaurid migration: inferences based on stable isotope comparisons among Late Cretaceous dinosaur localities. *Paleobiology* 35, 270.
- Gao, K., Norell M.A., 2000. Taxonomic composition and systematics of Late Cretaceous lizard assemblages from Ukhaa Tolgod and adjacent localities, Mongolian Gobi Desert. *Bulletin of the American Museum of Natural History* 1-118.
- Gonfiantini, R., Gratzu S., Tongiorgi E., 1965. Oxygen isotopic composition of water in leaves. *Isotopes and Radiation in Soil-Plant Nutrition Studies* 405-410.
- Gradzinski, R., 1970. Sedimentation of dinosaur-bearing Upper Cretaceous deposits of the Nemegt Basin, Gobi Desert. *Palaeontologica Polonica* 21, 147-210.
- Gradzinski, R., Jerzykiewicz T., 1974. Dinosaur-and mammal-bearing aeolian and associated deposits of the Upper Cretaceous in the Gobi Desert (Mongolia). *Sedimentary Geology* 12, 249-278.
- Grellet-Tinner, G., Norell M., 2002. An avian egg from the Campanian of Bayn Dzak, Mongolia. *Journal of Vertebrate Paleontology* 22, 719-721
- Grellet-Tinner, G., Chiappe L., Norell M., Bottjer D., 2006. Dinosaur eggs and nesting behaviors: A paleobiological investigation. *Palaeogeography, Palaeoclimatology, Palaeoecology* 232, 294-321.
- Grellet-Tinner, G., Corsetti F., Buscalioni D., 2010. The importance of microscopic examinations of eggshells: Discrimination of bioalteration and diagenetic overprints from biological features. *Journal of Iberian Geology* 36, 181-192.

- Hasegawa, T., Pratt L.M., Maeda H., Shigeta Y., Okamoto T., Kase T., Uemura K., 2003. Upper Cretaceous stable carbon isotope stratigraphy of terrestrial organic matter from Sakhalin, Russian Far East: a proxy for the isotopic composition of paleoatmospheric CO₂. *Palaeogeography, Palaeoclimatology, Palaeoecology* 189, 97-115.
- Hasegawa, H., Tada R., Ichinnorov N., Minjin C., 2009. Lithostratigraphy and depositional environments of the Upper Cretaceous Djadokhta Formation, Ulan Nuur basin, southern Mongolia, and its paleoclimatic implication. *Journal of Asian Earth Sciences* 35, 13-26.
- Jerzykiewicz, T., 1998. Okavango Oasis, Kalahari Desert: a contemporary analogue for the Late Cretaceous vertebrate habitat of the Gobi Basin, Mongolia. *Geoscience Canada* 25, 15-26.
- Jerzykiewicz, T., Russell D.A., 1991. Late Mesozoic stratigraphy and vertebrates of the Gobi Basin. *Cretaceous Research* 12, 345-377.
- Johnson, B.J., Fogel M.L., Miller G.H., 1998. Stable isotopes in modern ostrich eggshell: a calibration for paleoenvironmental applications in semi-arid regions of southern Africa. *Geochimica Et Cosmochimica Acta* 62, 2451-2461.
- Johnson, B.J., Miller G.H., Fogel M.L., Beaumont P.B., 1997. The determination of late Quaternary paleoenvironments at Equus Cave, South Africa, using stable isotopes and amino acid racemization in ostrich eggshell. *Palaeogeography, Palaeoclimatology, Palaeoecology* 136, 121-137.
- Kielan-Jaworowska, Z., Sochava A.V., 1969. The first multituberculate from the uppermost Cretaceous of the Gobi Desert (Mongolia). *Acta Palaeontologica Polonica* 14, 355-367.
- Kielan-Jaworowska, Z., Barsbold R., 1972. Narrative of the Polish-Mongolian palaeontological expeditions 1967-1971. *Palaeontologia Polonica* 5-12.
- Koch, P.L., 1998. Isotopic reconstruction of past continental environments. *Annual Review of Earth and Planetary Sciences* 26, 573-613.
- Koch, P.L., 2007. Isotopic study of the biology of modern and fossil vertebrates, in: Michener, R., Lajtha, K. (eds.), *Stable Isotopes in Ecology and Environmental Science*. Blackwell Publishing, Boston, pp. 99-154.
- Kohn, M.J., 2010. Carbon isotope compositions of terrestrial C₃ plants as indicators of (paleo) ecology and (paleo) climate. *Proceedings of the National Academy of Sciences* 107, 19691.

- Lee-Thorp, J.A., Van Der Merwe N.J., Brain C.K., 1989. Isotopic evidence for dietary differences between two extinct baboon species from Swartkrans. *Journal of Human Evolution* 18, 183-189.
- Levin, N.E., Quade J., Simpson S.W., Semaw S., Rogers M., 2004. Isotopic evidence for Plio-Pleistocene environmental change at Gona, Ethiopia. *Earth and Planetary Science Letters* 219, 93-110.
- Lockheart, M.J., Poole I., Van Bergen P.F., Evershed R.P., 1998. Leaf carbon isotope compositions and stomatal characters: important considerations for palaeoclimate reconstructions. *Organic Geochemistry* 29, 1003-1008.
- Longinelli, A., 1984. Oxygen isotopes in mammal bone phosphate: a new tool for paleohydrological and paleoclimatological research?. *Geochimica Et Cosmochimica Acta* 48, 385-390.
- Loope, D.B., Dingus L., Swisher C.C., Minjin C., 1998. Life and death in a Late Cretaceous dune field, Nemegt basin, Mongolia. *Geology* 26, 27.
- Luz, B., Kolodny Y., 1985. Oxygen isotope variations in phosphate of biogenic apatites, IV. Mammal teeth and bones. *Earth and Planetary Science Letters* 75, 29-36.
- MacFadden, B.J., Higgins P., 2004. Ancient ecology of 15-million-year-old browsing mammals within C3 plant communities from Panama. *Oecologia* 140, 169-182.
- Mikhailov, K.E., Bray E.S., Hirsch K.E., 1996. Parataxonomy of Fossil Egg Remains (Veterovata): Principles and Applications. *Journal of Vertebrate Paleontology* 16, 763-769.
- Mlynarski, M., Narmandach P., 1972. New turtle remains from the Upper Cretaceous of the Gobi Desert, Mongolia. *Palaeontologia Polonica* 7, 95-102.
- Norell, M.A., Clark J.M., Demberelyin D., Rhinchen B., Chiappe L.M., Davidson A.R., McKenna M.C., Altangerel P., Novacek M.J., 1994. A theropod dinosaur embryo and the affinities of the Flaming Cliffs dinosaur eggs. *Science* 266, 779-782.
- Norell, M.A., Clark J.M., Chiappe L.M., Dashzeveg D., 1995. A nesting dinosaur. *Nature* 378, 774-776.
- O'Leary, M.H., 1988. Carbon isotopes in photosynthesis. *Bioscience* 38, 328-336.
- Osborn, H.F., 1924. Three new theropoda, Protoceratops zone, central Mongolia. *American Museum Novitates* 144, 1-12.

- Pol, D., Norell M.A., 2004. A new gobiosuchid crocodyliform taxon from the Cretaceous of Mongolia. *American Museum Novitates* 1-31.
- Quade, J., Roe L.J., 1999. The stable-isotope composition of early ground-water cements from sandstone in paleoecological reconstruction. *Journal of Sedimentary Research* 69, 667-67.
- Royer, D.L., 1999. Depth to pedogenic carbonate horizon as a paleoprecipitation indicator?. *Geology* 27, 1123-1126.
- Sage, R.F., 2004. The evolution of C4 photosynthesis. *New Phytologist* 161, 341-370.
- Sarkar, A., Bhattacharya S., Mohabey D., 1991. Stable-isotope analyses of dinosaur eggshells: Paleoenvironmental implications. *Geology* 19, 1068-1071.
- Schaffner, F.C., Swart P.K., 1991. Influence of diet and environmental water on the carbon and oxygen isotopic signatures of seabird eggshell carbonate. *Bulletin of Marine Science* 48, 23-38.
- Shuvalov, V.F., 2000. The Cretaceous stratigraphy and palaeobiogeography of Mongolia, in: Benton M.J., Shishkin M.A., Unwin D.M., Kurochkin E.N., (eds.), *The Age of Dinosaurs in Russia and Mongolia*, Cambridge University Press, pp. 256-278.
- Stanton Thomas, K.J., Carlson S.J., 2004. Microscale $\delta^{18}\text{O}$ and $\delta^{13}\text{C}$ isotopic analysis of an ontogenetic series of the hadrosaurid dinosaur *Edmontosaurus*: implications for physiology and ecology. *Palaeogeography, Palaeoclimatology, Palaeoecology* 206, 257-287.
- Sternberg, L.D., Mulkey S.S., Wright S.J., 1989. Ecological Interpretation of Leaf Carbon Isotope Ratios: Influence of Respired Carbon Dioxide. *Ecology* 70, 1317-1324.
- Tieszen, L.L., 1991. Natural variations in the carbon isotope values of plants: implications for archaeology, ecology, and paleoecology. *Journal of Archaeological Science* 18, 227-248.
- Trueman, .N., Tuross N., 2002. Trace Elements in Recent and Fossil Bone Apatite. *Reviews in Mineralogy and Geochemistry* 48, 489-521.
- Von Schirnding, Y., Van Der Merwe N.J., Vogel J.C., 1982. Influence of diet and age on carbon isotope ratios in ostrich eggshell. *Archaeometry* 24, 3-20.

- Weishampel, D.B., Fastovsky D.E., Watabe M., Varricchio D., Jackson F., Tsogtbaatar K., Barsbold R., 2008. New oviraptorid embryos from Bugin-Tsav, Nemegt Formation (Upper Cretaceous), Mongolia, with insights into their habitat and growth. *Journal of Vertebrate Paleontology* 28, 1110-1119.
- Wible, J.R., Rougier G.W., Novacek M.J., Asher R.J., 2007. Cretaceous eutherians and Laurasian origin for placental mammals near the K/T boundary. *Nature* 447, 1003-1006.
- Withers, P.C., 1983. Energy, Water, and Solute Balance of the Ostrich *Struthio camelus*. *Physiological Zoology* 56, 568-579.
- Zazzo, A., Lécuyer C., Sheppard S.M., Grandjean P., Mariotti A., 2004. Diagenesis and the reconstruction of paleoenvironments: A method to restore original $\delta^{18}\text{O}$ values of carbonate and phosphate from fossil tooth. *Geochimica Et Cosmochimica Acta* 68, 2245-2258.
- Zhao, Z., Mao X., Chai Z., Yang G., Zhang F., Yan Z., 2009. Geochemical environmental changes and dinosaur extinction during the Cretaceous-Paleogene (K/T) transition in the Nanxiong Basin, South China: Evidence from dinosaur eggshells. *Chinese Science Bulletin* 54, 806-815.

CHAPTER VII

GENERAL CONCLUSIONS

In the previous chapters, I document how I have used new tools and techniques to answer paleobiological and paleoecological questions relating to vertebrate paleontology. These contributions illustrate some chemical and physical methods that can be used in vertebrate paleontology, and in addition what future directions need to be taken to advance the science in this field. I present the general conclusions from the preceding chapters:

- An important holotype specimen of edopoid temnospondyl from the Carboniferous of Ohio, USA, *Macrerpeton huxleyi*, is redescribed and included in a comprehensive phylogenetic analysis with 13 taxa. The phylogenetic analysis recovers *Macrerpeton huxleyi* as the sister taxon of *Cochleosaurus* within the newly renamed clade Macrerpetidae, formerly used the name of Cochleosauridae. Two other specimens are also referred to this species. Although the preserved material is limited, we are able to positively identify the presence of lateral line sulci, which indicate a potential semi-aquatic lifestyle. Due to its comparatively smaller size and curved, sharp dentition, *M. huxleyi* was likely a gracile predator that lived in a wetland environment near a larger source of water, like an oxbow lake.
- Through the development of new methods in measuring the variation of osteocyte lacunae size throughout the vertebrate skeleton, it is shown that substantial naturally occurring variance does exist. However, this is not what causes errors in

genome size estimation. Overall, phylogenetic estimation methods are more accurate than those not based on phylogeny, but they are still highly variable and remain uninformative on a fine scale in spite of the more precise results provided by the new methods and analyses presented in this chapter. A new method of automated bone cell measuring is introduced, and this method will prove useful for large batch measuring of other features in bones, both fossil and modern.

- The Pliocene Chinchilla Local Fauna of southeastern Queensland is a diverse vertebrate assemblage and is analyzed using stable isotopes ($\delta^{18}\text{O}$ and $\delta^{13}\text{C}$) for the first time. It is shown that there is distinct niche separation between the sampled vertebrates living contemporaneously in this locality. Additionally, despite the fact this environment has been interpreted to represent a habitat that is primarily grassland, stable isotope values show that this was a mixed C4 and C3 vegetation environment with a C3 dominated vegetation landscape. Oxygen isotopes in particular suggest a much more mesic environment than is present today. This could indicate that the tropical climate of modern day north Queensland extended much further south approximately 3 million years ago.
- In this synthesis chapter (chapter 5), I emphasize the viability of a little used ecological and environmental proxy- eggs. Eggs are prevalent in modern ecosystems and in the fossil record, so they can be a useful tool for stable isotope analysis. Fractionation of certain isotopes occur in a systematic fashion in different parts of the egg (e.g., membrane, inorganic shell) so all portions of an egg may be used for environmental, ecological, and dietary reconstruction. Eggs from birds and dinosaurs, both modern and fossil, have primarily been sampled

for carbon, oxygen, and nitrogen isotopes, but turtle and other reptile eggs remain understudied and will provide a useful venue for future research.

- Late Cretaceous dinosaur fossils of Mongolia are analyzed using stable isotopes in order to determine the paleoenvironment and paleoecology of dinosaurs living in two localities. I show that dinosaur eggshell and teeth from the Djadokhta and Nemegt Formations have not been significantly altered through diagenesis. The isotopic analyses reflect an environment of dry dunes during deposition of the Djadokhta Formation and a more mesic stream environment in the Nemegt Formation. This study represents the first geochemical analysis of vertebrate remains from the Cretaceous of Mongolia and illustrates the potential of utilizing dinosaur fossil geochemistry of both eggs and teeth to reconstruct Mesozoic environments.

Comparative biological methods are critical for the understanding of evolution of ecology and life history in vertebrates. The use of multiple proxies, such as microscopy and stable isotope mass spectroscopy, gives us an unprecedented way to look at questions that have existed in paleontology for centuries. It is critical to learn cutting-edge methods and phylogenetic approaches to answer these questions in the best, most comprehensive way possible.

APPENDIX A

SUPPLEMENTARY MATERIAL FOR CHAPTER II:

**ANATOMY AND RELATIONSHIPS OF *MACRERPETON HUXLEYI*
(TEMNOSPONDYLI: MACRERPETIDAE) FROM THE LATE
CARBONIFEROUS OF LINTON, OHIO**

Appendix A 2.1. Characters used in the phylogenetic analysis from Steyer et al. (2006).

Character states are polarized with respect to outgroup *Dendrepeton*. All characters are unordered. Characters marked with “*” are new to this analysis.

- 1 Interparietal (pineal) foramen open in skulls ≥ 120 mm midline length (0), or interparietal (pineal) foramen closed in skulls > 120 mm midline length (1)
- 2 Lacrimal enters the orbit margin (0), or excluded from the orbit margin (1)
- 3 Jugal excluded from cheek margin (0), or jugal enters cheek margin separating maxilla from quadratojugal (1)
- 4 Nasals do not contact maxilla (0), or nasals contact maxilla (1)
- 5 Preorbital length: short, less than 40% of skull length, as measured from tip of snout to anterior margin of orbit and middle of quadrate (0), intermediate, between 45-55% of skull length (1), or long, greater than 60% of skull length (2)
- 6 Postparietal lappets absent (0), present (1)
- 7 Jugal – lacrimal contact: short contact (0), extensive contact (1)
- 8 Postorbital with finger-like posterior process: absent (0), present (1)
- 9 Premaxillary elongation: absent, marginal length equal to medial length (0), present, marginal length much greater than medial length (1).
- 10 Maximum length of external naris much less than half orbit length (0), maximum length of external naris approximately half orbit length (1)
- 11 Width of skull table relative to maximum skull width: wide, $\geq 65\%$ (0), or narrow, less than 60% (1)
- 12 Jugal deep below orbit (vs narrow process): $< 50\%$ orbit diameter (0); $\geq 50\%$ (1)
- 13 Jugal alary process on palate: absent (0); present (1)

- 14 Prefrontal/postfrontal suture: middle of orbit (0); in anterior half of orbit (1)
- 15 Septomaxillary: small, entirely within the naris margin (0); barely exposed on the dorsal surface (1); triangular, substantially exposed on dorsal skull surface (2)
- 16 Squamosal – intertemporal contact: absent (0), present (1)
- 17 Premaxillary alary process: absent (0); present (1)
- 18 Width of interpterygoid vacuity: width \geq total skull table width (0); $<$ half of skull table width (1)
- 19 Anterior palatal fossa: absent (0); present (1)
- 20 Anterior extent of pterygoid: contacts contralateral pterygoid on midline anterior to cultriform process (0), contacts cultriform process, but do not meet on midline (1), extends anteriorly but does not contact cultriform process or contralateral pterygoid (2)
- 21 Depressions in vomers anterior to choanae: absent (0); shallow, dished depressions present (1)
- 22 Vomerine denticle patch: uniformly distributed on body of vomer (0), denticles restricted to posterior vomerine surface (1); denticles absent (2)
- 23 Denticles extend along the quadrate ramus of the pterygoid (0); denticles absent from quadrate ramus of pterygoid (1)
- 24 Vomerine fangs: larger than marginal teeth (0); same size or smaller than marginal teeth (1)
- 25 Upper marginal teeth: not enlarged near premaxillary-maxillary suture (0), enlarged near premaxillary-maxillary suture (1)

- 26 Pterygoid posterolateral edge: expanded into gently convex flange (0), extends at almost a right angle to quadrate ramus (1)
- 27 Prechoanal length of vomer: less than postchoanal length (0); greater than or equal to postchoanal width (1)
- 28 Premaxillary tooth number: fewer than 20 (0), greater than 20 (1).
- 29 Vomerine fang pair: aligned parallel to the marginal tooth row (0); not parallel (1)
- 30 Vomerine ridges radiate towards snout margins anterior to choanae: absent (0); present (1)
- 31 Basicranial joint: mobile, unfused (0), or sutural (1)
- 32 Sphenethmoid: rhomboidal (0); almost square (1); elongate and narrow (2)
- 33 Parasphenoid denticles: restricted to a discrete zone (0), shagreen covers much of ventral surface (1); absent (2)
- 34 Shape of choana: as wide anteriorly as posteriorly (0); wider anteriorly than posteriorly (1)
- 35 Location of parasphenoid carotid grooves: lie posteromedial to basiptyergoid process (0), curve far around the basiptyergoid process (1)
- 36 Anterior splenial: excluded from jaw symphysis (0), enters jaw symphysis (1)
- 37 Number of teeth in dentary: fewer than 48 (0), greater than 48 (1)
- 38 Para-articular (chordatympanic) foramen: present (0); absent (1)
- 39 Zone of subdued dermal ornament adjacent to midline suture: absent (0); present (1)
- 40 Position of quadrate condyles: posterior to exoccipital condyles (0), at same level as exoccipital condyles (1), anterior to exoccipital condyles (2)

- 41 Position of external naris: terminal (0), partially retracted (1), or retracted well back from tip of snout (at least 15% of skull length) (2)
- 42* Lateral line sulci: present (0); absent (1)
- 43* Ratio of interorbital distance at midline of orbit/total skull width at midline of orbit < 50% (0) or > 50% (1)

APPENDIX B

SUPPLEMENTARY MATERIAL FOR CHAPTER III:

**VARIATION OF OSTEOCYTE LACUNAE SIZE WITHIN THE TETRAPOD
SKELETON: IMPLICATIONS FOR PALAEOGENOMICS**

Appendix B 3.1. Materials and methods

Measuring osteocyte lacunae

The method of osteocyte lacuna size measuring is carried out using an automated approach. We utilize scanning electron microscopy to photograph the thin section slides to obtain the finest available resolution. Since lacunae are so small, a difference of a few pixel widths can make a large difference in calculating the area of an osteocyte lacuna. The threshold of the image is altered in the program ImageJ (Abramoff *et al.* 2004), so that the osteocyte lacunae are easily distinguishable from the rest of the bone matrix. The “Analyze Particles” feature is utilized to outline and automatically measure the lacunar areas in the photograph. The length and width calculated by this algorithm were subsequently used to calculate cell volume using the equation $(4/3 \times \pi \times \text{width axis radius}^2 \times \text{length axis radius})$ like in Organ *et al.* (2007).

Estimating missing values using phylogeny

The calculated volume values for each bone of each of the four studied taxa were then added to the most complete lacunar and genome size data set from Organ *et al.* (2009). As opposed to estimating the missing genome size values using the program BayesTraits (as used in Organ *et al.* (2007), Organ & Shedlock 2009, and Organ *et al.* (2009), a similar web based program called PhyloPars was employed. PhyloPars is extremely user friendly, able to easily handle missing data, and uses a maximum likelihood based method for inferring missing values (see Bruggeman *et al.* 2009 for more details). Additionally, the genome sizes used to check the accuracy of the estimated C-values from PhyloPars were obtained from the Animal Genome Size Database. To be

consistent, only C-values obtained using the method of Feulgen Densitometry were averaged if more than one genome size was available for the given taxon.

The phylogenetic tree used in analysis was the extant taxon tree from Organ and Shedlock (2009). Each taxon in this study was added to this tree using Mesquite v. 2.73(Maddison & Maddison 2007) and the StratAdd package (Faure *et al.* 2006). Details of how this tree was assembled can be found in the electronic supplementary information of Organ *et al.* (2009).

In this sensitivity analysis, the “ln genome” for the 35 extant taxa was replaced with the minimum and maximum C-values reported in the Animal Genome Size Database. Subsequently, all of the analyses were rerun for each the minimum C-value and maximum C-value. It was shown that no matter which C-value (min, max or average) was used, the estimated genome size for the unknown value did not significantly differ (Table S3). Additionally, using the 3rd quartile of the cell size measurements did not make a significant difference in the estimated genome size as compared to using the mean (Table S4). It is important to note that Organ *et al.* (2011) has presented an improved multiple regression method for estimating the genome sizes of amphibians- that have inordinately large genomes that improves the accuracy of the estimation.

Appendix B 3.2. Results

Table S3.1: A summary of measured values from the 44 slides. The natural log of the mean lacuna volume presented here is the value that was used in reconstructing the genome size for that skeletal element in the program PhyloPars. The column “n lacunae” is how many lacunae were automatically measured per slide.

Taxon	Bone element	Ln Lacuna Volume (Mean)	Standard Deviation	n lacunae
<i>Alligator sinensis</i>	Tibia	3.908	0.749	15
<i>Alligator sinensis</i>	Fibula	3.776	0.666	13
<i>Alligator sinensis</i>	Rib	3.637	0.915	7
<i>Alligator sinensis</i>	Ulna	3.653	0.839	54
<i>Alligator sinensis</i>	Femur	4.953	0.706	10
<i>Alligator sinensis</i>	Thoracic	4.970	0.787	6
<i>Alligator sinensis</i>	Metatarsal	4.121	0.800	47
<i>Alligator sinensis</i>	Humerus	3.678	0.757	47
<i>Alligator sinensis</i>	Skull	4.588	0.560	8
<i>Alligator sinensis</i>	Caudal	2.539	1.646	11
<i>Alligator sinensis</i>	Radius	4.285	1.118	17
<i>Ambystoma</i>	Tibia	8.634	0.867	7

<i>tigrinum</i>				
<i>Ambystoma tigrinum</i>	Fibula	8.934	0.735	16
<i>Ambystoma tigrinum</i>	Rib	10.274	0.371	3
<i>Ambystoma tigrinum</i>	Ulna	8.584	0.615	8
<i>Ambystoma tigrinum</i>	Femur	9.172	0.572	6
<i>Ambystoma tigrinum</i>	Thoracic	9.378	0.584	5
<i>Ambystoma tigrinum</i>	Metatarsal	9.270	1.007	6
<i>Ambystoma tigrinum</i>	Humerus	8.192	0.740	10
<i>Ambystoma tigrinum</i>	Skull	8.979	0.699	7
<i>Ambystoma tigrinum</i>	Caudal	7.979	1.258	6
<i>Ambystoma tigrinum</i>	Radius	7.837	1.046	8
<i>Marmota monax</i>	Tibia	3.517	0.741	36
<i>Marmota monax</i>	Fibula	3.628	0.772	37
<i>Marmota monax</i>	Rib	3.655	0.851	42
<i>Marmota monax</i>	Ulna	4.076	1.200	46
<i>Marmota monax</i>	Femur	3.900	0.885	71
<i>Marmota</i>	Thoracic	4.320	1.028	46

<i>monax</i>				
<i>Marmota monax</i>	Metatarsal	4.997	1.230	40
<i>Marmota monax</i>	Humerus	4.874	1.651	60
<i>Marmota monax</i>	Skull	3.807	1.570	28
<i>Marmota monax</i>	Caudal	4.764	1.109	25
<i>Marmota monax</i>	Radius	4.338	1.045	54
<i>Columba livia</i>	Tibia	4.128	0.862	14
<i>Columba livia</i>	Fibula	3.447	0.501	6
<i>Columba livia</i>	Rib	4.070	0.921	8
<i>Columba livia</i>	Ulna	3.233	0.864	26
<i>Columba livia</i>	Femur	3.047	0.664	17
<i>Columba livia</i>	Thoracic	4.449	1.653	12
<i>Columba livia</i>	Metatarsal	3.011	0.723	8
<i>Columba livia</i>	Humerus	3.223	0.941	10
<i>Columba livia</i>	Skull	4.059	1.227	8
<i>Columba livia</i>	Caudal	3.950	1.621	6
<i>Columba livia</i>	Radius	3.104	0.836	8

Table S3.2: A summary of the genome sizes estimated from the program PhyloPars for each skeletal element. The estimated genome size in picograms (pg) is the exponential of the estimated ln genome value.

Taxon	Bone element	Est. ln genome	SD	Est. Genome in pg
<i>Alligator sinensis</i>	Tibia	0.372	0.126	1.451
<i>Alligator sinensis</i>	Fibula	0.317	0.126	1.373
<i>Alligator sinensis</i>	Rib	0.253	0.126	1.288
<i>Alligator sinensis</i>	Ulna	0.261	0.126	1.298
<i>Alligator sinensis</i>	Femur	0.813	0.126	2.255
<i>Alligator sinensis</i>	Thoracic	0.821	0.126	2.273
<i>Alligator sinensis</i>	Metatarsal	0.461	0.126	1.586
<i>Alligator sinensis</i>	Humerus	0.274	0.126	1.315
<i>Alligator sinensis</i>	Skull	0.660	0.126	1.935
<i>Alligator sinensis</i>	Caudal	-0.209	0.126	0.811
<i>Alligator sinensis</i>	Radius	0.533	0.126	1.704
<i>Ambystoma tigrinum</i>	Tibia	2.600	0.457	13.464
<i>Ambystoma tigrinum</i>	Fibula	2.720	0.457	15.180

<i>Ambystoma tigrinum</i>	Rib	3.292	0.457	26.897
<i>Ambystoma tigrinum</i>	Ulna	2.580	0.457	13.197
<i>Ambystoma tigrinum</i>	Femur	2.830	0.457	16.945
<i>Ambystoma tigrinum</i>	Thoracic	2.910	0.457	18.357
<i>Ambystoma tigrinum</i>	Metatarsal	2.870	0.457	17.637
<i>Ambystoma tigrinum</i>	Humerus	2.410	0.457	11.134
<i>Ambystoma tigrinum</i>	Skull	2.750	0.457	15.643
<i>Ambystoma tigrinum</i>	Caudal	2.320	0.457	10.176
<i>Ambystoma tigrinum</i>	Radius	2.260	0.457	9.583
<i>Marmota monax</i>	Tibia	0.440	0.212	1.553
<i>Marmota monax</i>	Fibula	0.487	0.212	1.627
<i>Marmota monax</i>	Rib	0.496	0.212	1.642
<i>Marmota monax</i>	Ulna	0.678	0.212	1.970
<i>Marmota monax</i>	Femur	0.780	0.212	2.181
<i>Marmota monax</i>	Thoracic	0.780	0.212	2.181
<i>Marmota monax</i>	Metatarsal	1.070	0.212	2.915

<i>Marmota monax</i>	Humerus	1.010	0.212	2.746
<i>Marmota monax</i>	Skull	0.563	0.212	1.756
<i>Marmota monax</i>	Caudal	0.966	0.212	2.627
<i>Marmota monax</i>	Radius	0.788	0.212	2.199
<i>Columba livia</i>	Tibia	0.411	0.240	1.508
<i>Columba livia</i>	Fibula	0.123	0.240	1.131
<i>Columba livia</i>	Rib	0.386	0.240	1.471
<i>Columba livia</i>	Ulna	0.030	0.240	1.030
<i>Columba livia</i>	Femur	-0.050	0.240	0.951
<i>Columba livia</i>	Thoracic	0.550	0.240	1.733
<i>Columba livia</i>	Metatarsal	-0.064	0.240	0.938
<i>Columba livia</i>	Humerus	0.025	0.240	1.025
<i>Columba livia</i>	Skull	0.382	0.240	1.465
<i>Columba livia</i>	Caudal	0.335	0.240	1.398
<i>Columba livia</i>	Radius	-0.025	0.240	0.975

Table S3.3: A summary of estimated values from the sensitivity analysis. Maximum, minimum and average C-values were used in three separate sets of analyses to determine if the value selected for C-value from the Animal Genome Size Database affected the estimated genome size for the one unknown value. The difference in mean estimated genome size is not significant with the standard deviation taken into account.

Taxon	Bone	Est. In genome (Max C-val)	SD	Est. In genome (Min C-val)	SD
<i>Ambystoma tigrinum</i>	Tibia	2.500	0.483	2.651	0.62
<i>Ambystoma tigrinum</i>	Caudal	2.274	0.483	2.334	0.62
<i>Ambystoma tigrinum</i>	Radius	2.225	0.483	2.266	0.62
<i>Ambystoma tigrinum</i>	Fibula	2.605	0.483	2.797	0.62
<i>Ambystoma tigrinum</i>	Rib	3.072	0.483	3.451	0.62
<i>Ambystoma tigrinum</i>	Ulna	2.483	0.483	2.483	0.62
<i>Ambystoma tigrinum</i>	Femur	2.689	0.483	2.914	0.62
<i>Ambystoma tigrinum</i>	Thoracic	2.762	0.483	3.017	0.62
<i>Ambystoma tigrinum</i>	Metatarsal	2.723	0.483	2.963	0.62
<i>Ambystoma tigrinum</i>	Humerus	2.347	0.483	2.436	0.62
<i>Ambystoma tigrinum</i>	Skull	2.622	0.483	2.822	0.62
<i>Marmota monax</i>	Tibia	0.651	0.224	0.191	0.288
<i>Marmota monax</i>	Caudal	1.083	0.224	0.795	0.288
<i>Marmota monax</i>	Ulna	0.846	0.224	0.464	0.288
<i>Marmota monax</i>	Fibula	0.690	0.224	0.244	0.288
<i>Marmota monax</i>	Rib	0.696	0.224	0.254	0.288

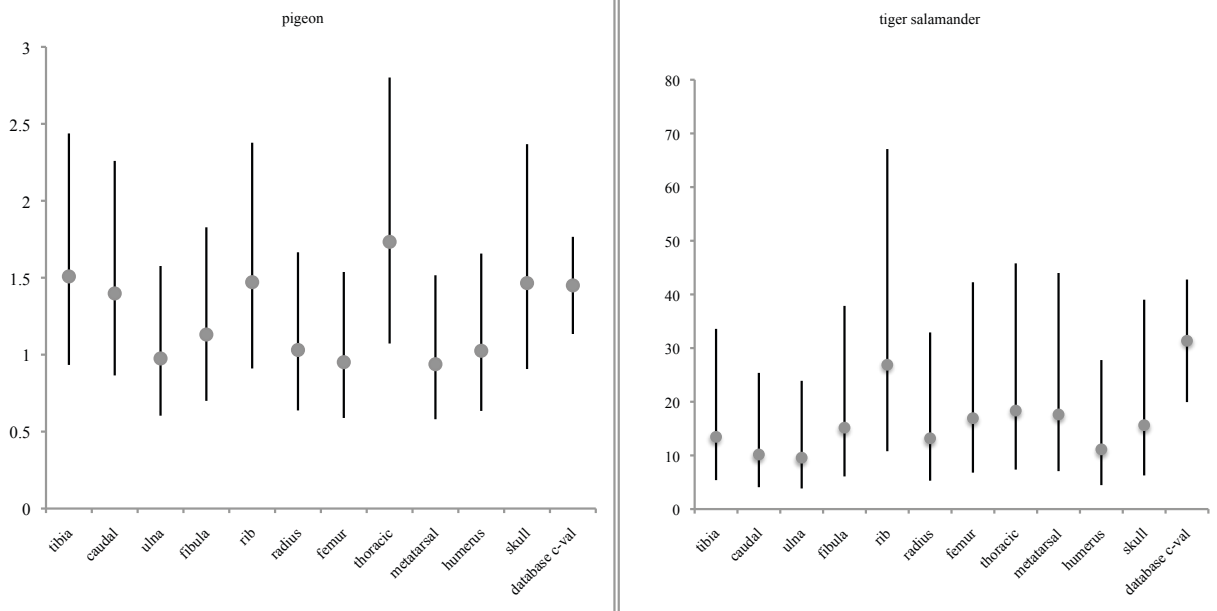
<i>Marmota monax</i>	Radius	0.937	0.224	0.590	0.288
<i>Marmota monax</i>	Femur	0.930	0.224	0.581	0.288
<i>Marmota monax</i>	Thoracic	0.930	0.224	0.581	0.288
<i>Marmota monax</i>	Metatarsal	1.167	0.224	0.912	0.288
<i>Marmota monax</i>	Humerus	1.122	0.224	0.849	0.288
<i>Marmota monax</i>	Skull	0.752	0.224	0.332	0.288
<i>Columba livia</i>	Tibia	0.446	0.254	0.493	0.325
<i>Columba livia</i>	Caudal	0.335	0.254	0.405	0.325
<i>Columba livia</i>	Radius	0.087	0.254	-0.010	0.325
<i>Columba livia</i>	Fibula	0.209	0.254	0.161	0.325
<i>Columba livia</i>	Rib	0.426	0.254	0.463	0.325
<i>Columba livia</i>	Ulna	0.133	0.254	0.054	0.325
<i>Columba livia</i>	Femur	0.070	0.254	-0.034	0.325
<i>Columba livia</i>	Thoracic	0.558	0.254	0.649	0.325
<i>Columba livia</i>	Metatarsal	0.056	0.254	-0.053	0.325
<i>Columba livia</i>	Humerus	0.129	0.254	0.049	0.325
<i>Columba livia</i>	Skull	0.422	0.254	0.459	0.325
<i>Alligator sinensis</i>	Tibia	0.549	0.135	0.275	0.171
<i>Alligator sinensis</i>	Caudal	0.075	0.135	-0.393	0.171
<i>Alligator sinensis</i>	Radius	0.685	0.135	0.460	0.171
<i>Alligator sinensis</i>	Fibula	0.504	0.135	0.212	0.171
<i>Alligator sinensis</i>	Rib	0.455	0.135	0.138	0.171
<i>Alligator sinensis</i>	Ulna	0.462	0.135	0.148	0.171
<i>Alligator sinensis</i>	Femur	0.915	0.135	0.782	0.171
<i>Alligator sinensis</i>	Thoracic	0.922	0.135	0.792	0.171

<i>Alligator sinensis</i>	Metatarsal	0.626	0.135	0.377	0.171
<i>Alligator sinensis</i>	Humerus	0.472	0.135	0.163	0.171
<i>Alligator sinensis</i>	Skull	0.790	0.135	0.607	0.171

Table S3.4. Due to the fact lacunae are 3-dimensional objects, the thin section preserve only one plane, and the most accurate representation of the size of that cell should be the largest 2-dimensional slice. Although we have shown that using the 3rd Quantile (75th percentile) of the cell size volumes to make genome size estimations did not result in statistically different values than when the mean was used.

Taxon	ln(Genome) est. 3rd Q	ln(Genome) est. mean	StDev
<i>Alligator</i>	0.49	0.26	0.13
<i>Ambystoma</i>	2.60	2.58	0.46
<i>Columba</i>	0.14	0.03	0.24
<i>Marmota</i>	1.12	0.79	0.21

Figure S3.1: An example of the intraspecific variation (95% CI) of reported C-values in the Animal Genome Size Database (www.genomesize.com). The variation in the database is most likely caused by different modes of measurement and associated error, but the spread of the estimated genome size values is still greater than the range of values presented in the database (Note: Not all species have multiple entries).



Appendix B 3.3 References

- Abramoff, M.D., Magelhaes, P.J., Ram, S.J. 2004. Image Processing with ImageJ. *Biophotonics International* **11**, 36-42.
- Bruggeman, J., Heringa, J. & Brandt, B. W. 2009. PhyloPars: estimation of missing parameter values using phylogeny. *Nucleic Acid Research* **37**, W179-W184.
- Faure, E., Lony, E., Lovigny, R., Menegoz, A., Ting, Y. & Laurin, M. 2006 StratAdd module for Mesquite. (<http://mesquiteproject.org/packages/stratigraphicTools/>)
- Maddison, W. P. & Maddison, D.R. 2010. Mesquite: a modular system for evolutionary analysis. Version 2.73 (<http://mesquiteproject.org>)
- Organ, C.L., Canoville, A., Reisz, R.R. & Laurin, M. 2011. Paleogenomic data suggest mammal-like genome size in the ancestral amniote and derived large genome size in amphibians. *Journal of Evolutionary Biology* **24**, 372-380.
- Organ, C. L., Brusatte, S. L. & Stein, K. 2009. Sauropod dinosaurs evolved moderately sized genome unrelated to body size. *Proceedings of the Royal Society B* **276**, 4303-4308.
- Organ, C. L. & Shedlock, A. 2009. Palaeogenomics of pterosaurs and the evolution of small genome size in flying vertebrates. *Biology Letters* **5**, 47-50.
- Organ, C. L., Shedlock, A. M., Meade, A., Pagel, M. & Edwards, S. 2007. Origin of avian genome size and structure inc non-avian dinosaurs. *Nature* **446**, 180-184.

APPENDIX C

SUPPLEMENTARY DATA FOR CHAPTER IV:

**PLIOCENE PALEOENVIRONMENTS OF SOUTHEASTERN QUEENSLAND,
AUSTRALIA INFERRED FROM STABLE ISOTOPES OF MARSUPIAL TOOTH
ENAMEL**

Table S4.1 Carbon and oxygen stable isotope values. Raw stable isotope data of Pliocene fossil tooth enamel used in this chapter. Isotope values are relative to the VPDB standard and are presented in per mil (‰). The column of $\delta^{13}\text{C}$ diet is the $\delta^{13}\text{C}$ enamel with the diet to enamel fractionation added, per Forbes et al. (2010). The “Suess effect” column is -1.2‰ added to the $\delta^{13}\text{C}$ enamel value to take into account the atmospheric depletion in $\delta^{13}\text{C}$ due to the burning of fossil fuels; this follows the convention of Yeakel et al. 2007.

Sample Number	Taxon	$\delta^{13}\text{C}$ enamel	with Suess effect (add -1.2)	$\delta^{13}\text{C}$ diet (add -12)	$\delta^{18}\text{O}$ (VPDB)
1	<i>Euryzygoma dunense</i>	-7.3	-8.5	-20.5	-1.7
2	<i>Euryzygoma dunense</i>	-5.9	-7.1	-19.1	-1.6
3	<i>Euryzygoma dunense</i>	-10.3	-11.53	-23.53	0.8
4	<i>Euryzygoma dunense</i>	-10.1	-11.3	-23.3	0.8
5	<i>Euryzygoma dunense</i>	-13.8	-15	-27	-0.5
6	<i>Euryzygoma dunense</i>	-14	-15.2	-27.2	-1.3
7	<i>Euryzygoma dunense</i>	-9.6	-10.8	-22.8	-1.8
8	<i>Euryzygoma dunense</i>	-13.5	-14.7	-26.7	-1.5
9	<i>Euryzygoma dunense</i>	-13.6	-14.8	-26.8	-1.8
10	<i>Euryzygoma dunense</i>	-13.4	-14.6	-26.6	1.3
11	<i>Euryzygoma dunense</i>	-9.3	-10.5	-22.5	2.9
12	<i>Euryzygoma dunense</i>	-12.9	-14.1	-26.1	2.1
13	<i>Macropus</i> sp.	-10.6	-11.8	-23.8	-4.6
14	<i>Macropus</i> sp.	-10.6	-11.8	-23.8	-4.2
15	<i>Macropus</i> sp.	-5.3	-6.5	-18.5	-5.6
16	<i>Macropus</i> sp.	-13.6	-14.8	-26.8	-1.9
17	<i>Macropus</i> sp.	-10.5	-11.7	-23.7	-2.8
18	<i>Macropus</i> sp.	-10	-11.2	-23.2	-1.3
19	<i>Macropus</i> sp.	-3.5	-4.7	-16.7	-1.9
20	<i>Macropus</i> sp.	-5.9	-7.1	-19.1	-1.5
21	<i>Macropus</i> sp.	-6.3	-7.5	-19.5	-2.0

22	<i>Macropus</i> sp.	-8.9	-10.1	-22.1	-0.5
23	<i>Macropus</i> sp.	-6.3	-7.5	-19.5	-2.9
24	<i>Macropus</i> sp.	-7.5	-8.7	-20.7	-2.2
25	<i>Macropus</i> sp.	-9.0	-10.22	-22.22	-2.3
26	<i>Macropus</i> sp.	-10.4	-11.59	-23.59	1.5
27	<i>Macropus</i> sp.	-9.7	-10.94	-22.94	-3.3
28	<i>Macropus</i> sp.	-11.5	-12.67	-24.67	0.1
29	<i>Macropus</i> sp.	-9.9	-11.13	-23.13	-0.2
30	<i>Macropus</i> sp.	-9.3	-10.47	-22.47	-1.2
31	<i>Macropus</i> sp.	-10.6	-11.8	-23.8	-1.7
32	<i>Macropus</i> sp.	-10.9	-12.1	-24.1	-1.4
33	<i>Macropus</i> sp.	-11.4	-12.55	-24.55	0.3
34	<i>Macropus</i> sp.	-7.5	-8.67	-20.67	-0.3
35	<i>Macropus</i> sp.	-8.1	-9.34	-21.34	1.2
36	<i>Macropus</i> sp.	-10.4	-11.61	-23.61	2.3
37	<i>Protemnodon chinchillensis</i>	-15.4	-16.61	-28.61	-0.5
38	<i>Protemnodon</i> sp.	-11.5	-12.7	-24.7	-6.0
39	<i>Protemnodon</i> sp.	-10.1	-11.3	-23.3	-4.1
40	<i>Protemnodon</i> sp.	-12.3	-13.5	-25.5	-5.7
41	<i>Protemnodon</i> sp.	-13.5	-14.65	-26.65	-1.7
42	<i>Protemnodon</i> sp.	-14.7	-15.88	-27.88	0.0
43	<i>Protemnodon</i> sp.	-12.7	-13.89	-25.89	-0.1
44	<i>Protemnodon</i> sp.	-15.9	-17.1	-29.1	-2.7
45	<i>Troposodon minor</i>	-11.9	-13.1	-25.1	-1.5
46	<i>Troposodon minor</i>	-6.9	-8.08	-20.08	0.1
47	<i>Troposodon minor</i>	-10.9	-12.06	-24.06	-1.0
48	<i>Troposodon minor</i>	-13.5	-14.71	-26.71	-1.7
49	<i>Troposodon</i> sp.	-12.9	-14.1	-26.1	-3
50	<i>Troposodon</i> sp.	-13.5	-14.72	-26.72	-1.8

Table S4.2. Carbon and oxygen stable isotope values. The stable isotope values used in this chapter of modern *Macropus* tooth enamel obtained from Murphy et al. (2007a). Oxygen and carbon values are reported relative to the VPDB standard. The final column of $\delta^{13}\text{C}$ diet is the $\delta^{13}\text{C}$ enamel with the diet to enamel fractionation added, per Forbes et al. (2010). Regional abbreviations: CYP (Cape York Peninsula), ARP (Arnhem Plateau), BBS (Brigalow Belt South), and SEQ (South East Queensland), SEH (South Eastern Highlands) and MGD (Miller Grass Downs).

Specimen number	$\delta^{13}\text{C}$ enamel	$\delta^{18}\text{O}$ (VPDB)	Region	$\delta^{13}\text{C}$ diet (add -12)
S664	-3.17	-0.14	SEQ	-15.17
S665	-8.68	-0.75	SEQ	-20.68
S666	-3.35	-0.78	SEQ	-15.35
S667	-4.27	0.24	SEQ	-16.27
S668	-2.33	1.11	SEQ	-14.33
S669	-2.48	-0.28	SEQ	-14.48
S670	-1.8	-0.37	SEQ	-13.8
S675	-6.04	0.05	SEQ	-18.04
S676	-3.87	-2.82	SEQ	-15.87
S671	-5.42	0.8	SEQ	-17.42
S672	-2.32	1.3	SEQ	-14.32
S673	-3	-0.54	SEQ	-15
S674	-2.89	0.75	SEQ	-14.89
S682	-2.09	0.41	SEQ	-14.09
S617	-2.76	3.1	BBS	-14.76
S618	-5.46	2.57	BBS	-17.46
S619	-2.49	1.91	BBS	-14.49
S620	-2.5	2.15	BBS	-14.5
S621	-3.3	2.83	BBS	-15.3
S612	-4.62	1.77	BBS	-16.62
S616	-2.67	1.7	BBS	-14.67
S615	-4.9	2.34	BBS	-16.9
S611	-8.56	2.33	BBS	-20.56
S613	-2.98	2.08	BBS	-14.98
S614	-3	2.82	BBS	-15
S600	-8.99	1.91	BBS	-20.99
S601	-11	2.12	BBS	-23
S610	-2.99	4.2	BBS	-14.99
S609	-6.61	2.16	BBS	-18.61
S604	-6.36	1.84	BBS	-18.36
S602	-6.47	1.93	BBS	-18.47
S603	-5.94	0.84	BBS	-17.94
S608	-6.02	3.1	BBS	-18.02

S605	-8.01	2.88	BBS	-20.01
S607	-3.51	2.97	BBS	-15.51
S606	-2.88	2.81	BBS	-14.88
S662	-4.37	0.12	BBS	-16.37
S677	-10.43	1.99	BBS	-22.43
S393	-1.51	-0.42	CYP	-13.51
S392	-7.42	-1.4	CYP	-19.42
S394	-7.53	-1.05	CYP	-19.53
S395	-11.63	-1.14	CYP	-23.63
S391	-7.09	0.16	CYP	-19.09
S390	-8.67	-0.9	CYP	-20.67
S396	-8.46	2.09	CYP	-20.46
S397	-13.89	0.2	CYP	-25.89
S398	-6.85	-1.35	CYP	-18.85
S358	-8	0.28	ARP	-20
S359	-8.31	-3.4	ARP	-20.31
S290	-6.29	-1.95	ARP	-18.29
S295	-7.99	0.3	ARP	-19.99
S50	-8.82	-3.11	ARP	-20.82
S294	-7.63	-2.33	ARP	-19.63
S70	-4.89	3.5	MGD	-16.89
S71	-5.85	5.34	MGD	-17.85
S69	-5.46	2.04	MGD	-17.46
S68	-4.92	1.28	MGD	-16.92
S67	-5.72	5.92	MGD	-17.72
S32	-6.99	4.53	MGD	-18.99
S66	-4.58	4.95	MGD	-16.58
S33	-3.35	7.76	MGD	-15.35
S34	-6.94	6.57	MGD	-18.94
S65	-5.23	6.79	MGD	-17.23
S64	-4.23	4.5	MGD	-16.23
S63	-3.26	3.07	MGD	-15.26
S62	-5.2	2.67	MGD	-17.2
S61	-4.37	4.22	MGD	-16.37
S60	-5.37	7.46	MGD	-17.37
S59	-2.88	0.56	MGD	-14.88
S57	-5.86	3.71	MGD	-17.86
S58	-6.5	4.92	MGD	-18.5
S56	-2.29	1.77	MGD	-14.29
S17	-7.18	3.48	MGD	-19.18
S43	-9.11	0.88	MGD	-21.11
S16	-12.07	0.83	MGD	-24.07
S55	-8.12	5.08	MGD	-20.12
S15	-12.62	1.36	MGD	-24.62

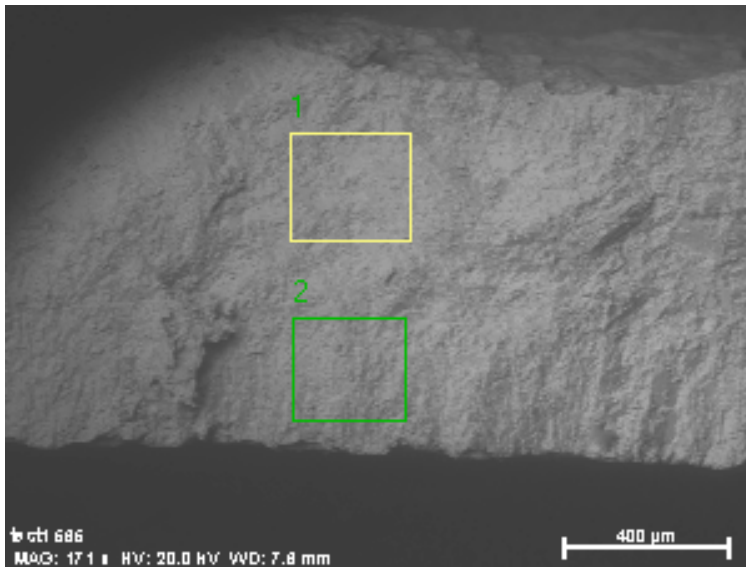
S54	-8.86	2.9	MGD	-20.86
S53	-2.83	1.94	MGD	-14.83
S52	-3.67	0.19	MGD	-15.67
S46	-5.84	3.34	MGD	-17.84
S47	-6.52	2.42	MGD	-18.52
S51	-4.05	2.7	MGD	-16.05
S48	-6.05	0.53	MGD	-18.05
S49	-5.69	1.61	MGD	-17.69
S478	-13.5	-1.06	SEH	-25.5
S477	-10.82	-1.61	SEH	-22.82
S476	-13.63	-2.06	SEH	-25.63
S475	-11.97	-2.66	SEH	-23.97
S474	-12.47	-0.2	SEH	-24.47
S458	-12.52	-2.06	SEH	-24.52
S473	-9.94	-0.56	SEH	-21.94
S472	-9.09	-2.59	SEH	-21.09
S459	-14.13	-1.58	SEH	-26.13
S469	-14.68	-2.64	SEH	-26.68
S470	-13.96	-3.23	SEH	-25.96
S471	-13.68	-0.22	SEH	-25.68
S465	-12.81	-3.07	SEH	-24.81
S466	-17.16	-2.91	SEH	-29.16
S464	-16.09	-3.98	SEH	-28.09
S460	-15.29	-3.1	SEH	-27.29
S461	-15.42	-1.87	SEH	-27.42
S462	-14.96	-2.61	SEH	-26.96
S463	-12.56	-3.14	SEH	-24.56
S456	-17.22	-1.78	SEH	-29.22
S457	-12.04	-3.12	SEH	-24.04
S479	-15.52	-2.94	SEH	-27.52
S480	-15.61	-2.81	SEH	-27.61
S455	-12.81	-2.62	SEH	-24.81
S468	-15.54	-3.73	SEH	-27.54
S467	-14.66	-2.68	SEH	-26.66
S454	-11.67	-2.94	SEH	-23.67
S481	-16.08	-0.25	SEH	-28.08
S482	-17.43	-2.9	SEH	-29.43
S483	-14.59	-1.03	SEH	-26.59
S493	-18.38	-3.74	SEH	-30.38

APPENDIX D

SUPPLEMENTARY MATERIAL FOR CHAPTER VI:

**DINOSAUR EGGSHELL AND TOOTH ENAMEL GEOCHEMISTRY AS AN
INDICATOR OF CENTRAL ASIAN CRETACEOUS PALEOENVIRONMENTS**

Figure S6.1 EDS output from Bruker Esprit 1.9.3 software. Eggshell IGM 100/1189 from the locality Bugin Tsav. Most abundant elements are listed in the “Element” column with the uncorrected and corrected weight percentages. Error is presented in weight percent. Two regions of the eggshell cross-section are compared, labeled on the micrograph in yellow (1) and green (2).

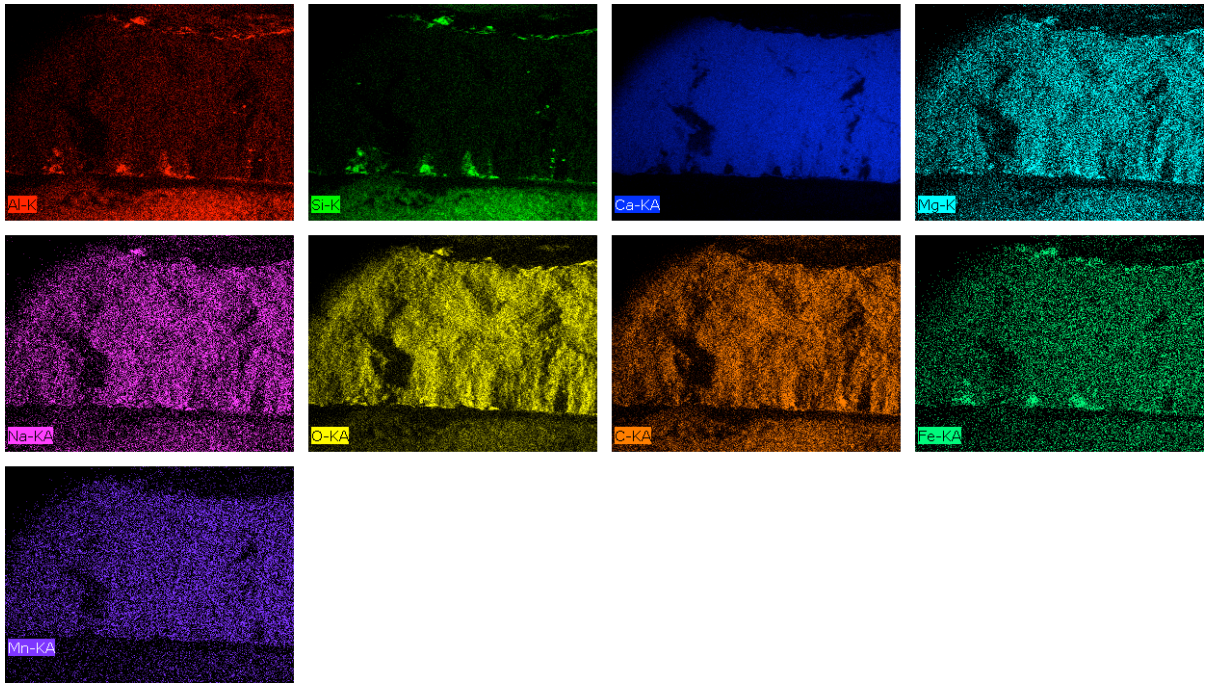


Spectrum: 1

Element	Series	unn. C [wt.%]	norm. C [wt.%]	Atom. C [at.%]	Error (1 Sigma) [wt.%]
Carbon	K-series	20.27	16.54	26.24	2.65
Oxygen	K-series	58.30	47.57	56.67	7.21
Calcium	K-series	43.81	35.75	17.00	1.31
Aluminium	K-series	0.10	0.08	0.06	0.03
Silicon	K-series	0.07	0.06	0.04	0.03
Total:		122.55	100.00	100.00	

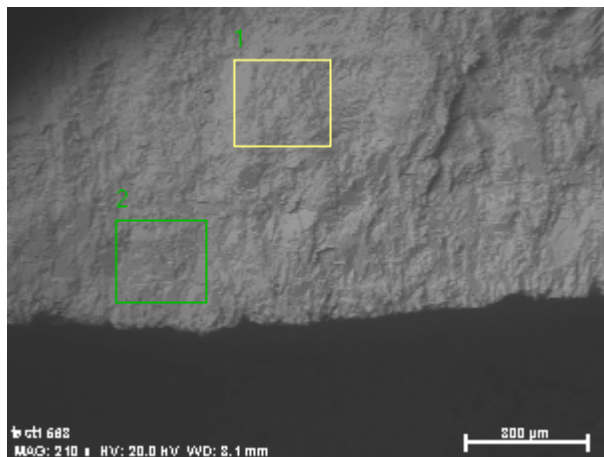
Spectrum: 2

Element	Series	unn. C [wt.%]	norm. C [wt.%]	Atom. C [at.%]	Error (1 Sigma) [wt.%]
Carbon	K-series	20.72	16.96	26.76	2.73
Oxygen	K-series	58.25	47.67	56.47	7.25
Calcium	K-series	42.64	34.90	16.50	1.27
Strontium	L-series	0.11	0.09	0.02	0.03
Aluminium	K-series	0.18	0.15	0.10	0.04
Silicon	K-series	0.27	0.22	0.15	0.04
Total:		122.18	100.00	100.00	



Al-K, Si-K, Ca-KA, Mg-K, Na-KA, O-KA, C-KA, Fe-KA, Mn-KA,
 Date:3/5/2012 1:15:03 PM
 Image size:300 x 225
 Mag:171.24136x
 HV:20.0kV

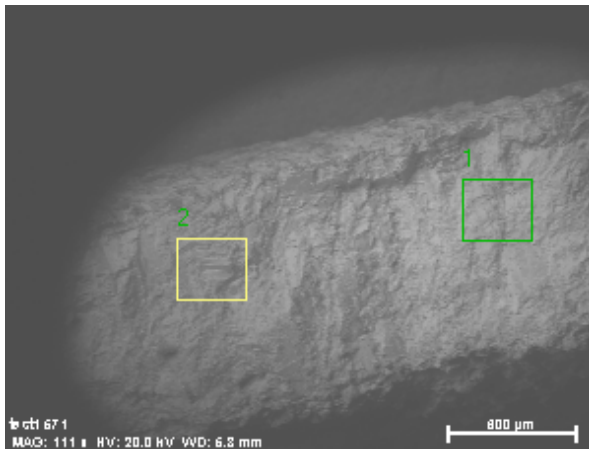
Figure S6.2. Element map from IGM 100/1189 radial view. Illustrates adheared sand grains are accounting for the presence of silicon and aluminum in the element spectrum. Each square is colored for a specific element listed in that square



Spectrum: 1

Element	Series	unn. C [wt.%]	norm. C [wt.%]	Atom. C [at.%]	Error (1 Sigma) [wt.%]
Carbon	K-series	18.30	16.23	25.95	2.40
Oxygen	K-series	53.03	47.03	56.45	6.58
Calcium	K-series	41.39	36.72	17.59	1.24
Silicon	K-series	0.03	0.02	0.02	0.03
Total:		112.74	100.00	100.00	

Figure S6.3 EDS output from Bruker Esprit 1.9.3 software. Eggshell from the locality Bugin Tsav. Most abundant elements are listed in the “Element” column with the uncorrected and corrected weight percentages. Error is presented in weight percent. Two regions of the eggshell cross-section are compared, labeled on the micrograph in yellow (1) and green (2).

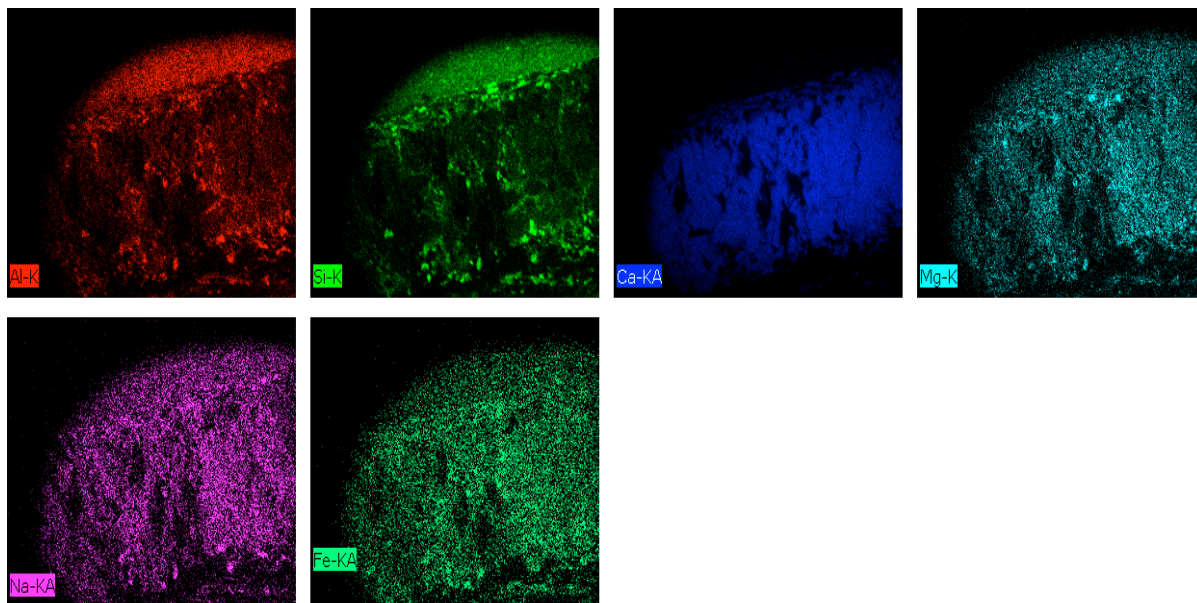


El AN Series uncorr. C norm. C Atom. C Error (1 Sigma)
 [wt.%) [wt.%) [at.%) [wt.%)

C	6	K-series	17.68	14.84	23.79	2.73
O	8	K-series	58.05	48.74	58.63	7.90
Mg	12	K-series	0.15	0.12	0.10	0.04
Al	13	K-series	0.58	0.49	0.35	0.06
Si	14	K-series	1.07	0.90	0.62	0.08
Ca	20	K-series	40.26	33.80	16.23	1.21
Fe	26	K-series	0.40	0.34	0.12	0.05
Sr	38	L-series	0.92	0.78	0.17	0.08

 Total: 119.12 100.00 100.00

Figure S6.4 EDS output from Bruker Esprit 1.9.3 software. Eggshell IGM 100/1066 from the locality Bayn Dzak. Most abundant elements are listed in the “Element” column with the uncorrected and corrected weight percentages. Error is presented in weight percent. Two regions of the eggshell cross-section are compared, labeled on the micrograph in yellow (1) and green (2).



Al-K, Si-K, Ca-KA, Mg-K, Na-KA, Fe-KA,
Date:3/5/2012 4:37:58 PM
Image size:300 x 225
Mag:111.24155x
HV:20.0kV

Figure S6.5. Element map from IGM 100/1066 radial view. Illustrates adheared sand grains are accounting for the presence of silicon and aluminum in the element spectrum. Each square is colored for a specific element listed in that square. The EDS map shows no obvious areas of inclusion of exotic elements not typically found in calcium carbonate eggshells.

Table S6.1. Raw carbon and oxygen stable isotope values of carbonates and tooth enamel used in the analyses in this chapter. Values are presented in per mil (‰)

Sample ID	Carbon ($\delta^{13}\text{C}$)	Oxygen ($\delta^{18}\text{O}$)
Ukhaa Tolgod Eggshells		
UT01	-5.1	-4.8
UT02	-5.2	-8.2
UT03	-6.1	-2.6
UT04	-3.8	-5.0
UT05	-5.7	-2.8
UT06	-5.4	-0.9
UT07	-4.3	-6.1
UT08	-6.6	-1.8
UT15	-5.0	-3.6
UT16	-4.5	-6.4
UT17	-4.4	-7.6
A5	-7.5	-4.6
A6	-6.0	-11.8
A7	-5.3	-10.7
SM06 untreated	-6.7	-1.4
SM13 treated	-4.7	-2.6
SM12 treated	-4.4	-2.2
SM 14 treated	-3.7	-6.3
SM03 untreated	-3.7	-9.9
Carbonate nodules		
UT09	-3.7	-10.5
UT10	-5.8	-11.2
UT11	-3.9	-10.4
UT12	-2.9	-10.8
UT13	-4.4	-11.4
UT14	-4.1	-11.1
UT18	-5.3	-11.7
UT19	-3.8	-11.2
UT20	-5.0	-11.4
UT21	-3.6	-10.9
UT22	-3.7	-10.8
Bayn Dzak Eggshell		
SM 15 treated	-5.4	-8.6
SM07 treated	-5.1	-11.7
SM08 treated	-5.1	-12.1
A26	-4.4	-9.6
A27	-3.2	-10.7

Bugin Tsav		
Eggshell		
SM11 treated	-6.1	-9.6
SM09 treated	-5.9	-10.2
SM10 treated	-5.5	-10.3
SM04 untreated	-5	-10.8
BB01	-5.7	-9.8
BB02	-6.1	-7.8
BB03	-6.4	-9.0
BB04	-4.8	-9.0
BB05	-4.4	-9.1
BB06	-6.5	-8.4
BB07	-6.5	-9.9
BB08	-5.5	-8.8
BB09	-5.2	-8.9
BB10	-5.4	-9.3
BB13	-4.9	-8.4
BB14	-5.2	-9.0
BB15	-6.5	-10.5
Ukhaa Tolgod		
<i>Protoceratops</i> teeth		
A8	-2.34	-7.13
A9	-3.93	-9.83
A11	-5.29	-5.86
A13	-6.78	-5.01
A17	-5.82	-5.13
A19	-6.51	-4.10
A21	-5.93	-4.90
A23	-6.50	-4.60